EVOLUTIONARY DYNAMICS OF SELFISH MITOCHODRIAL MUTATIONS IN *CAENORHABDITIS ELEGANS*

A Dissertation

by

JOSEPH JAMES DUBIE

Submitted to the Graduate and Professional School of
Texas A&M University
in partial fulfillment of the requirements for the degree of

DOCTOR OF PHILOSOPHY

Chair of Committee,	Vaishali Katju
Committee Members,	Ulfar Bergthorsson
	Luis Rene Garcia
	William J. Murphy
Head of Department,	David W. Threadgill

May 2022

Major Subject: Genetics

ABSTRACT

Despite mitochondrial DNA being one of the most popular and powerful molecular markers used to study eukaryotic evolution, much about its biology remains poorly understood. Mitochondrial genomes are challenging to engineer, reducing the power of experiments aimed at disentangling mitochondria's complex and dynamic biology. In this dissertation, we take advantage of both long-term mutation accumulation experiments — which spontaneously generate new deletion-bearing mitotypes in *Caenorhabditis elegans* — and the large catalog of *C. elegans* natural isolates. This allows us to avoid the difficulty of engineering mitochondrial genomes and explore how selection shapes the fate of new mitochondrial mutations. We first demonstrate the selfish nature of a mitotype bearing a deletion in the *ctb-1* gene (Δ*ctb-1*), namely its transmission advantage and host fitness costs. Δ*ctb-1* is then used to highlight the importance of population size for the intracellular dynamics of mitochondrial mutations. Next, we disentangle the mutational history of Δ*ctb-1*. In doing so, we found that selfish drive can be seen in a variety of classes of mitochondrial mutations, and that some mutations may hitchhike to high frequency by arising on a mitotype bearing a selfish mutation. We then demonstrate the selfish nature of another deletion-bearing mitotype and compare its intracellular dynamics to that of Δ*ctb-1*. Finally, we created lines of *C. elegans* bearing mutations in their sex determination pathways, and in key components of the electron transport chain. We then used these lines to determine if any of the electron transport chain mutations had sex system-specific or male-specific detrimental effects.

ACKNOWLEDGEMENTS

Pursuing a Ph.D. is a long and arduous process. Mine has required all the standard long hours in the lab, not getting to see your family as often as you'd like , and intellectual rigors, but it has also had a few surprises. In my second year my house burned down, and in my fourth year a major pandemic swept the world. Despite these setbacks I have consistently received the support from my colleagues, friends, and family that I needed to keep my head up and push through to the end. Here I would like to thank a few of the folks who provided that support.

I would first like to thank my advisor Dr. Vaishali Katju, who provided me the opportunity and guidance to explore this line of research. It was through her that I have developed a love of experimental evolution and the charismatic little worms we spend so much time with. She also helped me to travel overseas and supported me as I traveled around the world to present my research. Finally, I can never fully express how grateful I was when, after our house burned down, she went out her way to sell art and fundraise to help my wife and I as we rebuilt our life.

Next, I would like to thank Dr. Ulfar Bergthorsson for his contributions to my PhD experience. Dr. Bergthorsson's intellectual fingerprints can be found on all of my projects. I always valued his expertise and quiet encouragement as we designed experiments and discussed every piece of data I generated. He has also advised me every step of the way, always feeding into my excitement about new avenues to explore but reminding me to be realistic about what is accomplishable.

I would like to thank my committee members, Dr. William Murphy and Dr. L. Rene Garcia, for their valuable guidance throughout my studies. You helped me to discover the tools I would need to successfully complete my dissertation.

The projects included in this dissertation are all labor intensive, and I have greatly appreciated the help of our stellar undergraduate lab assistants and lab managers. In particular I would like to thank Avery Caraway and McKenna Stout, who lightened the load by assisting in the near-endless transferring and genotyping of worms. I would also like to thank Meghan Brady, Nicholas Edenhoffer, Robert Melde, and Austin Daigle, who kept the lab running so that I could focus on my experiments.

I would also like to thank Dr. Andrew Hillhouse, associate director of the Texas A&M Institute for Genome Sciences and Society, for his help in establishing new molecular tools for the lab. He has always been more than generous in offering support and helping to troubleshoot new problems as they arise.

I would like to thank my fellow graduate students and the administrative staff of the Texas A&M University Interdisciplinary Graduate Program in Genetics. Their consistent validation and care have kept me driven during my time at Texas A&M. I am also grateful for the kindness and help we received after our house burned down; without them we would not have been able to recover from our losses nearly as quickly. I would also like to thank Dr. Evelyn Tiffany-Castiglioni for helping me to find the program and my future advisor and for being our first home away from home in Texas.

Finally, I would like to thank my family. Chantal, thank you for your loving support and for putting up with my late hours in the lab and tired grumbling. Thank you

to my parents for encouraging me to pursue my passions, even if it means we are so far apart. Thank you to my brothers and sisters for keeping me grounded and for reminding me how cool it is that I have this opportunity.

CONTRIBUTORS AND FUNDING SOURCES

Contributors

This work was supervised by a dissertation committee consisting of Professors Dr. Vaishali Katju, Dr. Ulfar Bergthorsson, and Dr. William Murphy of the Department of Veterinary Integrative Biosciences and Professor L. Rene Garcia of the Department of Biology.

Several of the lines used in chapter V were generated by Dr. Suzanne Estes of Portland State University. All other work conducted for this dissertation was completed by the student independently.

Funding Sources

Graduate study was supported by fellowships from Texas A&M University.

This work was also made possible in part by the National Science Foundation under grant numbers MCB-1565844 to Dr. Katju, MCB-1330245 to Drs. Katju and Bergthorsson, and by the National Institutes of Health under grant number 1R01GM127433 to Dr. Katju. Its contents are solely the responsibility of the authors and do not necessarily represent the official views of the National Science Foundation or the National Institutes of Health.

TABLE OF CONTENTS

Page

LIST OF FIGURES

Page

LIST OF TABLES

Page

CHAPTER I

INTRODUCTION

Mitochondrial DNA has been one of the most popular and powerful molecular markers used to study the evolution and diversity of eukaryotic life. Its multicopy nature, lack of recombination, and high mutation rate have made mitochondrial DNA the first choice among molecular markers for evolutionary biologists and ecologists (Avise et al. 1987; Mortiz 1994; Arif et al. 2015). Many assumptions about mitochondrial DNA, such as its neutrality (Ballard and Rand 2005), constant mutational rate (Broz et al. 2021), and lack of recombination (Ladoukakis and Eyre-Walker 2004), have come into question. Mitochondrial biology is much more complex than previously understood, and a more nuanced understanding of mitochondria is needed if we are going to use it as a molecular marker (Galtier et al. 2009; Hurst and Jiggins 2005; Zhaoke et al. 2021).

In addition, many diseases associated with mitochondrial mutations have been identified in humans, with some studies suggesting that mitochondrial diseases affect one in 4,300 people globally (Chinnery et al. 2000; Gorman et al. 2015). Some studies have suggested that intracellular selection affects the occurrence and fate of mutations that cause mitochondrial diseases (Stewart and Chinnery 2015), and treatments that manipulate biogenesis and degradation in mitochondria have been shown to ameliorate or prevent disease progression (Filograna et al. 2021). It is imperative to have a greater understanding of the factors affecting the intracellular dynamics of disease-causing mitochondrial mutations if we are to develop effective treatments for these diseases.

The studies that follow examine mitochondrial mutations using *Caenorhabditis elegans* as a model system. *C. elegans* is a favored model organism for basic biological research. This is due to its short generation time, ease of maintenance, relatively simple genome, high homology between *C. elegans* and human genes, invariant cell lineages, and extensive genetic tools available (Xu and Kim 2011). Recently, *C. elegans* has become a popular model for studying mitochondrial evolution and disfunction. In addition to *C. elegans* being a good model generally, many genes associated with mitochondrial diseases in humans have orthologs in *C. elegans* (Maglioni and Ventura 2016).

One of the greatest challenges in studying mitochondrial mutations is the mutations' creation. While the tools for manipulating nuclear genes have advanced rapidly in the past few years, the technology required to manipulate mitochondrial genomes are still lacking (Klucnika and Ma 2020). The use of *C. elegans* can bypass this hurdle, because lines bearing mitochondrial mutations are available from numerous previously collected natural isolates (Cook et al. 2017) and from long-term mutation accumulation experiments (Katju and Bergthorsson 2019), which are conducted over many generations, and produce libraries of lines with spontaneously arising mutations.

In the following studies, we used *C. elegans* to better understand what factors shape the intracellular dynamics of mitochondrial mutations. The first study characterizes a deletion in the *C. elegans* mitochondrial gene *ctb-1*, which selfishly increases its intra-individual frequency despite severe fitness consequences for its host. In this study, we also compare the intra-individual dynamics of the *ctb-1* deletion in

conditions with low and high levels of inter-individual selection. The second study examines the effect of multiple subsequent mitochondrial mutations on the intracellular drive of a single selfish mitotype. The third study characterizes a selfishly acting mitotype bearing a deletion in the *COI* gene and compares it to the previously characterized selfish mitotype bearing a *ctb-1* deletion. The final study examines the effect of mitonuclear mutations on overall fitness and mitochondrial respiration in *C. elegans*. Further, this final study seeks to identify any sex-specific differences in respiration and what impact sexual system has on mitonuclear dysfunction.

References

Arif IA, Khan HA, Bahkali AH, Al Homaidan AA, Al Farhan AH, Al Sadoon M, Shobrak M. 2011. DNA marker technology for wildlife conservation. *Saudi J Biol Sci.* **18**(3):219-25. (doi:10.1016/j.sjbs.2011.03.002)

Avise JC, Arnold J, Ball RM, Bermingham E, Lamb T, Neigel JE, Reeb CA, Saunders NC. 1987. Intraspecific Phylogeography: The Mitochondrial DNA Bridge Between Population Genetics and Systematics. *Annu Rev Ecol Evol Syst*. **18**(1): 489-522. (doi:10.1146/annurev.es.18.110187.002421)

Ballard JW, Rand DM. 2005. The population biology of mitochondrial DNA and its phylogenetic implications. *Annu. Rev. Ecol. Evol. Syst.*. **36**:621-42. (doi:10.1146/annurev.ecolsys.36.091704.175513)

Broz AK, Waneka G, Wu Z, Fernandes Gyorfy M, Sloan DB. 2021. Detecting de novo mitochondrial mutations in angiosperms with highly divergent evolutionary rates. *Genetics*. **218**(1):iyab039. (doi:10.1093/genetics/iyab039)

Chinnery PF, Johnson MA, Wardell TM, Singh-Kler R, Hayes C, Brown DT, Taylor RW, Bindoff LA, Turnbull DM. 2000. The epidemiology of pathogenic mitochondrial DNA mutations. *Ann Neurol.* **48**(2):188-93. (doi:10.1002/1531-8249(200008)48:2<188::AID-ANA8>3.0.CO;2-P)

Cook DE, Zdraljevic S, Roberts JP, Andersen EC. 2017. CeNDR, the *Caenorhabditis elegans* natural diversity resource. *Nucleic Acids Res.* **45**(D1):D650-D657. (doi:10.1093/nar/gkw893)

Filograna R, Mennuni M, Alsina D, Larsson NG. 2021. Mitochondrial DNA copy number in human disease: the more the better? *FEBS Lett.* **595**(8):976-1002. (doi:10.1002/1873-3468.14021)

Galtier N, Nabholz B, Glémin S, Hurst G.D.D. 2009. Mitochondrial DNA as a marker of molecular diversity: a reappraisal. *Mol. Ecol.* **18**: 4541-4550. (doi:10.1111/j.1365-294X.2009.04380)

Gorman GS, Schaefer AM, Ng Y, Gomez N, Blakely EL, Alston CL, Feeney C, Horvath R, Yu-Wai-Man P, Chinnery PF, Taylor RW, Turnbull DM, McFarland R. 2015. Prevalence of nuclear and mitochondrial DNA mutations related to adult mitochondrial disease. *Ann Neurol.* **77**(5):753-9. (doi:10.1002/ana.24362)

Hurst GD, Jiggins FM. 2005. Problems with mitochondrial DNA as a marker in population, phylogeographic and phylogenetic studies: the effects of inherited symbionts. *Proc Biol Sci.* **272**(1572):1525-34. (doi:10.1098/rspb.2005.3056)

Katju V, Bergthorsson U. 2019. Old Trade, New Tricks: Insights into the spontaneous mutation process from the partnering of classical mutation accumulation experiments with high-throughput genomic approaches. *Genome Biol Evol*. **11**(1):136-165. (doi:10.1093/gbe/evy252)

Klucnika A, Ma H. 2020. Mapping and editing animal mitochondrial genomes: can we overcome the challenges? *Philos Trans R Soc Lond B Biol Sci*. **375**(1790):20190187. (doi:10.1098/rstb.2019.0187)

Ladoukakis ED, Eyre-Walker A. 2004. Evolutionary genetics: direct evidence of recombination in human mitochondrial DNA. *Heredity*. **93**(4):321. (doi:10.1038/sj.hdy.6800572)

Maglioni S, Ventura N. 2016. *C. elegans* as a model organism for human mitochondrial associated disorders. *Mitochondrion*. **30**:117-25. (doi:10.1016/j.mito.2016.02.003)

Moritz C. 1994. Applications of mitochondrial DNA analysis in conservation: a critical review. *Mol. Ecol.*, **3**:401-411. (doi:10.1111/j.1365-294X.1994.tb00080)

Stewart JB, Chinnery PF. 2015. The dynamics of mitochondrial DNA heteroplasmy: implications for human health and disease. *Nat Rev Genet*. **16**(9):530-42. (doi:10.1038/nrg3966)

Xu X, Kim SK. 2011. The early bird catches the worm: new technologies for the *Caenorhabditis elegans* toolkit. *Nat Rev Genet*. **12**(11):793-801. (doi:10.1038/nrg3050)

Zhaoke D, Yangzhou W, Chao L, Lili L, Xingyuan M. 2021. Mitochondrial DNA as a molecular marker in insect ecology: Current status and future prospects. *Ann. Entomol. Soc. Am*, **114**(4):470-76. (doi:10.1093/aesa/saab020)

CHAPTER II

THE CONFLICT WITHIN: ORIGIN, PROLIFERATION AND PERSISTENCE OF A SPONTANEOUSLY ARISING SELFISH MITOCHONDRIAL GENOME*

Introduction

Across the eukaryotic branches on the tree of life, there exists significant variation in the number of protein-coding genes in the genomes of mitochondria, ranging from three to 66 (Kairo et al. 1994; Gray 2018). However, most animal species typically contain the same 13 protein-coding mitochondrial genes, a small fraction of their complete protein-coding capacity. In spite of this limited protein-coding capacity, mitochondria may have had disproportionate effects on eukaryotes, starting with their origin and influencing major aspects of their subsequent evolution, from speciation (Burton et al. 2013; Chang et al. 2016; Telschow et al. 2019) and evolution of sex (Havird et al. 2015; Radzvilavicius and Blackstone 2015) to adaptation to different environments (Das 2006; da Fonseca et al. 2008; Scott et al. 2011) and senescence (Correia-Melo et al. 2016).

The population biology of mitochondria can be described as nested hierarchies, and competition, random genetic drift and natural selection can operate at different

levels of organization (Rand 2001). Thus, competition can take place between species, between populations and individuals of the same species (intraspecific), between the cells of an individual and between molecules of mitochondrial DNA (mtDNA) within a cell. Eukaryotic cells, depending on the species and the stage of development, can harbor from one to hundreds of thousands of mitochondria, and each mitochondrion can contain multiple copies of the mitochondrial genome. Hence, a cell with multiple copies of mtDNA can possess different genotypes (mitotypes or haplotypes) owing to spontaneously occurring mtDNA mutations or partial biparental transmission, a condition referred to as heteroplasmy (Harrison et al. 1985; Kmiec et al. 2006; Stewart and Chinnery 2015; Karavaeva et al. 2017). While the ratio of different types of mtDNAs in a heteroplasmic population may fluctuate, usually one mitotype predominates in frequency with other mitotypes observed at low frequencies. Hence, a mutant mitochondrial genome may have minimal effect on the physiology of the cell and the individual when its copy number is low in the cell. In such instances, the organismal phenotype is thought to be determined by the predominant mtDNA variant (Kmiec et al. 2006). The forces of genetic drift and selection operating within cells can increase the copy number of a mutant mitotype to a degree that it starts affecting the physiology and fitness of the cell and the individual, which are usually detrimental and likely to result in selection against the mutation. While most detrimental heteroplasmic mutations are removed from populations either by genetic drift, selection or by cells targeting defective mitochondria for degradation (mitophagy) (Knorre 2019), they sometimes increase in frequency and reach fixation. Indeed, heteroplasmy has been implicated in mitochondrial

diseases associated with senescence, infertility, and cancer in animals (Zeviani and Antozzi 1997; Wallace 1999; Wallace and Chalkia 2013; Greaves et al. 2014; Stewart and Chinnery 2015; Lakshmanan et al. 2018).

Because selection can operate on different levels of organization, it can also operate in opposing directions at different levels. In addition to the creation of a heteroplasmic state, mtDNA mutations may also give rise to variants that can be described as 'selfish' or 'parasitic' mtDNA molecules that possess a transmission advantage over their wild-type (WT) counterparts despite being neutral or detrimental to organismal fitness (Hurst and Werren 2001; Clark et al. 2012; Ma and O'Farrell 2016). A mitochondrial mutation can increase the fitness of a DNA molecule within cells and yet be detrimental at the level of individuals, contributing to genetic conflict. The potential of mitochondria to incur mutations that result in such genetic conflict is well recognized (Eberhard 1980; Cosmides and Tooby 1981; Barr et al. 2005). Not only can there be selection within cells that is opposed by selection between individuals, but because mitochondria are usually uniparentally inherited, mutations can arise that are beneficial to the sex that transmits its mitochondria to the next generation to the disadvantage of the opposite sex. Examples of the latter category include the multiple varieties of cytoplasmic male sterility mutations that are commonly observed in the mitochondrial genomes of flowering plants (Schnabel and Wise 1998). Such selfish mtDNA molecules, originating owing to mutations, commence at a low frequency but can rapidly exceed the frequency of the WT mtDNA within the cytoplasm, if their spread is left unabated.

Recent research has demonstrated that deletion-bearing mtDNA molecules often bear the signature of selfish genetic elements. Large-deletion bearing mtDNA molecules resulting in a petite mutant phenotype in small experimental populations of the yeast *Saccharomyces cerevisiae* were among the first to be described as selfish mtDNA elements, and were often observed to replicate along with the WT mtDNA in a state of heteroplasmy (MacAlpine et al. 2001; Taylor et al. 2002, Jasmin and Zeyl 2014). These petite mutations in yeast are one of the best characterized examples of within-cell selection for deleterious mitochondrial mutations, and are thought to gain a transmission advantage owing to faster replication. Additionally, germline mtDNA deletions that are transmitted to progeny have also been reported in humans (Poulton et al. 1991) and nematodes (Tsang and Lemire 2002; Howe and Denver 2008). Deletions of mitochondrial genes in the nematode genus *Caenorhabditis* exhibit patterns that are consistent with selfishness in that they are strongly detrimental to the individual, and yet, reach high intracellular frequency and persist over long periods in populations (Tsang and Lemire 2002; Liau et al. 2007; Estes et al. 2011; Clark et al. 2012). In the first documented case of a selfish mitochondrial deletion (*uaDf5*) in *Caenorhabditis elegans*, close to 25% (11 genes) of the mitochondrial genome was eliminated during mutagenesis, including *atp6*, *ctb-1*, *nd1* and *nd2* (Tsang and Lemire 2002). The *uaDf5* deletion persisted in laboratory populations despite significant negative consequences for fitness-related traits. Additionally, natural populations of *Caenorhabditis briggsae* were found to harbor a heteroplasmic mitochondrial deletion that included a portion of *nd5* (Howe and Denver 2008; Clark et al. 2012). The *nd5* deletion-bearing mitochondrial

genomes exist in a heteroplasmic state at 30-40% frequency within *C. briggsae*. As was the case of the large deletion in *C. elegans*, these deletions are detrimental to fitness. In both *C. elegans* and *C. briggsae*, the negative effects on individual fitness are countered by transmission advantage of the mitochondria that harbor the deletions. mtDNA deletions are thought to be functionally recessive, with a phenotype manifesting beyond a high threshold level of heteroplasmy (greater than or equal to 60%) (Hayashi et al. 1991; Porteous et al. 1998), although there can be considerable variation in the phenotypic onset of mtDNA genetic defects (Rossignol et al. 2003). Intriguingly, a small percentage of normal mtDNA (2-27%) can have a disproportionately large ameliorative effect on the phenotype despite a high frequency of the heteroplasmic mtDNA deletion (Shoffner et al. 1990).

The reduced ability of populations to rid themselves of strongly deleterious mitochondrial mutations by natural selection can give rise to compensatory mutations, either in nuclear or other mitochondrial genes, that mitigate the effects of the original mutations. An important mechanistic question regarding large-scale heteroplasmic mtDNA deletions is whether they are indeed propagating as selfish genetic elements, a designation that is met if the said elements fulfil two key criteria, namely: (i) possess a transmission advantage relative to other DNA encoded in the genome of the organism, and (ii) are neutral or detrimental with respect to organismal fitness (Hurst and Werren 2001). *Caenorhabditis elegans* provides an attractive multicellular system to understand the evolutionary dynamics of mitochondrial mutations in real time and the mechanisms by which deleterious mutations are maintained in populations. To that end, we have

begun to investigate mitochondrial mutations, including mtDNA deletions, that arose spontaneously and reached high frequencies in a mutation accumulation (MA) experiment in *C. elegans* (Konrad et al. 2017). One MA line (line 1G) was found to harbor five heteroplasmic mtDNA mutations relative to the ancestral control, of which three exceeded frequencies of 50%. Of these, a 499 bp frameshift deletion in the *cytochrome b(1)* (*ctb-1*) gene had reached a frequency of 96%. For simplicity, we refer to this mutant mtDNA genome as Δ*ctb-1*-bearing mtDNA given that (i) the large *ctb-1* deletion had the highest frequency among all of the detected mtDNA heteroplasmies within this line, and (ii) the *ctb-1* deletion serves as a convenient, easily detectable marker for mutant mtDNA within this experimental line. Herein we analyze the fitness consequences of this mutant Δctb-1 mtDNA genome, the timing of its origin and its population dynamics that enable its evolutionary persistence in populations despite a significant fitness cost.

Methods

Identification of Δctb-1-bearing mtDNA in a spontaneous mutation accumulation experiment

A 499 bp deletion in the mitochondrial *ctb-1* gene originated in one replicate line (1G) of a long-term *C. elegans* spontaneous MA experiment with varying population sizes (Katju et al. 2015; Konrad et al. 2017; Katju et al. 2018). The MA experiment was conducted over 409 consecutive MA generations. Line 1G was one of twenty replicate MA lines that were propagated via single hermaphrodite descent each generation (n = 1) and had reached MA generation 346 when submitted for genome sequencing. The lower MA generation number (generation 346) was owing to frequent backups during the course of the MA experiment, presumably because of the build-up of a mutation load leading to reduced fitness relative to the ancestor. Following the termination of the MA experiment, whole-genome sequencing of all 35 MA lines and their ancestral pre-MA control was conducted via Illumina paired-ends sequencing and all mtDNA mutations across the 35 MA lines were identified (Konrad et al. 2017). MA line 1G was found to harbor five heteroplasmic mtDNA mutations relative to the ancestral control: (i) a G → T substitution in the *tRNA-Asn* gene (frequency 13%), (ii) a 499 bp frameshift deletion in the *ctb-1* gene (frequency 96%), (iii) a single T insertion in a homopolymeric run within the *nd5* gene [(T)8 → (T)9; frequency 3%], (iv) an insertion of a T pair in a homopolymeric run within the *nd5* gene [(T)8 → (T)10; frequency 70%], and (v) a C → T nonsynonymous substitution (Thr → Ile) in the *nd5* gene (frequency 94%). Owing to the presence of three high-frequency (greater than or equal to 70%) heteroplasmic

mtDNA mutations in line 1G, it is likely that the majority of mtDNA molecules within this lineage harbor more than one of these heteroplasmic mtDNA variants. Given that the *ctb-1* deletion is the heteroplasmy with the highest frequency and is easily genotyped by polymerase chain reaction (PCR), we refer to the mutant mitotypes as Δ*ctb-1*-bearing mtDNA or Δ*ctb-1* mitotype for the sake of simplicity.

Timing the spontaneous origins of multiple heteroplasmies in mutation accumulation line 1G

An immense advantage of *C. elegans* as a model system for experimental evolution studies is the species' ability to survive long-term cryogenic storage at −86°C. During the course of the spontaneous MA experiment, the MA lines had been cryogenically preserved at regular time-intervals. In addition to the pre-MA ancestral control, we thawed stocks of line 1G frozen at nine additional time-intervals, namely MA generations 25, 51, 72, 96, 137, 157, 221, 300 and 346, and isolated genomic DNA from L4 larvae using a previously described supplemental nematode protocol with a Puregene Genomic DNA Tissue Kit (Konrad et al. 2017). These genomic DNA samples were initially screened for the frequency of Δ*ctb-1* via droplet digital PCR (ddPCR, henceforth). The sequence context of the other mtDNA mutations in line 1G were not suitable for designing reliable ddPCR probes and the frequency of these mutations was estimated from peak heights in chromatograms generated by Sanger sequencing.

Droplet digital polymerase chain reaction to estimate the frequency of Δctb-1 and mtDNA copy number

We used ddPCR to determine the frequency of the Δ*ctb-1* mitotype, and the relative copy number of Δ*ctb-1* and WT mtDNA. We refer to the mitochondrial alleles present in the ancestral control of our MA lines as WT alleles in this study. Bio-Rad ddPCR probes targeted a sequence within the *ctb-1* deletion, a region of *cox-1*, and a conserved region of the second exon of *actin-2* (supplementary material available online, https://royalsocietypublishing.org/doi/suppl/10.1098/rstb.2019.0174, table S1). To determine the degree of heteroplasmy, a single L4 worm was lysed in 5 µl worm lysis buffer (90 µl 10×PCR buffer + 10 µl 10 mg ml^{-1} proteinase K). The single worm lysate was diluted 1:5 in molecular grade water and 2.2 µl of the diluted worm lysate was added to 19.8 µl of ddPCR master mix, which included both *ctb-1* and *cox-1* Bio-Rad Digital PCR assays in a single multiplexed PCR reaction. In an adjacent well, the *actin-2* Bio-Rad Digital PCR assay was performed on the same single worm lysate to measure the concentration of nuclear genomes in the sample. The fluorescin (FAM) probe in the *ctb-1* assay only hybridizes to the WT mtDNA whereas the hexachlorofluorescin (HEX) probe in the *cox-1* assay hybridizes to both Δ*ctb-1* and WT mtDNA in the sample. Heteroplasmic frequency was determined by subtracting the concentration (copies μl^{-1}) of WT mtDNA in the sample from the total mtDNA concentration and dividing it by the total:

$$f(\Delta\text{mtDNA}) = \frac{\text{total mtDNA concentration} - \text{WT mtDNA concentration}}{\text{total mtDNA concentration}}$$

This quantity was then compared to the nuclear DNA concentration to determine relative mtDNA copy number per cell. Droplets were generated using the BioRad Automated Droplet Generator. Droplet generation was considered successful if more than 7000 droplets were generated. Subsequently, the PCR droplets were read on a BioRad QX200 Droplet Reader and droplet distribution was analyzed by the automated threshold setting in QUANTISOFT and inspected visually. The FAM probe used for the *ctb-1* WT is slightly more efficient than the HEX probe used for *cox-1*. As a result, when *C. elegans* N2 DNA is used as a template for these ddPCR reactions, the heteroplasmic Δ*ctb-1* are negative (−0.099, s.d. = 0.028). This is owing to the fact that the heteroplasmy frequency was calculated by subtracting the frequency of *ctb-1* WT from that of *cox-1*.

Estimating the frequencies of heteroplasmic mutations in nd5 and tRNA-Asn

The intracellular frequencies of *nd5* and *tRNA-Asn* mutations were determined from Sanger sequencing. The following primers were used to sequence the region of nd5 that contained three previously detected mutations: forward, 5'-TCATCTTCATCTTGG GAGGATTT-3' and reverse, 5'-GTGTCCTCAAGGCTACCACC-3'. The peak heights at heteroplasmic sites were measured from sequencing chromatograms using ImageJ. For the *nd5* nonsynonymous mutation at mtDNA:12,304, the height of the mutant allele peak T_{mut} and the height of the WT allele peak C_{wt} were used to estimate the frequency of mtDNA containing the nonsynonymous mutation as follows:

$$f(\text{nonsynonymous}) = \frac{T_{mut}}{T_{mut} + C_{wt}}$$

The same approach was used to calculate the frequency of the *tRNA-Asn* base substitution at mtDNA:1679.

For the $T_8 \rightarrow T_9$ frameshift mutation at mtDNA:11,778, the heteroplasmy frequency was determined from the average of two sites. The sequence context at the boundaries at the end of the homopolymeric run and the downstream nucleotides is *TAG* and we used the first *T* + *A* and *A* + *G* in the chromatograms to determine the frequency as follows:

$$f(T_8 \rightarrow T_9) = \frac{\left(\frac{T_9}{A_1 + T_9}\right) + \left(\frac{A_2}{A_2 + G_1}\right)}{2}$$

where T_9 is the *T* in the first double peak, A_1 is the *A* in the first double peak, A_2 is the *A* in the second double peak and G_1 is the *G* in the second double peak. When the $T_8 \rightarrow T_{10}$ insertion is present in addition to the $T_8 \rightarrow T_9$ insertion, the following calculations were performed to calculate the frequencies of both $T_8 \rightarrow T_9$ and $T_8 \rightarrow T_{10}$ mutations as follows:

$$f(T_8 \rightarrow T_9) = \frac{A}{A + G + T_{10}}$$

and

$$f(T_8 \rightarrow T_{10}) = \frac{T_{10}}{A + G + T_{10}}$$

where *A*, *G* and T_{10} are the corresponding bases in the first triple peak downstream of the insertion.

A forward primer (5'-GGT GTT ACA GGG GCA ACA TT-3') within the region that is deleted in *ctb-1* and a reverse primer (5'-GTG TCC TCA AGG CTA CCA CC-3')

downstream of the *nd5* missense mutation amplified a 7,470 bp region of the non-deletion-bearing mtDNA to test if any of the *nd5* mutations were associated with the WT *ctb-1*. PCR was performed using Promega GoTaq Long PCR reagents. Gel purified (QIAEXII Gel Extraction Kit) PCR products were used to reamplify the *nd5* region (forward primer: 5'-TCA TCT TCA TCT TGG GAG GAT TT-3', reverse primer: 5'-GTG TCC TCA AGG CTA CCA CC-3') for sequencing. Similarly, a forward primer (5'-ATC AAT TGC CCA AAG GGG AGT-3') upstream of the *tRNA-Asn* mutation and a reverse primer (5'-TGG CCC TCA AAT TGG AAT AA-3') within the *ctb-1* deletion amplified a 3,435 bp region to test if the *tRNA-Asn* mutation was associated with the WT *ctb-1*. Gel purified PCR products were sequenced using the *tRNA-Asn* forward primer and a *tRNA-Asn* reverse primer. DNA sequencing of *nd5* and *tRNA-Asn* was done on 1G worms sampled at every time point during the original MA experiment, and at the beginning and termination (generation 75) of the experimental evolution in large populations. Sanger sequencing was performed by Eton Biosciences.

Sequestering the Δctb-1-bearing mtDNA in a wild- type background

In order to assess the fitness effects and population dynamics of Δ*ctb-1*-bearing mtDNA relative to WT mtDNA, we first isolated the mitochondria of line 1G in a WT nuclear background, free of other nuclear mutations that arose in line 1G during the MA procedure. This was accomplished by crossing 1G hermaphrodites to males belonging to a line bearing a mutation in the nuclear *fog-2* gene. In WT *C. elegans*, hermaphrodites have two X chromosomes and males have one X chromosome.

The *fog-2* gene functions in a pathway responsible for sperm production in hermaphrodites. Hence, a *fog-2* loss-of-function [*fog-2(lf)*] mutation turns XX individuals that would have been hermaphrodites into functional females only capable of reproduction via outcrossing with males. After two generations of crosses to males of the mutant *fog-2* strain, XX individuals were rendered homozygous for the *fog-2(lf)* and therefore incapable of self-fertilizing. This conversion of XX selfing hermaphrodites into obligate outcrossing females facilitated subsequent outcrossing with males bearing a WT nuclear genome. Commencing with the F3 generation, females with Δ*ctb-1*-bearing mtDNA were subjected to 11 additional generations of backcrosses to *fog-2(lf)* males with a WT (non-MA) nuclear background during which the contribution of the nuclear DNA of the MA line was reduced by half in each generation (supplementary material available online, https://royalsocietypublishing.org/doi/suppl/10.1098/rstb.2019.0174, figure S1). Finally, backcrossed females with Δ*ctb-1*-bearing mtDNA were backcrossed with WT N2 males in the last two generations (generations 14 and 15), thereby replacing the WT *fog-2* allele in the females and restoring them to functional hermaphrodites with the ability to self-fertilize. After 15 generations, the proportion of the nuclear DNA from the original 1G line is estimated to be 0.5^{15} of the total nuclear DNA, or approximately 3×10^{-5}, which virtually removes all other nuclear mutations that arose during MA. This backcrossing experiment yielded six replicate lines comprising worms with the Δ*ctb-1*-bearing mtDNA from line 1G in a WT nuclear background. These six lines (1G.C, 1G.L, 1G.M, 1G.N, 1G.T and 1G.U) were cryogenically preserved at −80°C.

Assays for four fitness-related traits

The fitness effects of Δ*ctb-1*-bearing mtDNA from line 1G were assayed in the six 1G lines harboring the mutant DNA in a WT nuclear background relative to WT N2 controls. Frozen stocks of the six experimental WT backcrossed 1G lines (1G.C, 1G.L, 1G.M, 1G.N, 1G.T and 1G.U) and the N2 control line were thawed and one and three individuals, respectively, were selected and expanded into 15 replicates to establish within-line replication (n = 90 and 45 worms for the 1G and N2 lines, respectively). The 15 Δ*ctb-1*-bearing hermaphrodites from each of the generated 1G lines (n = 90) were assayed for four fitness-related traits (productivity, survivorship to adulthood, developmental time and longevity) and compared to WT N2 nematodes (n = 45) using standard *C. elegans* protocols (Katju et al. 2015; Lee et al. 2016; Katju et al. 2018). These 135 lines (90 Δ*ctb-1*- bearing and 45 N2 control) were then maintained by transferring single L4 (fourth larval stage) hermaphrodite individuals for two additional generations to remove environmental effects (maternal and grandmaternal). A single third-generation descendant from each thawed replicate was subsequently employed in the actual fitness assay. For logistic purposes, the fitness assays were performed in three rounds, each with two of the Δ*ctb-1*-bearing lines (n = 30) and an ancestral N2 control (n = 15). All assays were performed under benign laboratory conditions at 20°C, an optimal temperature for *C. elegans* growth. A schematic of the design of the four fitness assays is presented in supplementary materials available online (https://royalsocietypublishing.org/doi/suppl/10.1098/rstb.2019.0174, figure S2).

To assay survivorship to adulthood (also referred to as survivorship), 10 L1 (first larval stage) progeny of each third-generation hermaphrodite were randomly selected upon hatching and isolated on a separate 35 mm nematode growth medium (NGM) Petri dish seeded with an *Escherichia coli* OP50 lawn; then 36 h after isolation, the number of individuals surviving past the L4 larval stage to reach adulthood were quantified. Survivorship values can range from 0 to 1, and were calculated by dividing the number of adult worms by the number of L1 larvae originally sequestered (Katju et al. 2015; Katju et al. 2018).

To measure productivity, a single worm, a full sibling of the 10 individuals assayed for survivorship, was randomly selected as an L4 larva and transferred to a new 35 mm NGM Petri dish seeded with an *E. coli* OP50 lawn. Every 24 h ± 30 min thereafter, each hermaphrodite being assayed was transferred to a fresh Petri dish over 8 days after reaching the L4 (last) larval stage. Transfers were terminated if the worm was found dead prior to the completion of these 8 days. Following each daily transfer of the assayed individuals, plates with eggs were placed at 20°C for an additional 24 h period to enable hatching. To enable progeny counts, the plates were then stored at 4°C to kill the progeny larvae. Progeny were counted by staining the agar pad and *E. coli* lawn with a 0.075% water dilution of toluidine blue, which rendered the dead worms transparent and visible on the contrasting purple background for the approximately 2-5 min period required for counting. Productivity was calculated as the total number of progeny produced; non-reproductive individuals were scored as having zero productivity (Katju et al. 2015; Katju et al. 2018).

The single worm assayed for productivity above was additionally used to measure developmental time. Following its sequestration as a lone L4 larva onto a seeded Petri dish, the worm was visually inspected under a dissecting scope every 2 h. The hermaphrodite was determined to be an adult hermaphrodite if it had: (i) undergone its L4 larval molt, (ii) had a developed vulva, and (iii) displayed at least one developed egg in the uterus. Developmental time was calculated as the number of hours it took a newly-hatched L1 larva to reach adulthood (Lee et al. 2016).

We measured longevity (number of days) on the same worm that was assayed for productivity and developmental time. After day 8 of egg laying, the worms were transferred to a new 35 mm NGM plate seeded with OP50 for a longevity assay. Each day thereafter, these nematodes that had largely ceased egg production were visualized under the dissecting scope until mortality. A nematode was determined to be dead if it was no longer locomoting, did not respond to gently tapping the plate or agar, did not respond to gentle prodding of the tail with a pick and had no pharyngeal activity. Longevity was measured as the total number of days from a newly-hatched L1 larva to mortality.

Relative fitness values for three traits (productivity, survivor- ship to adulthood and longevity) were generated by assigning the mean absolute fitness value of the WT N2 control a value of 1 (n = 45). Fitness measures for these three traits were standardizing by dividing a replicate line's observed fitness value by the mean fitness value of the WT N2 control to yield relative fitness values. Developmental rate was expressed as the inverse of the relative developmental time.

Competition experiments

Stocks of five experimental replicate *C. elegans* lines bearing the Δ*ctb-1* mtDNA in a WT nuclear background (1G.C, 1G.L, 1G.N, 1G.T and 1G.U) were thawed along with WT N2 worms. Worms were picked from each thaw and placed on separate 60 mm NGM plates with *E. coli* OP50 seed. A single worm from the progeny of each thaw was transferred for two generations to remove potential freezer effects. The F3 generation worms were used to initiate an experimental evolution study to investigate the population dynamics of Δ*ctb-1*-bearing lines under competitive and non-competitive conditions.

For each of the five experimental lines (1G.C, 1G.L, 1G.N, 1G.T and 1G.U), we established two populations, one competitive and one non-competed control. Hence, the competition experiment comprised 10 populations in total (five competition and five non-competed controls) (supplementary material available online, https://royalsocietypublishing.org/doi/suppl/10.1098/rstb.2019.0174, figure S3). Each competition population was initiated by adding 50 L4 hermaphrodites from a Δ*ctb-1*-bearing experimental line and 50 L4 worms from the WT N2 stock onto a 100 mm NGM plate seeded with an *E. coli* OP50 lawn (1 ml), for a total population size of $n = 100$ worms with Δ*ctb-1* and WT mtDNA-bearing worms in equal frequencies. In addition, we established five non-competed control populations by transferring 50 L4 hermaphrodites from a Δ*ctb-1*-bearing experimental line in isolation onto a fresh 100 mm NGM plate. In summary, the first generation (generation 0 in supplementary

material available online, https://royalsocietypublishing.org/doi/suppl/10.1098/rstb.2019.0174, figure S3) of the competition lines comprised an equal ratio of Δ*ctb-1* mtDNA: WT mtDNA worms whereas the non-competed control lines were established with 100% Δ*ctb-1* mtDNA worms. A standard *C. elegans* bleaching protocol was used to synchronize the evolving populations at the first larval stage (L1) of each generation and ensure that adult worms from a previous generation did not continue to contribute to the gene pool across multiple generations. Four days after L4 worms were placed onto a fresh plate to establish a new generation, each plate was bleached with a 30% bleach and 15% 5M NaOH solution. Bleaching killed living worms but rendered eggs unharmed. The eggs that survived the bleach were re-plated onto new 100 mm NGM plates with OP50 to establish the next generation. The competition experiment was conducted over 16 consecutive generations (supplementary material available online, https://royalsocietypublishing.org/doi/suppl/10.1098/rstb.2019.0174, figure S3).

To determine the population frequencies of the Δ*ctb-1*-bearing and WT mtDNA haplotypes on each plate in each generation, we randomly selected 30 L4 worms for genotyping from each of the 10 experimental plates (five competition and five non-competed controls). The worms were added to worm lysis buffer (10× PCR buffer and proteinase K) and the digests were used in single-worm PCR with *cytb-1* primers to assess the presence/absence of the Δ*ctb-1* mitotype. The *ctb-1* forward and reverse primers are 5'-TAG CAT TTT CAA CAG TGC AG-3' and

5’-CGC AAA ATT GCA TAA CTC AAA T-3’, respectively. The expected WT and Δ*ctb-1* PCR products are 661 and 162 bp in length, respectively. The PCR products were run on a 1% agarose gel (100 ml 1× tris-acetate-EDTA; 1 g RA agarose; 1 µl GelRed) at 105 V for 30 min.

In addition, large populations that were established from replicate lines 1G.C, 1G.N, 1G.T and 1G.U were maintained on 100 mm NGM plates seeded with an *E. coli* OP50 lawn (1 ml) for 75 generations and maintained in the same manner as that outlined for the competed and non-competed lines. At generations 0, 30 and 75, a random sample of 15 individuals were used to determine the frequency of Δ*ctb-1* and relative mtDNA copy number in individual worms by ddPCR. The frequency results were analyzed in a two-way ANOVA after arcsine transformation. The Pearson correlation coefficient between relative copy numbers of Δ*ctb-1* and WT *ctb-1* were calculated for these 15 individuals per line at each of the three time-points.

Estimating the relative fitness of Δ*ctb-1*-bearing *mtDNA from competition experiments*

The composite relative fitness, *w*, of the Δ*ctb-1* mitotype was calculated from its average frequency pooled across the competition experiments comprising the five replicate lines across generations. First, the log of the ratio (p/q) in each generation t was calculated, where p equals the average frequency of the Δ*ctb-1* mitotype, and q equals the average frequency of the WT *ctb-1* allele. The log ratio of p/q was mapped as a function of generation and linear regression was performed on the data. The slope of the

regression line, *b*, equals log(*w*). Hence, the relative fitness, *w*, was calculated as 10^b where *b* represents the slope of the $\log(p/q)_t$ over *t* generations.

Role of selfish drive versus genetic drift in the proliferation of the Δctb-1 mitotype within individuals

To test if the Δ*ctb-1* mitotype's rapid increase in frequency was owing to selfish drive or genetic drift, we first performed directional selection for a lower frequency of Δ*ctb-1*. From each of the populations at generation 75 (1G.C, 1G.N, 1G.T and 1G.U), five L4 hermaphrodites were transferred to individual 35 mm NGM plates seeded with OP50. After allowing 2 days for egg-laying, these adult (parent) nematodes were subsequently genotyped by single-worm PCR using primers for *ctb-1*. Five progeny of one parent per line that produced the strongest WT PCR product were used to establish the next generation. After five rounds of selection for a Δ*ctb-1* PCR product of reduced intensity, the offspring of a single individual from line 1G.T with a low frequency of the Δ*ctb-1* mitotype (37%) were used to establish 25 lines that were propagated by picking a single L4 hermaphrodite at random in each generation to establish the next generation. After six generations of propagating 25 lines by single-progeny descent, single-worm ddPCR was used to determine the frequency of the Δ*ctb-1* mitotype.

Results

Appearance and proliferation of the Δctb-1 mitotype as a heteroplasmy during mutation accumulation

A 499 bp frameshift deletion in *ctb-1* arose during a spontaneous MA experiment in *C. elegans* and was detected via whole-genome sequencing at the termination of the MA experiment (figure 2.1a) (Konrad et al. 2017). The frequency of the deletion within individuals of this particular MA line (1G) was estimated to be 96%. The deletion encompassed approximately 45% of the *ctb-1* gene (figure 2.1b). Hence, not only does this Δ*ctb-1* allele have the potential to result in a truncated protein product with no residual function, it may also generate frameshifted transcripts leading to altered proteins. Specifically, this Δ*ctb-1* allele is predicted to produce a 106 aa peptide, whereas the original WT CTB-1 protein comprised 370 aa, owing to the introduction of a stop codon downstream of the deleted segment.

We screened previously cryopreserved stocks of MA line 1G at several time-intervals of the MA experiment via PCR and ddPCR to determine: (i) the approximate timing of origin of the Δ*ctb-1* mitotype, and (ii) the change in its frequency within line 1G during the course of the MA experiment. The Δ*ctb-1* mitotype was not detected in worms at MA generation 25, but was present at 7% frequency by MA generation 51. Its frequency rose rapidly until it had reached 90% by MA generation 91. Following MA generation 91 and until MA generation 364, its frequency remained high, fluctuating between 80% and 98% (figure 2.2).

Additional high-frequency mtDNA mutations in mutation accumulation line 1G originated after Δctb-1

Following the origin of the Δ*ctb-1* allele in line 1G, an insertion of a single *T* nucleotide in *nd5* was detected in 26% frequency in a run of 8*T*s at location 11,778 by MA generation 90 and subsequently reaching a frequency of 81% by MA generation 137 (figure 2.2). This single *T* insertion in *nd5* remained in high frequency at MA generations 157 and 221, with an estimated frequency of 78% at both time-points. However, when a second *T* insertion had appeared at the same site by MA generation 300, the single *T* mutation declined in frequency until it had been largely replaced by the double *T* insertion. The combined frequencies of the single and double *T* insertion at this site were 86% and 92% in MA generations 300 and 346, respectively. In addition to these insertions, a nonsynonymous mutation in *nd5* had reached a frequency of 38% by generation 137 (figure 2.2). This mutation also reached high frequency and fluctuated around 90% from generation 222 until the end of the MA experiment. Based on their high frequencies, it seemed likely that these mutations were on the same molecule as the Δ*ctb-1* mutant allele and not linked to the low frequency *ctb-1* WT mtDNA. We tested this assumption by first performing PCR with one primer within the deleted *ctb-1* sequence and a reverse primer downstream of the *nd5* mutations, followed by Sanger sequencing of *nd5*. The PCR product only contained sequence from the *ctb-1* WT allele. At each time-point analyzed in the MA experiment, and in each experimental population established with the mtDNA from MA line 1G, the *ctb-1* WT allele is associated with the *nd5* WT allele. Similarly, the *nd5* mutations were associated with the Δ*ctb-1* mutant

allele and we found no evidence of recombination between the *ctb-1* WT and Δ*ctb-1* molecules. In addition to these mutations that persisted in the mtDNA genome of line 1G until the end of the MA experiment, a *T* insertion at site 11,722 within the *nd5* gene was detected at 41% frequency in MA generation 137 but subsequently went extinct (figure 2.2). A single nucleotide insertion at this site occurred in multiple independent lines during the original MA experiment, suggesting that it is a mutational hotspot (Konrad et al. 2017) The intracellular frequencies of the *nd5* mutations in this study were primarily assessed via Sanger sequencing, but their frequencies can be compared to those previously obtained by whole-genome Illumina sequencing from the end of the MA experiment (Konrad et al. 2017). The single and double *T* insertions were estimated to be at 14% and 78% frequency by Sanger sequencing, respectively, but at 3% and 70% by Illumina sequencing. The nonsynonymous *nd5* mutant allele was estimated at 91% and 94% frequency by Sanger and Illumina sequencing, respectively. In addition to mutations in *ctb-1* and *nd5*, whole-genome sequencing of MA lines had identified a *tRNA-Asn* mutation with 13% frequency in line 1G (Konrad et al. 2017). Based on Sanger sequencing, this mutation was in 8% frequency at the end of the MA experiment, and at 5% at MA generation 300. There is no evidence of this mutation prior to MA generation 300. Sanger sequencing of PCR products from the WT *ctb-1* molecule, which used a reverse primer to the deleted region in *ctb-1* and a forward primer upstream of *tRNA-Asn*, only yielded a WT *tRNA-Asn* sequence. We conclude that the Δ*ctb-1* mutant allele is linked to other mutations in *nd5* and *tRNA-Asn*, which arose sequentially after

the original *ctb-1* deletion, and there is no evidence of recombination between any of these mutations in the mitochondrial genome of line 1G or its derivatives.

Δ*ctb-1-bearing mtDNA engender a significant fitness cost*

In order to test the fitness effects of Δ*ctb-1*-bearing mtDNA relative to WT mtDNA, the mutant mitochondria were sequestered in a WT N2 genetic background, free of other nuclear mutations that arose during MA within line 1G (supplementary material available online, https://royalsocietypublishing.org/doi/suppl/10.1098/rstb.2019.0174, figure S1). Four fitness traits, namely productivity, survivorship to adulthood, longevity and developmental time were measured in six lines (1G.C, 1G.L, 1G.M, 1G.N, 1G.T, 1G.U) harboring the Δ*ctb-1* mtDNA from line 1G in a WT N2 nuclear background (supplementary material available online, https://royalsocietypublishing.org/doi/suppl/10.1098/rstb.2019.0174, figure S2; table 2.1). The Δ*ctb-1*-bearing worms varied significantly from the WT mtDNA lines with respect to all of the four fitness traits assayed (figure 2.3; supplementary material available online, https://royalsocietypublishing.org/doi/suppl/10.1098/rstb.2019.0174, table S2).

Δ*ctb-1*-bearing lines exhibited a significant decline in productivity relative to the WT N2 control (figure 3; Wilcoxon rank sum, $z = 8.88$, d.f. = 1, $p < 0.0001$). The mean productivity of 109 offspring per hermaphrodite in Δ*ctb-1*-bearing lines is only 35% of the 311 offspring produced by the WT N2 control. Mean relative productivity of the

Δ*ctb-1*-bearing lines ranged from 28% (lines 1G.M and 1G.N) to 55% (line 1G.T) of the average WT productivity. There was no significant difference in the mean productivity of the six individual 1G lines bearing the Δ*ctb-1* mitotype (table 2.1; Wilcoxon/ Kruskal-Wallis, $\chi 2 = 8.47$, $p = 0.13$).

Δ*ctb-1*-bearing lines exhibited a significant decline in survivorship to adulthood relative to the N2 control (figure 2.3; Wilcoxon rank sum, z = 4.11, d.f. = 1, $p < 0.0001$). The mean survivorship of Δ*ctb-1*-bearing and N2 control worms is 90% and 99%, respectively. Hence, Δ*ctb-1*-bearing worms have a relative mean survivorship of 92% (8% mean decline) compared to WT worms. Mean survivorship of the Δ*ctb-1*-bearing lines ranged from 77% (line 1G.N) to 96% (lines 1G.L, 1G.M, 1G.T and 1G.U) of the average WT survivorship. There was a significant difference in the mean survivorship of the six individual 1G lines bearing the Δ*ctb-1* mitotype (table 2.1; Wilcoxon/Kruskal-Wallis, $\chi 2 = 12.79$, $p = 0.026$), with lines 1G.C and 1G.N in particular having lowered survivorship of 77-88% relative to the N2 control.

There was a significant reduction in the developmental rate of Δ*ctb-1*-bearing lines versus the N2 control (figure 2.3; Wilcoxon rank sum, z = 5.1, d.f. = 1, $p < 0.0001$). Δ*ctb-1*-bearing worms took, on average, 6.3 h longer than WT to lay their first fertilized egg, representing an average 13.7% increase in the time taken to reach reproductive maturity. Δ*ctb-1*-bearing lines took 2-27% longer relative to the N2 control to reach reproductive maturity. There was a significant difference in the mean developmental time of the six individual 1G lines bearing the Δ*ctb-1* mitotype (table 2.1; Wilcoxon/Kruskal-Wallis, $\chi 2 = 34.19$, $p < 0.0001$).

The longevity of Δ*ctb-1*-bearing lines was significantly lower than that of the N2 control (figure 2.3; Wilcoxon rank sum, z = 2.54, d.f. = 1, $p = 0.011$). On average, the lifespan of Δ*ctb-1*-bearing worms was approximately 3 days shorter relative to the N2 control, representing an average 19% decrease in the former. The mean longevity of Δ*ctb-1*-bearing lines ranged from 71-88% of the N2 control's mean longevity. However, there was no significant difference in the mean longevity of the six individual 1G lines bearing the Δ*ctb-1* mitotype (table 2.1; Wilcoxon/Kruskal-Wallis, $\chi 2 = 1.42$, $p = 0.92$).

Rapid extinction of Δctb-1 when competed with wild-type mtDNA

A competition assay was performed to test the fitness of the Δ*ctb-1* mitotype in the replicate 1G lines when in competition with the WT N2 mtDNA. Five replicate 1G lines with the Δ*ctb-1*-bearing mtDNA in a WT nuclear background (1G.C, 1G.L, 1G.N, 1G.T, 1G.U) were competed against WT N2 worms in a mixed population commencing with equal frequencies of deletion-bearing and WT mtDNA worms (supplementary material available online, https://royalsocietypublishing.org/doi/suppl/10.1098/rstb.2019.0174, figure S3). All five competition populations showed a steep decline in the frequency and rapid extinction of Δ*ctb-1* mtDNA across successive generations of competition with worms bearing WT mitochondria (figure 2.4a). The frequency of Δ*ctb-1*-bearing worms had fallen below levels of detection in all populations by the eighth generation (figure 2.4a). The competition experiment was continued until generation 16, with 30 individuals sampled

from each population in every generation, but no individuals were detected as harboring the Δ*ctb-1* mitotype from generations 9-16.

The five replicate Δ*ctb-1*-bearing 1G lines were also used to establish large populations that were maintained in parallel to the competition experiment, but without any WT N2 worms. In these non-competed populations, the Δ*ctb-1* was never observed to go extinct (figure 2.4a). This suggests that the decline in the population frequency and eventual loss of Δ*ctb-1* under competitive conditions was owing to the substantially lower fitness of Δ*ctb-1*-bearing worms relative to WT, and not because of the loss of the Δ*ctb-1* mitotype within worms that contained the deletion at the beginning of the experiment.

The relative fitness reduction associated with the Δ*ctb-1* mitotype was also calculated from its average frequency pooled across the five replicate competition populations across generations. First, the log of the ratio (p/q) in each generation t was calculated, where, p and q equal the average frequency of the Δ*ctb-1* and WT *ctb-1* mitotype, respectively. The log ratio of p/q was mapped as a function of generation and linear regression was performed on the data (figure 2.4b). The slope of the regression line, b, was determined to be −0.3174, which yielded a relative fitness (w) value of 0.4815. Hence, the overall competitive fitness of Δ*ctb-1*-bearing worms is only 48% of worms with WT mitochondria. A negative selection coefficient of approximately 0.52 (52%) represents an extremely significant fitness cost for Δ*ctb-1*-bearing worms.

Frequency of Δctb-1 declines with time in large populations

Four Δ*ctb-1*-bearing lines (1G.C., 1G.N, 1G.T and 1G.U) were maintained as large populations for 75 generations. The initial average frequency of the heteroplasmic Δ*ctb-1* in these worms was 93.4% (figure 2.5). There was a slight, but significant, difference in the frequency of the heteroplasmic Δ*ctb-1* between the lines at the beginning of their evolution in large populations (ANOVA, $F = 11.07$, $p < 0.0001$). At the lower end of the spectrum, 1G.U and 1G.T had the Δ*ctb-1* mitotype in 91 and 92% frequency, respectively. At the higher end of the spectrum, the Δ*ctb-1* mitotype in 1G.C and 1G.N was at 95 and 96% frequency, respectively. We additionally determined the frequencies of four additional heteroplasmies in these four 1G-derived lines after their mutant mtDNA genomes were sequestered in a WT nuclear background. The single *T* insertion heteroplasmy in *nd5* in these experimental lines at the start of this experiment ranged from 13% to 24% with an average frequency of 20%. The frequency of the double *T* insertion heteroplasmy in *nd5* in these experimental lines ranged from 67% to 74% with an average frequency of 70%. The combined frequencies the single and double T insertions at this site ranged from 87% to 93% with an average of 90%. The frequency of the nonsynonymous mutation heteroplasmy in *nd5* ranged from 83% to 91% with an average frequency of 86%. Lastly, the base substitution in *tRNA-Asn* ranged from 0% to 17% with an average of 11% across the 1G-derived lines.

In the absence of worms homoplasmic for WT mtDNA, the frequency of Δ*ctb-1* within lines initially appeared to be stable at high frequency. After 30 generations at large population size, the average frequency in all four lines remained above 90%, with

an average of 93%. However, by generation 75, the average frequency of the heteroplasmic Δ*ctb-1* mitotype had declined to 74% (two-way ANOVA, generation effect: $F = 85.49$, $p < 0.0001$). In addition to the decline in the average frequency of the heteroplasmic Δ*ctb-1* mitotype in these populations, there was an increase in the variation in frequency of Δ*ctb-1* between individuals within lines. The standard deviation in the frequency of Δ*ctb-1* within the four populations at the beginning (generation 0) ranged from 1.3% to 3.8%, with an average of 2.7%. By generation 30, the average within-population standard deviation had increased slightly to 4.8% but was 14.8% by generation 75. The gradual increase in the within-population variation might explain why the frequency of the strongly deleterious Δ*ctb-1* mitotype declines very slowly at first. The efficiency of selection was probably impeded in the early generations of these populations because there was insufficient variation in the frequency of Δ*ctb-1* between individuals and hence, insufficient variation in fitness. As the population-level variation increased with time, so did the variation in fitness and subsequently, the reduction of Δ*ctb-1* mitotypes.

The frequencies of the three additional heteroplasmies in *nd5* (single *T* insertion, double *T* insertion and non-synonymous mutation) showed similar decline as the Δ*ctb-1* mutant after propagation at large population sizes over 75 generations. The average frequency of the nonsynonymous mutation declined to 70% and the combined frequency of the single and double *T* insertions was estimated to be at 77%. Interestingly, the frequency of the double *TT* insertion exhibited the greatest decline to 57%, whereas the

frequency of the single *T* insertion was virtually unchanged at 20%. In addition, the low frequency *tRNA-Asn* mutant went extinct in each of the four large populations.

mtDNA copy number was elevated in some, but not all Δctb-1-bearing lines

Previous work has shown that the mtDNA copy number is frequently elevated in individuals that are heteroplasmic for a mitochondrial gene deletion (Tsang and Lemire 2002; Gitschlag et al. 2016; Lin et al. 2016). This increase in mtDNA copy number is probably the result of compensatory mechanisms that cells resort to when their respirational demands are not being met (Lin et al. 2016). After backcrossing the Δ*ctb-1* mitochondrial genome into a WT nuclear background, four independently backcrossed lines were tested for mtDNA copy number. Immediately following the backcrossing regime, two of these lines, 1G.C and 1G.N, had elevated mtDNA copies compared to control lines with WT mitochondria (generation 0; figure 2.6; one-way ANOVA: F = 6.25, p = 0.0003). The average mtDNA copy number increase for lines 1G.C and 1G.N was 60% and 47%, respectively. By contrast, the total mtDNA copy number was not elevated in lines 1G.T and 1G.U relative to WT mitochondria. Lines 1G.T and 1G.U also had a slightly lower frequency of Δ*ctb-1*, but perhaps more importantly, they had almost two times (1.93×) higher frequency of the WT mitochondrial genome. On average, lines 1G.T and 1G.U also appeared to perform better in the fitness-related traits assays (table 2.1).

There was no significant change in mtDNA copy number in the large populations by generation 30 (two-way ANOVA, generation effect: F = 1.17, p = 0.28). However, by

generation 75, the total mtDNA copy number in lines 1G.C and 1G.N had declined to WT levels. At that stage in the experiment, all four populations that were established as independently WT-backcrossed replicates of the original 1G line had total mtDNA copy numbers indistinguishable from N2 worms with WT mitochondrial genomes (Tukey-Kramer HSD: ancestral control versus 1G.C, $p = 0.27$; ancestral control versus 1G.N, $p = 1.0$; ancestral control versus 1G.T, $p = 0.64$; ancestral control versus 1G.U, $p = 1.0$). The reduction in total mtDNA copy number within these four replicate 1G lines with time could be an adaptation if the cost of increasing the total number of mitochondria is greater than the benefit from increasing the copy number of WT mtDNA.

Strength of correlation between Δctb-1 and wild- type mtDNA copy number weakened with time

There is a significant positive correlation between Δ*ctb-1* and WT mtDNA copy number ($r = 0.42$, $p = 0.001$; figure 2.7a). This correlation may stem from two principal sources. The first source of this correlation could be the compensatory processes that increase mtDNA copy number in response to mitochondrial dysfunction. In the event of a severe reduction of mitochondrial functions, such as would accompany a loss- of-function mutation in the mitochondrial genome, the cells might increase the replication of mtDNA indiscriminately, resulting in an increased copy number of both normal and defective mtDNA genomes. The second potential source is experimental variation that could affect the numbers of mutant and WT mtDNA in the same manner. Although we made every effort to sample individual worms at the same stage of development, it is

possible that there existed some experimental variation in the developmental stage of the worms at the time of analysis, which in turn resulted in variation in mtDNA copy number and a positive correlation between mutant and WT mtDNA copy number. The coefficient of variation (CV) for Δ*ctb-1* and WT mtDNA copy number across both populations and generations was 0.62 and 1.15, respectively. Calculating the CV separately within particular generations or populations does not change this conclusion. This suggests that the variation in Δ*ctb-1* mtDNA copy number was no greater than expected when its higher average copy number was taken into account. Furthermore, we find no evidence that the variation in Δ*ctb-1* mtDNA contributes disproportionally to the variation in total mtDNA copy number as has been previously suggested (Gitschlag et al. 2016).

Within the four Δ*ctb-1*-bearing lines that were evolved at large population size for 75 generations, the strength of the correlation between Δ*ctb-1* and WT copy number declined with time ($r = -0.69$, $p = 0.013$) and had all but disappeared by generation 75 (figure 2.7b). If the correlation between Δ*ctb-1* and WT mtDNA copy number is primarily an artefact of an asynchronous developmental stage of the worm (second explanation suggested in the preceding paragraph), it should exert a similar effect at both generations 0 and 75, which was not observed. The weakening of the correlation with time is, however, consistent with our first hypothesis in the preceding paragraph that the reduction in total mtDNA copy number is owing to adaptive mutations, presumably in the nuclear genome, that disable or reduce the compensatory increase in mtDNA replication in response to mitochondrial dysfunction. Alternatively, by generation 75, the

frequency of Δ*ctb-1* may have fallen below the levels that would trigger a compensatory increase in mtDNA copy number. However, at that stage in the evolution of these heteroplasmic Δ*ctb-1* populations, the Δ*ctb-1* mitotype was still present in high frequency, 74% on average, and the number of WT mtDNA genomes was only a quarter of the numbers observed in homoplasmic WT worms.

Δctb-1 is selfish

We conducted five generations of artificial selection for a reduction in the frequency of Δ*ctb-1*. The average heteroplasmy levels in eight worms that were descended from population 1G.T was 40%, with a range from 23 to 65%. We chose the descendants of an individual with a Δ*ctb-1* frequency of 37%, which was the closest to the mean, to establish 25 independent replicate lines. These 25 lines were maintained by single-progeny descent each generation to maximize the strength of genetic drift and minimize the efficacy of natural selection at the inter-individual level. If the intraindividual population dynamics of the Δ*ctb-1* mitotype are dominated by genetic drift, the changes in its frequency should be random. If there is selection against the Δ*ctb-1* mitotype, its frequency should decline. Conversely, if the Δ*ctb-1* mitotype has a transmission advantage despite its severe fitness cost at the individual level, its frequency should increase. After only six generations of single individual bottlenecks, there existed considerable variation between the 25 lines, with the frequency of Δ*ctb-1* ranging from 23 to 81% (figure 2.8). However, only one of the 25 lines (4%) had a reduced Δ*ctb-1* frequency. The average frequency of Δ*ctb-1* rose to 54%, a significant

increase from the original 37% (Student's: $t = 5.9$, $p < 0.0001$). Assuming that the change in Δ*ctb-1* frequency over time stems from changes in the germline frequency of heteroplasmy rather than fluctuations in Δ*ctb-1* in the somatic tissue, we conclude that Δ*ctb-1* has a transmission advantage over WT mitochondria despite engendering a severe fitness cost at the individual level.

Discussion

A spontaneous MA study in *C. elegans* with varying effective population sizes revealed that mitochondrial mutations predicted to be strongly deleterious reached high frequency within individual MA lines (Konrad et al. 2017). The focal mitochondrial mutations reached a higher frequency in MA lines with the most severe population bottlenecks (n = 1 individual) relative to larger-sized MA lines (n = 10 and 100 individuals), consistent with their detrimental effects on fitness. Specifically, two n = 1 MA lines (of a total 20 lines) possessed high- frequency mtDNA heteroplasmies comprising deletions of protein-coding or tRNA genes. In general, random genetic drift is assumed to be the major evolutionary force enabling the increase in frequency and/or fixation of deleterious mutations. This is especially pertinent in MA experiments, which typically involve passaging populations through severe genetic bottlenecks in order to maximize the effects of genetic drift. In the case of mitochondrial deletions, there is evidence that they can have a transmission advantage despite their serious consequences for the reproductive success of their hosts (Ephrussi et al. 1955; Bernardi 1979; Beziat et al. 1993; Taylor et al. 2002; Tsang and Lemire 2002; Howe and Denver 2008). However, the mechanisms that maintain deleterious mitochondrial mutations in populations are still poorly understood.

In this study, we focused on one of several previously identified spontaneous mitochondrial deletions in our *C. elegans* MA lines (Konrad et al. 2017), namely a high-frequency deletion in the *ctb-1* gene of MA line 1G referred to as the Δ*ctb-1* mitotype. As previously mentioned, the mtDNA genomes of line 1G also possessed two additional

high-frequency heteroplasmies in addition to Δ*ctb-1*, namely a nonsynonymous base substitution and a frameshift mutation in the mtDNA gene, *nd5*. The primary objective of this study was to determine if this mutant mitotype, which contains all three high-frequency heteroplasmic mutations including Δ*ctb-1* in addition to two low frequency mutations, is a selfish genetic element. We found no evidence for recombination between any of the mutations, given that the WT *ctb-1* was always associated with the WT alleles of both *nd5* and *tRNA-Asn*. For reasons explained earlier, we refer to this mutant mitotype as Δ*ctb-1* or Δ*ctb-1*-bearing mtDNA. To qualify as a selfish genetic element, a particular mitotype should have negative or neutral effects on fitness in conjunction with a transmission advantage over other mitochondrial genotypes. A previous whole genome sequencing analysis of MA line 1G (in which the Δ*ctb-1* deletion originated) suggested that at the termination of the MA experiment, an unprecedented 96% of the mtDNA genomes within individuals of this line contained this deletion (Konrad et al. 2017). This mutation frequency seemed extraordinarily high and is likely to be severely deleterious given that approximately 50% of the coding sequence was deleted while simultaneously altering the reading frame of the coding sequence downstream of the deletion. For comparison, two other mitochondrial deletions, *uaDf5* and *mptDf1*, that were discovered in laboratory strains of *C. elegans*, are frequently in 60-80% frequency (Tsang and Lemire 2002; Gitschlag et al. 2016). Herein, we demonstrate that in high frequency, the Δ*ctb-1* mitotype is indeed severely deleterious for each of four assayed fitness-related traits. In this respect, the Δ*ctb-1* mitotype is similar to deletions *uaDf5* and *mptDf1* that have been previously described in *C. elegans*,

resulting in delayed development, reduced productivity, shorter lifespan and lowered survivorship to adulthood (Tsang and Lemire 2002; Liau et al. 2007; Gitschlag et al. 2016). Furthermore, Δ*ctb-1*-bearing worms are rapidly driven to extinction when competed against WT worms. However, we are unable to delineate the specific contribution of each of the five linked mutations comprising the Δ*ctb-1* mitotype to the composite 52% fitness decline. Indeed, one or more mutations may in fact be compensatory in nature. Irrespective, this compensatory role, if present, does not preclude or offset the substantial fitness cost to the worms bearing this mitotype.

Given that *C. elegans* is amenable to long-term cryopreservation, we were offered a unique opportunity to retroactively screen stocks of line 1G frozen at several time-intervals during the progression of the MA experiment and thereby determine the approximate timing of the origin of Δ*ctb-1* and reconstruct its population trajectory over approximately 364 generations of experimental evolution. Δ*ctb-1* first appeared between MA generations 25 and 50, and already existed at a 7% frequency by generation 51. Its rapid proliferation within line 1G is evident by its occurrence at 90% frequency by generation 90. Subsequently, mutations at two different sites in *nd5* also reach high frequency. Given the strongly negative fitness effects associated with this mitotype, combined with the extreme genetic drift that dominates in MA experiments, such a rapid rise could, in principle, be owing to either random drift within the germline of this MA line, or a transmission advantage of the mutant mitochondrial genome. Although the frequency of *Δctb-1* declined under directional selection, its frequency increased once again when selection for its reduction was relaxed. If genetic drift within the germline

was the primary reason for the initial rapid proliferation of the Δ*ctb-1* mitotype in the original MA experiment, we expect the frequency of Δ*ctb-1* to change at random, with no significant net increase or decrease after we relaxed selection for lower abundance. Instead, our results suggest that the Δ*ctb-1* mitotype has a replication or transmission advantage over WT mitochondria. Hence, our data demonstrating (i) strongly deleterious fitness consequences of the Δ*ctb-1* mitotype, and (ii) its transmission advantage over WT mitochondria, together qualify it as a selfish genetic element.

The importance of large population size for the containment of selfish mtDNA has been noted in different species, including yeast (Taylor et al. 2002) and *C. briggsae* (Phillips et al. 2015). In large populations, selection between individuals results in lower abundance of selfish mtDNA. Conversely, at small population size, selection within individuals results in greater abundance of selfish mtDNA. In our experiments comprising large, non-competed populations of the derivatives of line 1G over the course of 75 generations, the frequency of Δ*ctb-1* initially exhibited a very slight decline, but the rate of decline accelerated with time. In the initial stages of the experiment, when the frequency of Δ*ctb-1* was near its maximum whereas that of the WT was near its minimum, the variation in the numbers of mutant and WT mitochondria generated each generation probably did not translate into large differences in fitness between individuals. Increasing variation in the frequencies of Δ*ctb-1* and WT mtDNA with time concomitantly increases variation in fitness, resulting in greater efficiency of selection for individuals with reduced abundance of Δ*ctb-1*. Furthermore, as the frequencies of *Δctb-1* and WT become more equal, random partitioning of mitochondria

into eggs generates greater variation in the numbers of *Δctb-1* and WT within individuals than when *Δctb-1* was high. Subsequently, this engenders greater variation in fitness. It is currently unclear if Δ*ctb-1* would have reached an equilibrium frequency owing to the opposing forces of individual and within-individual selection, or if it would continue to decline until the Δ*ctb-1* mitotype became extinct. If there is a real threshold level below which detrimental mitochondria are selectively neutral, Δ*ctb-1* might also persist in the populations until it is eventually lost by genetic drift.

An upregulation of mtDNA copy number has been suggested to play a role in the proliferation of mutant mitochondrial genomes (Gitschlag et al. 2016; Lin et al. 2016). Although we observe an increase in mtDNA copy number in some replicate lines of 1G, this was not apparent in other lines that contained the same Δ*ctb-1* deletion in high frequency. There was a correlation between mutant and WT mtDNA quantity, which can be interpreted as the result of a nonspecific increase in mtDNA. That is, the mechanisms responsible for an increase in mtDNA do not discriminate between Δ*ctb-1* and WT and generically increase total mtDNA copy number. This interpretation is also supported by comparing the variation in the copy numbers of Δ*ctb-1* and WT mtDNA. If the increase in mtDNA is preferentially for the Δ*ctb-1* mtDNA while WT mtDNA was tightly regulated, we would expect greater variation in Δ*ctb-1* mtDNA between individuals and lines, as Δ*ctb-1* mtDNA would increase disproportionately. Although Δ*ctb-1* mtDNA did indeed exhibit greater variation, we found no significant differences in the CV between Δ*ctb-1* and WT mtDNA. It appears that this greater variation in Δ*ctb-1* is a function of a greater average number of Δ*ctb-1* than WT mtDNA per individual.

Within the large, non-competed populations of line 1G replicates evolved for 75 generations, there was selection for a lower frequency of the Δ*ctb-1* mitotype, but also an opportunity for compensatory evolution to mitigate the deleterious consequences of Δ*ctb-1*. During evolution in these large populations, the total mtDNA copy number dropped to levels that are typical of the WT N2 control. Furthermore, the correlations between Δ*ctb-1* and WT mtDNA were no longer significant after 75 generations, even though the average frequency of Δ*ctb-1* remained fairly high, at 74%. It is possible that the frequency of the Δ*ctb-1* mitotype had dropped to levels that did not stimulate a compensatory increase in mtDNA copy number. However, it is also possible that the lack of compensatory increase in mtDNA is itself adaptive. For example, the increased investment in mitochondria may be too costly and generate too little return on the investment, so that an increase in mtDNA copy number instead contributes to the fitness cost of the Δ*ctb-1* mitotype.

Mitochondrial mutations contribute to a multitude of age-related and degenerative diseases and understanding the persistence and proliferation of deleterious mtDNA variants could provide new ways to target and treat their debilitating effects (Ross et al. 2013; Hudson et al. 2014; Pinto and Moraes 2015). Furthermore, the sources of genetic conflict between the nuclear and mitochondrial genomes also have implications for the evolution of organellar genomes and the evolutionary history of eukaryotes. A key question remaining to be answered pertains to the mechanism by which mitochondrial deletions can have a competitive advantage within cells. One distinct feature of mitochondria is that they have highly reduced genome sizes, perhaps

in order to increase their replication rate (Wallace 1982; Anderson et al. 1998; Lang et al. 1999). It had been proposed that deletion-bearing mtDNA molecules gain a selfish transmission advantage because they replicate more rapidly owing to their smaller size (Wallace 1992). The experimental evidence for the hypothesis that shorter mitochondrial genomes are faster replicators is mixed. Some studies have demonstrated that shorter mitochondrial genomes can replicate more rapidly than larger, WT mtDNA genomes within the same cell (Tang et al. 2000; Diaz et al. 2002). Likewise, in vivo experiments in mouse neurons suggested that mitochondrial genomes with large deletions accumulate faster than genomes with small deletions (Fukui and Moraes 2009). This proposed characteristic of mitochondrial genomes could provide a transmission advantage for the Δ*ctb-1* mitotype because they replicate more rapidly owing to their smaller size. However, a recent study in *C. elegans* found no empirical support for this 'small-genome' hypothesis (Gitschlag et al. 2016) given that mtDNA heteroplasmies involving point mutations and smaller deletions show clonal expansion at a rate similar to that of large deletion-bearing mitochondria (Campbell et al. 2014). Rather, recent work in *C. elegans* suggest that mutant mtDNA molecules 'hijack' endogenous pathways of mitonuclear signalling to upregulate the mitochondrial unfolded protein response pathway to facilitate an increase in their copy number (Gitschlag et al. 2016; Lin et al. 2016).

Levels of mitochondrial heteroplasmy are the product of mutation and selection at different levels of organization. To address questions about replicative advantage of different mtDNA variants within individuals, it is imperative that one eliminate sources

of confounding factors, such as selection between individuals. Experiments on the population dynamics of selfish mtDNA have revealed that their abundance can be very sensitive to population size (Phillips et al. 2015). One of the advantages of using single individual bottlenecks to study the dynamics of mitochondrial mutations is the near absence of selection between individuals, which can reveal the relative contributions of selection and drift within the germline.

Tables

Table II-1: Fitness of Δ*ctb-1*-bearing mtDNA in a wild-type nuclear background relative to control worms of the laboratory strain, *N2*, bearing wild-type mtDNA. (Fifteen replicates each of three *N2* control and six experimental Δ*ctb-1*-bearing (1G.C-1G.U) lines were assayed. Estimates of the mean phenotype for four fitness traits are provided for the wild-type *N2* control ($\bar{Z}_{N2\ control}$; three lines each with 15 replicates, $n = 45$) and the six 1G-derived, Δ*ctb-1*-bearing lines ($\bar{Z}_{\Delta ctb\text{-}1\text{-}bearing\ line}$; $n = 90$). Mean fitness values across $n = 15$ replicates for individual control and experimental lines are also provided (three *N2* control and six Δ*ctb-1*-bearing lines).) Reprinted from Dubie et al. 2020.

	Fitness-related trait			
	Productivity	Survivorship to Adulthood	Developmental Time (hours)	Longevity (days)
$\bar{Z}_{N2\ control}$	311.31	0.990	45.89	15.51
$\bar{Z}_{\Delta ctb\text{-}1\ bearing\ line\ 1G}$	108.73	0.907	52.21	12.56
$\bar{Z}_{N2\ control\ 1}$	294.93	0.980	51.67	15.13
$\bar{Z}_{N2\ control\ 2}$	326.33	1.000	42.27	17.93
$\bar{Z}_{N2\ control\ 3}$	312.67	1.000	43.73	13.47
$\bar{Z}_{\Delta ctb\text{-}1\ bearing\ line\ 1G.C}$	91.73	0.873	51.73	12.07
$\bar{Z}_{\Delta ctb\text{-}1\ bearing\ line\ 1G.L}$	96.87	0.947	57.29	13.13
$\bar{Z}_{\Delta ctb\text{-}1\ bearing\ line\ 1G.M}$	87.00	0.953	58.14	13.07
$\bar{Z}_{\Delta ctb\text{-}1\ bearing\ line\ 1G.N}$	85.80	0.760	48.57	11.00
$\bar{Z}_{\Delta ctb\text{-}1\ bearing\ line\ 1G.T}$	169.93	0.953	46.80	12.40
$\bar{Z}_{\Delta ctb\text{-}1\ bearing\ line\ 1G.U}$	121.07	0.953	51.20	13.67

Figures

Figure II-1. Identification and location of the *ctb-1* deletion in MA line 1G. (a) A 499 bp frameshift mtDNA deletion in *ctb-1* (Δ*ctb-1*) occurred spontaneously in a *C. elegans* spontaneous mutation accumulation line, 1G, and was detected via whole-genome sequencing (Konrad et al. 2017). The figure shows the read depth from Illumina whole genome sequencing mapped to the *ctb-1* region of the *C. elegans* mitochondrial genome in line 1G. The read depth inside the deletion is only 4% of the read depth of the sequences immediately flanking the deletion, suggesting that the frequency of the Δ*ctb-1* mitotype is 96% within this MA line. (b) A map of the *C. elegans* mitochondrial genome (adapted from Okimoto et al. 1992), illustrating the location, extent, and the sequence context of Δ*ctb-1*. The protein-coding sequence of the *ctb-1* gene spans 1110 bp (protein length 370 aa). Reprinted from Dubie et al. 2020.

Figure II-2. Frequency trajectories of four spontaneous mtDNA mutations that arose in MA line 1G during the course of the MA experiment. The vertical axis represents the intracellular frequency of individual mtDNA mutations as estimated by ddPCR (Δ*ctb-1*) or Sanger sequencing. The horizontal axis represents the number of generations since the start of the MA experiment. Reprinted from Dubie et al. 2020.

Figure II-3. Relative trait means of Δ*ctb-1*-bearing 1G replicate lines and the wild-type N2 control. Mean fitness values for each of the four traits were measured across six 1G lines (orange), each with 15 replicates where possible (n = 87 or 90) and three N2 control lines (grey), each with 15 replicates (n = 45). Phenotypic assays were conducted

for four fitness-related traits, namely productivity, survivorship to adulthood, developmental rate and longevity. For simplicity, the mean relative fitness value for each of the four traits in the wild-type N2 control was scaled to a value of 1. All of the lines bearing the Δ*ctb-1* mtDNA perform significantly worse than the wild-type N2 line. ** $p \leq 0.01$, **** $p \leq 0.0001$. Error bars represent one standard error. Reprinted from Dubie et al. 2020.

Figure II-4. Evolutionary dynamics of Δ*ctb-1* mtDNA under competitive conditions. (a) Population-level frequencies of the Δ*ctb-1* mtDNA heteroplasmy in five 1G replicate lines under non-competed (gray lines) versus competitive conditions (colored lines). In competitive assay populations established with equal ratios of Δ*ctb-1* and wild-type mtDNA-bearing worms (50 Δ*ctb-1*-bearing 1G hermaphrodites+50 wild-type mtDNA-bearing N2 hermaphrodites), the population dynamics of the Δ*ctb-1* mitotype displays a steep decline in frequency with time. The Δ*ctb-1* mtDNA heteroplasmy remains in high frequency (approx. 1.0) within each replicate line across generations under noncompetitive (control) conditions. In general, there is a significant reduction in the frequency of the Δ*ctb-1* mitotype from 0.5 to less than 0.2 within two generations under competitive conditions, and eventual loss (undetectable via PCR) from the population between generations 3-8. The Δ*ctb-1* mitotype remained undetected between generations 9-16. (b) A linear regression of the change in log[f (Δ*ctb-1*/WT mtDNA)] with time (generations). The single data point for each generation represents the average values of the Δ*ctb-1* mutant mitotype and wild-type mtDNA across five independent replicates of

line 1G (1G.C, 1G.L, 1G.N, 1G.T and 1G.U). The relative fitness, *w*, of the Δ*ctb-1* mutant mitotype was calculated from the slope of the regression line and estimated to be 0.48, implicating a large deleterious fitness cost of the *ctb-1* deletion-bearing mtDNA and its gradual eradication in large competitive populations via purifying selection. Reprinted from Dubie et al. 2020.

Figure II-5. A box plot of the Δ*ctb-1* frequency across time in non-competed large populations of lines 1G.C, 1G.N, 1G.T and 1G.U. The average frequency of Δ*ctb-1* is 93.4%, 93.2% and 74.0% at generation 0, 30 and 75, respectively. Reprinted from Dubie et al. 2020.

Figure II-6. A box plot of the relative mtDNA copy number across time in non-competed large populations of lines 1G.C, 1G.N, 1G.T and 1G.U as determined by ddPCR. The relative mtDNA copy number for wild-type N2 mtDNA is displayed for reference. Reprinted from Dubie et al. 2020.

Figure II-7. Relationship between the copy number of Δ*ctb-1* and wild-type mtDNA. (a) A scatterplot of the relationship between relative copy number of Δ*ctb-1* and wild-type mtDNA at generation 0 in large populations. The plot combines ddPCR results for lines 1G.C, 1G.N, 1G.T and 1G.U. There is a significant correlation between Δ*ctb-1* and wild-type mtDNA copy number at generation 0 ($r = 0.42$, $p = 0.001$). (b) Individual correlation coefficients between Δ*ctb-1* and wild-type mtDNA copy number as a function of time (number of generations) for non-competed populations of 1G.C, 1G.N,

1G.T and 1G.U. The strength of the correlation between Δ*ctb-1* and wild-type mtDNA copy number declines with time ($r = -0.69$, $p = 0.013$). Reprinted from Dubie et al. 2020.

Figure II-8. The distribution of the frequency of Δ*ctb-1* mtDNA in 25 lines after six generations of bottlenecking via single progeny descent. All 25 lines were descended from an individual with a Δ*ctb-1* frequency of 37%, indicated by the dashed vertical line. The frequency of Δ*ctb-1* mtDNA exhibited a rapid and significant increase (average 54%) under this regime of minimal selection between individuals. Reprinted from Dubie et al. 2020.

Figure II-1: Identification and location of the *ctb-1* deletion in MA line 1G.

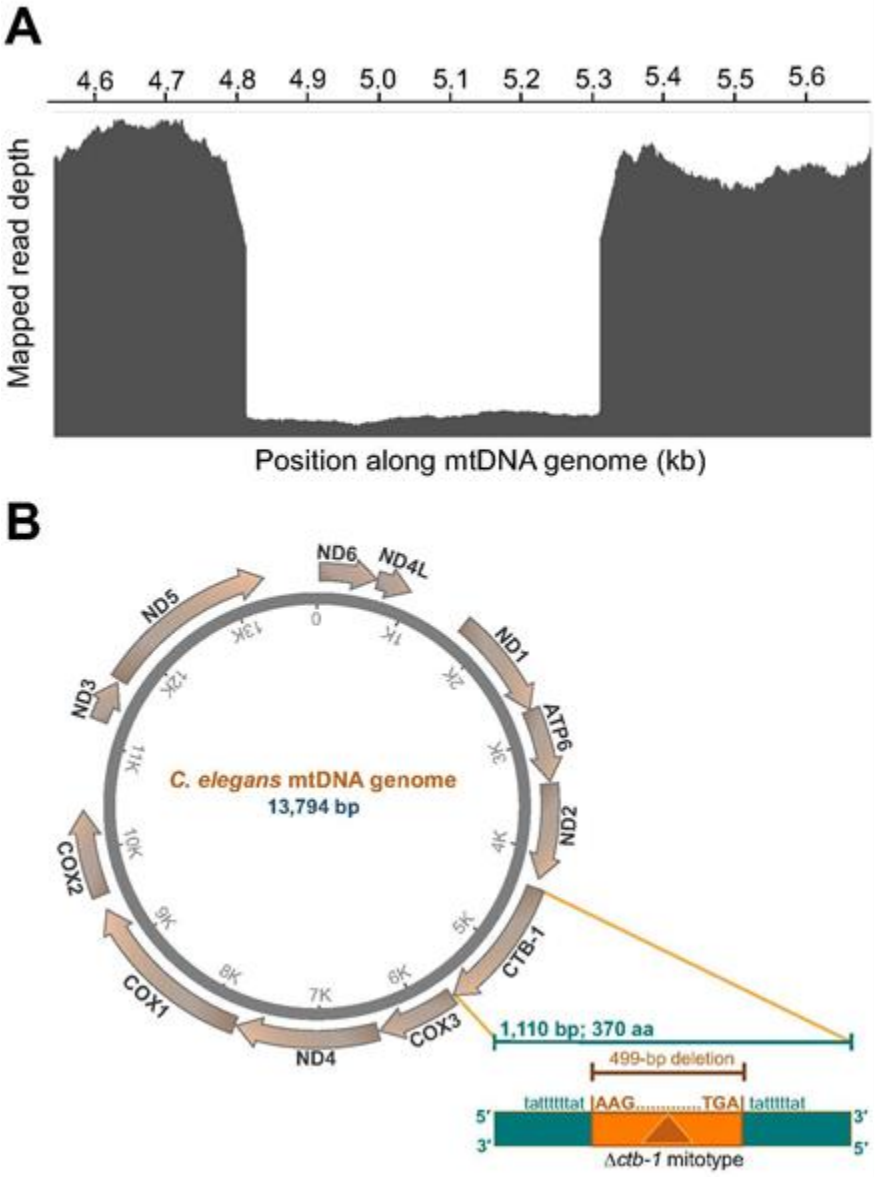

Figure II-2: Frequency trajectories of four spontaneous mtDNA mutations that arose in MA line 1G during the course of the MA experiment.

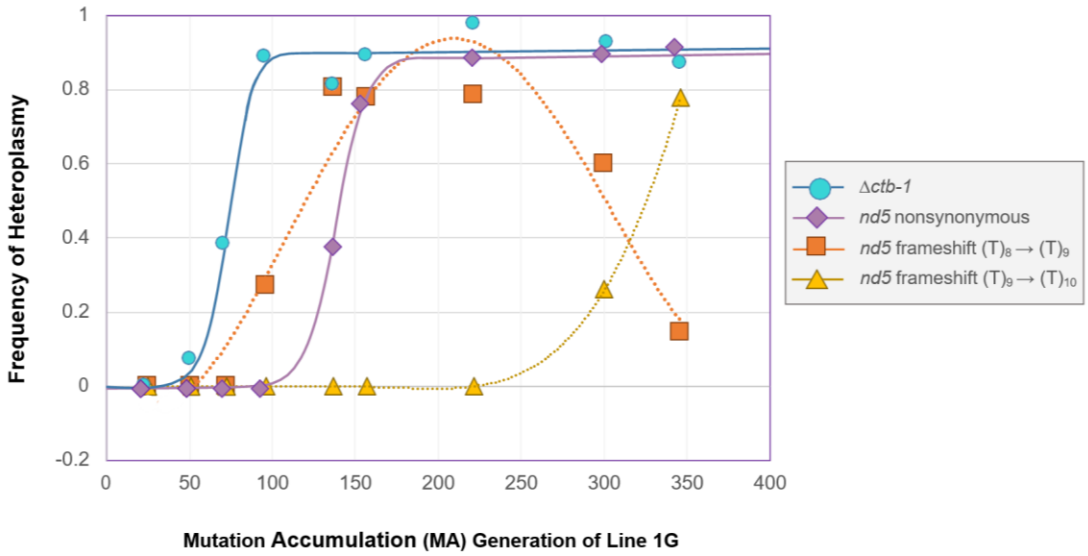

Figure II-3: Relative trait means of Δ*ctb-1*-bearing 1G replicate lines and the wild-type N2 control.

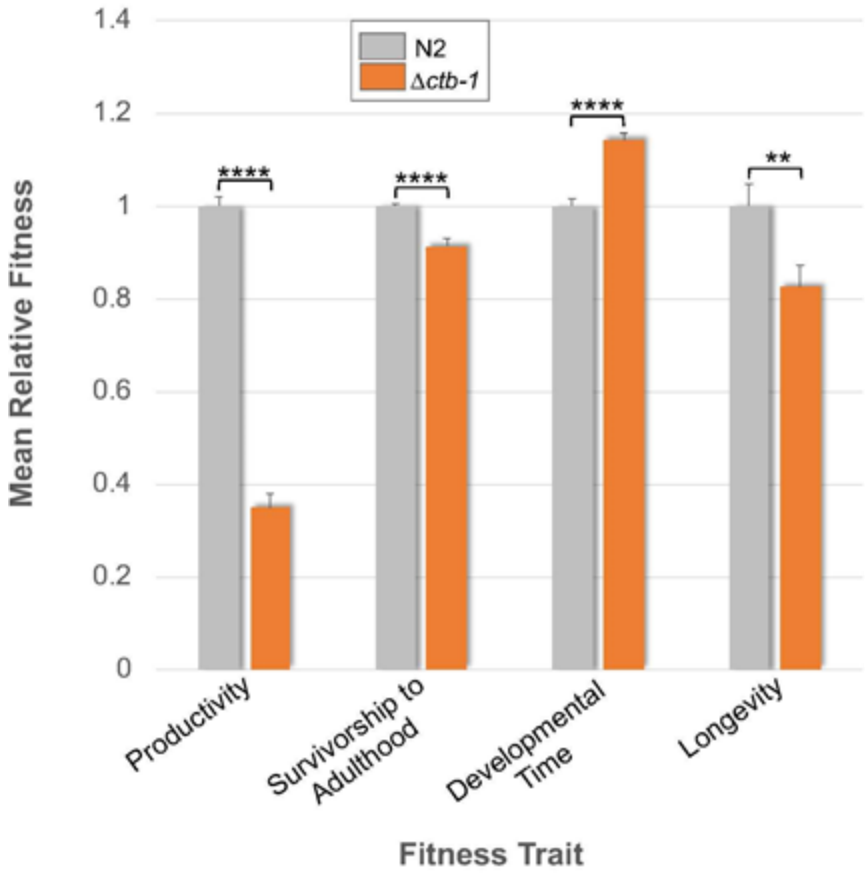

Figure II-4: Evolutionary dynamics of Δ*ctb-1* mtDNA under competitive conditions.

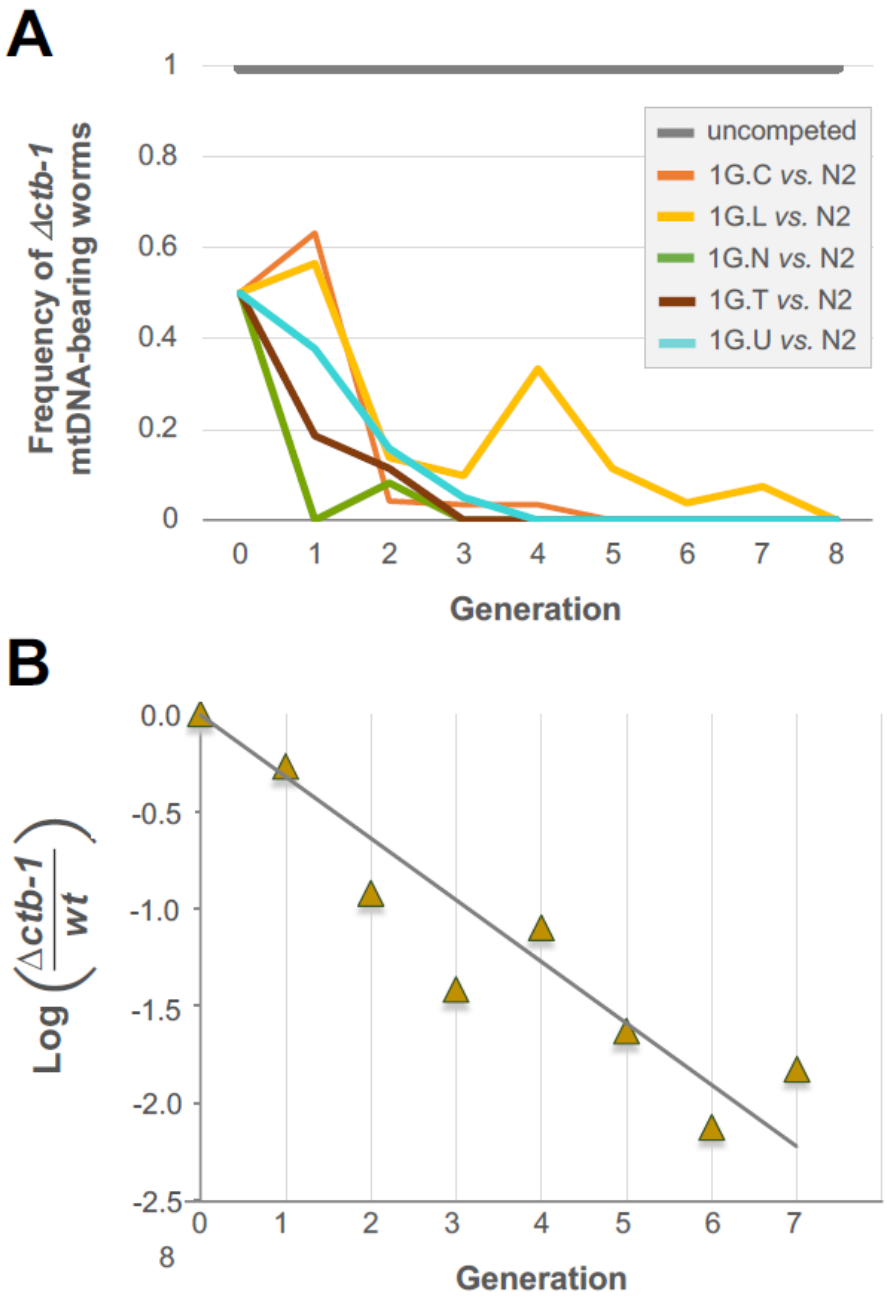

Figure II-5: A box plot of the Δ*ctb-1* frequency across time in non-competed large populations of lines 1G.C, 1G.N, 1G.T and 1G.U.

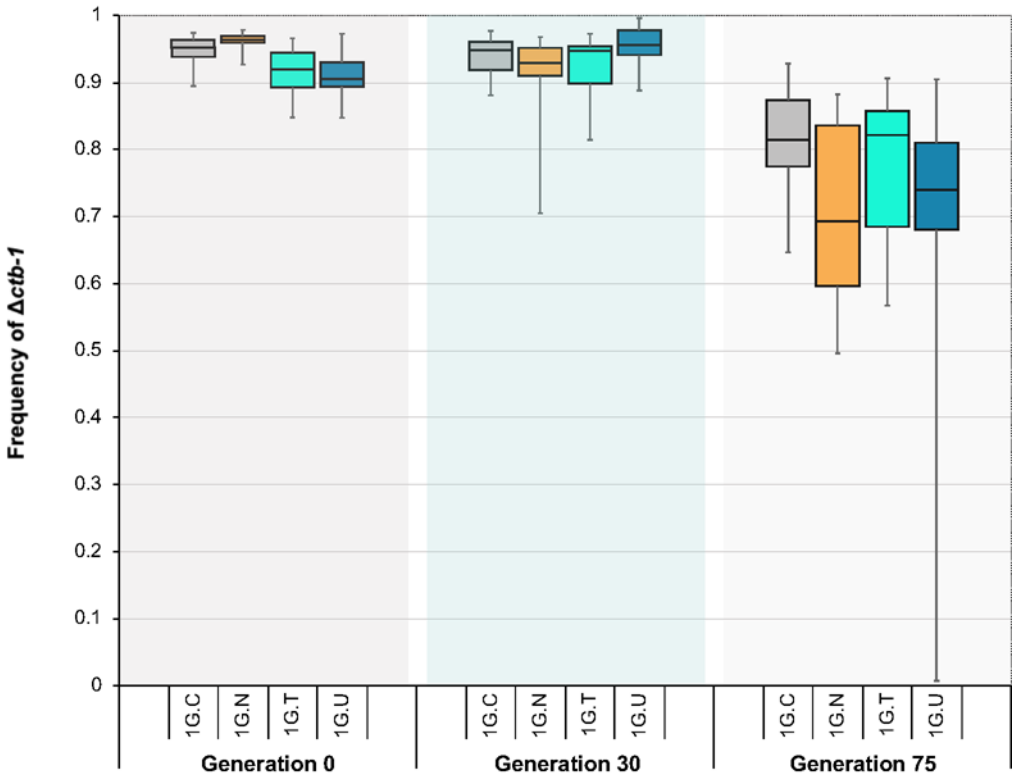

Figure II-6: A box plot of the relative mtDNA copy number across time in non-competed large populations of lines 1G.C, 1G.N, 1G.T and 1G.U as determined by ddPCR.

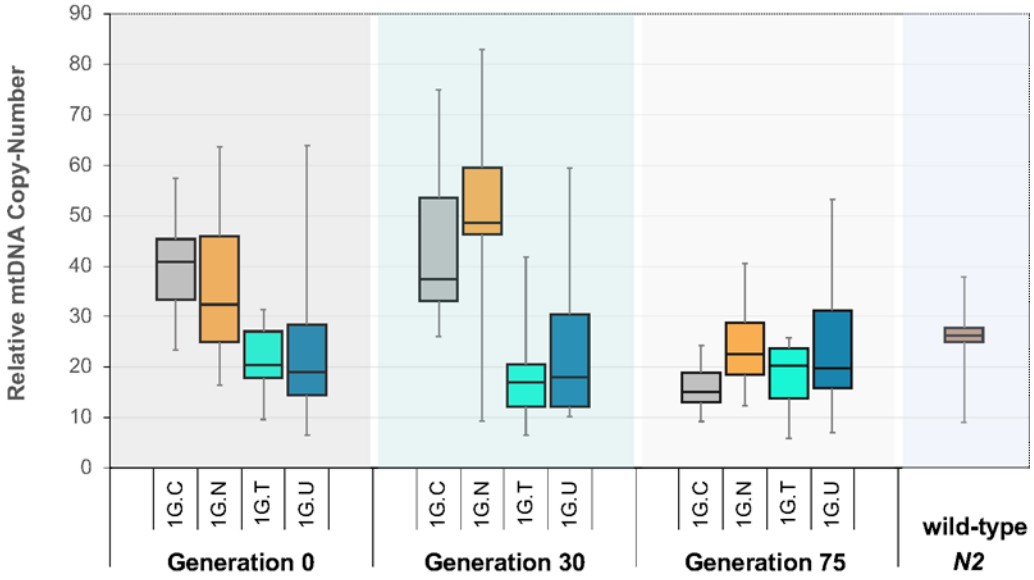

Figure II-7: Relationship between the copy number of Δ*ctb-1* and wild-type mtDNA.

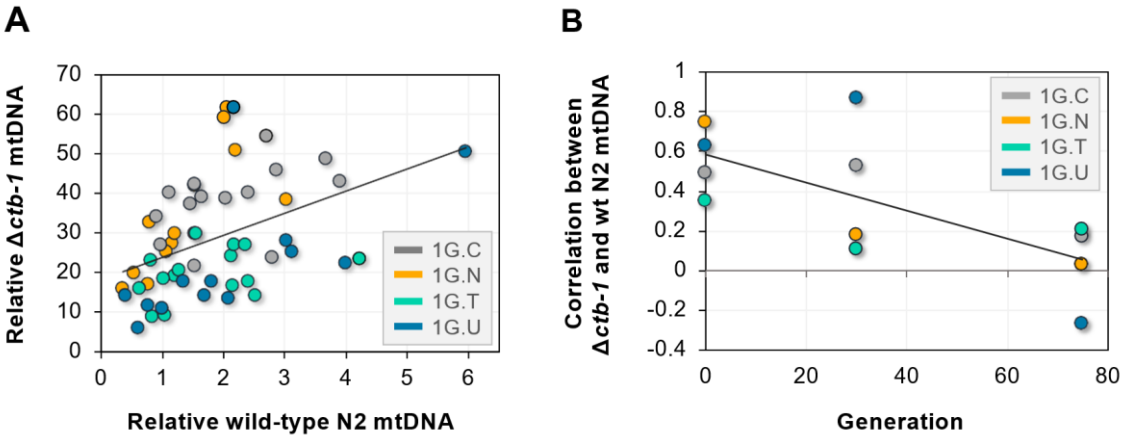

Figure II-8: The distribution of the frequency of Δ*ctb-1* mtDNA in 25 lines after six generations of bottlenecking via single progeny descent.

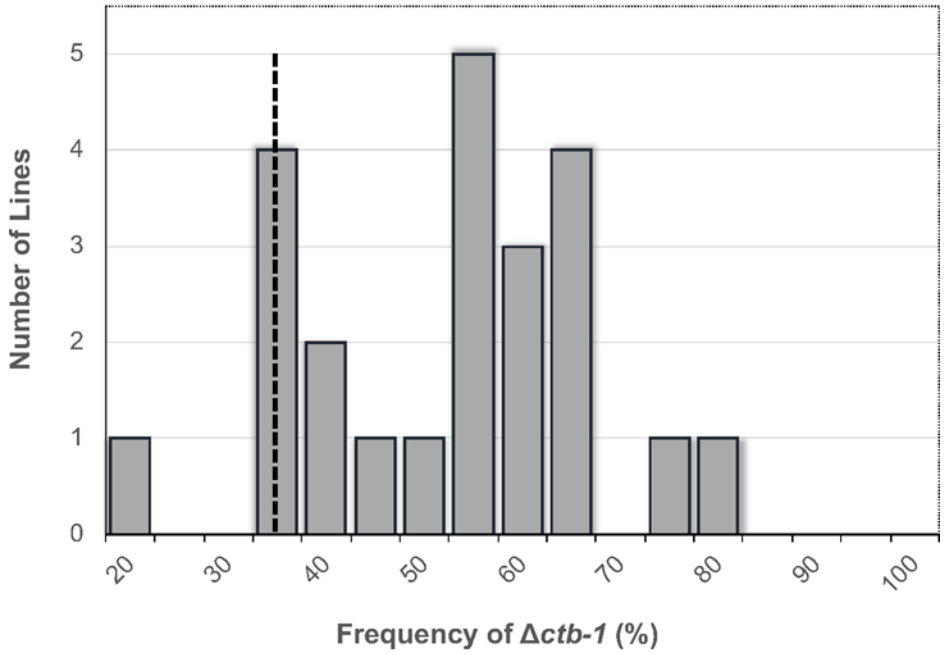

References

Andersson SG, Zomorodipour A, Andersson JO, Sicheritz-Pontén T, Alsmark UC, Podowski RM, Näslund AK, Eriksson AS, Winkler HH, Kurland CG. 1998. The genome sequence of *Rickettsia prowazekii* and the origin of mitochondria. *Nature*. **396**:133-140. (doi:10.1038/24094)

Barr CM, Neiman M, Taylor DR. 2005. Inheritance and recombination of mitochondrial genomes in plants, fungi and animals. *New Phytol*. **168**:39-50. (doi:10.1111/j.1469-8137.2005.01492.x)

Bernardi, G. 1979. The petite mutation in yeast. *Trends Biochem. Sci*. **4**:197-201. (doi:10.1016/0968-0004(79)90079-3)

Beziat F, Morel F, Volz-Lingenhol A, Saint Paul N, Alziari S. 1993. Mitochondrial genome expression in a mutant strain of *D. subobscura*, an animal model for large scale mtDNA deletion. *Nucleic Acids Res*. **21**:387-392. (doi:10.1093/nar/21.3.387)

Burton RS, Pereira RJ, Barreto FS. 2013. Cytonuclear genomic interactions and hybrid breakdown. *Annu. Rev. Ecol. Evol. Syst*. **44**:281-302. (doi:10.1146/annurev-ecolsys-110512-135758)

Campbell G, Krishnan KJ, Deschauer M, Taylor RW, Turnbull DM. 2014. Dissecting the mechanisms underlying the accumulation of mitochondrial DNA deletions in human skeletal muscle. *Hum. Mol. Genet*. **23**:4612-4620. (doi:10.1093/hmg/ddu176)

Chang CC, Rodriguez J, Ross J. 2016. Mitochondrial-nuclear epistasis impacts fitness and mitochondrial physiology of interpopulation *Caenorhabditis briggsae* hybrids. *G3*. **6**:209-219. (doi:10.1534/g3.115.022970)

Clark KA, Howe DK, Gafner K, Kusuma D, Ping S, Estes S, Denver DR. 2012. Selfish little circles: transmission bias and evolution of large deletion-bearing mitochondrial DNA in *Caenorhabditis briggsae* nematodes. *PLoS ONE*. **7**:e41433. (doi:10.1371/journal.pone.0041433)

Correia-Melo C, Birch J, Passos JF. 2016. Powering senescence: the ugly side of mitochondria. *Cell Cycle.* **15**:2541-2542. (doi:10.1080/15384101.2016.1204852)

Cosmides LM, Tooby J. 1981. Cytoplasmic inheritance and intragenomic conflict. *J. Theor. Biol*. **89**:83-129. (doi:10.1016/0022-5193(81)90181-8)

da Fonseca RR, Johnson WE, O'Brien SJ, Ramos MJ, Antunes A. 2008. The adaptive evolution of the mammalian mitochondrial genome. *BMC Genomics.* **9**:119. (doi:10.1186/1471-2164-9-119)

Das J. 2006. The role of mitochondrial respiration in physiological and evolutionary adaptation. *Bioessays.* **28**:890-901. (doi:10.1002/bies.20463)

Diaz F, Bayona-Bafaluy MP, Rana M, Mora M, Hao H, Moraes CT. 2002. Human mitochondrial DNA with large deletions repopulates organelles faster than full-length genomes under relaxed copy number control. *Nucleic Acids Res.* **30**:4626-4633. (doi:10.1093/nar/gkf602)

Dubie JJ, Caraway AR, Stout MM, Katju V, Bergthorsson U. 2020. The conflict within: origin, proliferation and persistence of a spontaneously arising selfish mitochondrial genome. *Phil. Trans. R. Soc. B*. **375**:20190174. (doi:10.1098/rstb.2019.0174)

Eberhard WG. 1980. Evolutionary consequences of intracellular organelle competition. *Q. Rev. Biol*. **55**:231-249. (doi:10.1086/411855)

Ephrussi B, de Margerie-Hottinguer H, Roman H. 1955. Suppressiveness: a new factor in the genetic determinism of the synthesis of respiratory enzymes in yeast. *Proc. Natl Acad. Sci. USA*. **41**:1065-1071. (doi:10.1073/pnas.41.12.1065)

Estes S, Coleman-Hulbert AL, Hicks KA, de Haan G, Martha SR, Knapp JB, Smith SW, Stein KC, Denver DR. 2011. Natural variation in life history and aging phenotypes is associated with mitochondrial DNA deletion frequency in *Caenorhabditis briggsae. BMC Evol. Biol*. **11**:11. (doi:10.1186/1471-2148-11-11)

Fukui H, Moraes CT. 2009. Mechanisms of formation and accumulation of mitochondrial DNA deletions in aging neurons. *Hum. Mol. Genet.* **18**:1028-1036. (doi:10.1093/hmg/ddn437)

Gitschlag BL, Kirby CS, Samuels DC, Gangula RD, Mallal SA, Patel MR. 2016. Homeostatic responses regulate selfish mitochondrial genome dynamics in *C. elegans. Cell Metab*. **24**:91-103. (doi:10.1016/j.cmet.2016.06.008)

Gray MW. 2018. Mitochondrial genomes. Molecular life sciences (eds RD Wells, JS Bond, J Klinman, BSS Masters), pp. 695-709. New York, NY: Springer.

Greaves LC, Nooteboom M, Elson JL, Tuppen HA, Taylor GA, Commane DM, Arasaradnam RP, Khrapko K, Taylor RW, Kirkwood TB, Mathers JC, Turnbull DM. 2014. Clonal expansion of early to mid-life mitochondrial DNA point

mutations drives mitochondrial dysfunction during human ageing. *PLoS Genet*. **10**(9):e1004620. (doi:10.1371/journal.pgen.1004620)

Harrison RG, Rand DM, Wheeler WC. 1985. Mitochondrial DNA size variation within individual crickets. *Science.* **228**:1446-1448. (doi:10.1126/science.228.4706.1446)

Havird JC, Hall MD, Dowling DK. 2015. The evolution of sex: a new hypothesis based on mitochondrial mutational erosion. *Bioessays*. **37**:951-958. (doi:10.1002/bies.201500057)

Hayashi J, Ohta S, Kikuchi A, Takemitsu M, Goto Y, Nonaka I. 1991. Introduction of disease-related mitochondrial DNA deletions into HeLa cells lacking mitochondrial DNA results in mitochondrial dysfunction. *Proc. Natl Acad. Sci. USA*. **88**:10614-10618. (doi:10.1073/pnas.88.23.10614)

Howe DK, Denver DR. 2008. Muller's Ratchet and compensatory mutation in *Caenorhabditis briggsae* mitochondrial genome evolution. *BMC Evol. Biol*. **8**:62. (doi:10.1186/1471-2148-8-62)

Hudson G, Gomez-Duran A, Wilson IJ, Chinnery PF. 2014. Recent mitochondrial DNA mutations increase the risk of developing common late-onset human diseases. *PLoS Genet*. **10**:e1004369. (doi:10.1371/journal.pgen.1004369)

Hurst GD, Werren JH. 2001. The role of selfish genetic elements in eukaryotic evolution. *Nat. Rev. Genet*. **2**:597-606. (doi:10.1038/35084545)

Jasmin JN, Zeyl C. 2014. Rapid evolution of cheating mitochondrial genomes in small yeast populations. *Evolution.* **68**:269-275. (doi:10.1111/evo.12228)

Kairo A, Fairlamb AH, Gobright E, Nene V. 1994. A 7.1 kb linear DNA molecule of *Theileria parva* has scrambled rDNA sequences and open reading frames for mitochondrially encoded proteins. *EMBO J.* **13**:898-905. (doi:10.1002/j.1460-2075.1994.tb06333.x)

Karavaeva IE, Golyshev SA, Smirnova EA, Sokolov SS, Severin FF, Knorre DA. 2017. Mitochondrial depolarization in yeast zygotes inhibits clonal expansion of selfish mtDNA. *J. Cell Sci*. **130**:1274-1284. (doi:10.1242/jcs.197269)

Katju V, Packard LB, Bu L, Keightley PD, Bergthorsson U. 2015. Fitness decline in spontaneous mutation accumulation lines of *Caenorhabditis elegans* with varying effective population sizes. *Evolution.* **69**:104-116. (doi:10.1111/evo.12554)

Katju V, Packard LB, Keightley PD. 2018. Fitness decline under osmotic stress in *Caenorhabditis elegans* populations subjected to spontaneous mutation

accumulation at varying population sizes. *Evolution.* **72**:1000-1008. (doi:10.1111/evo.13463)

Keogh M, Chinnery PF. 2013. Hereditary mtDNA heteroplasmy: a baseline for aging? *Cell Metab*. **18**:463-464. (doi:10.1016/j.cmet.2013.09.015)

Kmiec B, Woloszynska M, Janska H. 2006. Heteroplasmy as a common state of mitochondrial genetic information in plants and animals. *Curr. Genet*. **50**:149-159. (doi:10.1007/s00294-006-0082-1)

Knorre DA. 2019. Intracellular quality control of mitochondrial DNA: evidence and limitations. *Phil. Trans. R. Soc. B*. **375**:20190176. (doi:10.1098/rstb.2019.0176)

Konrad A, Thompson O, Waterston RH, Moerman DG, Keightley PD, Bergthorsson U, Katju V. 2017. Mitochondrial mutation rate, spectrum and heteroplasmy in *Caenorhabditis elegans* spontaneous mutation accumulation lines of differing population size. *Mol. Biol. Evol*. **34**:1319-1334. (doi:10.1093/molbev/msx051)

Korolchuk VI, Miwa S, Carroll B, von Zglinicki T. 2017. Mitochondria in cell senescence: is mitophagy the weakest link? *EBioMedicine*. **21**:7-13. (doi:10.1016/j.ebiom.2017.03.020)

Lakshmanan LN, Yee Z, Ng LF, Gunawan R, Halliwell B, Gruber J. 2018. Clonal expansion of mitochondrial DNA deletions is a private mechanism of aging in long-lived animals. *Aging Cell.* **17**:e12814. (doi:10.1111/acel.12814)

Lang BF, Gray MW, Burger G. 1999. Mitochondrial genome evolution and the origin of eukaryotes. *Annu. Rev. Genet*. **33**:351-397. (doi:10.1146/annurev.genet.33.1.351)

Lee Y, Hwang W, Jung J, Park S, Cabatbat JJ, Kim PJ, Lee SJ. 2016. Inverse correlation between longevity and developmental rate among wild *C. elegans* strains. *Aging.* **8**:986-999. (doi:10.18632/aging.100960)

Liau WS, Gonzalez-Serricchio AS, Deshommes C, Chin K, LaMunyon CW. 2007. A persistent mitochondrial deletion reduces fitness and sperm performance in heteroplasmic populations of *C. elegans*. *BMC Genet*. **8**:8. (doi:10.1186/1471-2156-8-8)

Lin YF, Schulz AM, Pellegrino MW, Lu Y, Shaham S, Haynes CM. 2016. Maintenance and propagation of a deleterious mitochondrial genome by the mitochondrial unfolded protein response. *Nature*. **533**:416-419. (doi:10.1038/nature17989)

Ma H, O'Farrell PH. 2016. Selfish drive can trump function when animal mitochondrial genomes compete. *Nat. Genet*. **48**:798-802. (doi:10.1038/ng.3587)

MacAlpine DM, Kolesar J, Okamoto K, Butow RA, Perlman PS. 2001. Replication and preferential inheritance of hypersuppressive petite mitochondrial DNA. *EMBO J.* **20**:1807-1817. (doi:10.1093/emboj/20.7.1807)

Okimoto R, Macfarlane JL, Clary DO, Wolstenholme DR. 1992. The mitochondrial genomes of two nematodes, *Caenorhabditis elegans* and *Ascaris suum. Genetics*. **130**:471-498. (doi:10.1093/genetics/130.3.471)

Phillips WS, Coleman-Hulbert AL, Weiss ES, Howe DK, Ping S, Wernick RI, Estes S, Denver DR. 2015. Selfish mitochondrial DNA proliferates and diversifies in small, but not large, experimental populations of *Caenorhabditis briggsae*. *Genome Biol. Evol.* **7**:2023-2037. (doi:10.1093/gbe/evv116)

Pinto M, Moraes CT. 2015. Mechanisms linking mtDNA damage and aging. *Free Radic. Biol. Med*. **85**:250-258. (doi:10.1016/j.freeradbiomed.2015.05.005)

Porteous WK, James AM, Sheard PW, Porteous CM, Packer MA, Hyslop SJ, Melton JV, Pang CY, Wei YH, Murphy MP. 1998. Bioenergetic consequences of accumulating the common 4977-bp mitochondrial DNA deletion. *Eur. J. Biochem*. **257**:192-201. (doi:10.1046/j.1432-1327.1998.2570192.x)

Poulton J, Deadman ME, Ramacharan S, Gardiner RM. 1991. Germ-line deletions of mtDNA in mitochondrial myopathy. *Am. J. Hum. Genet*. **48**, 649-653.

Rand DM. 2001. The units of selection on mitochondrial DNA. *Annu. Rev. Ecol. Evol. Syst*. **32**:415-448. (doi:10.1146/annurev.ecolsys.32.081501.114109)

Radzvilavicius AL, Blackstone NW. 2015. Conflict and cooperation in eukaryogenesis: implications for the timing of endosymbiosis and the evolution of sex. *J. R. Soc. Interface.* **12**:20150584. (doi:10.1098/rsif.2015.0584)

Ross JM, Stewart JB, Hagström E, Brené S, Mourier A, Coppotelli G, Freyer C, Lagouge M, Hoffer BJ, Olson L, Larsson NG. 2013. Germline mitochondrial DNA mutations aggravate ageing and can impair brain development. *Nature.* **501**:412-415. (doi:10.1038/nature12474)

Rossignol R, Faustin B, Rocher C, Malgat M, Mazat JP, Letellier T. 2003. Mitochondrial threshold effects. *Biochem. J*. **370**:751-762. (doi:10.1042/BJ20021594)

Schnabel PS, Wise RP. 1998. The molecular basis of cytoplasmic make sterility and fertility restoration. *Trends Plant Sci*. **3**:175-180. (doi:10.1016/S1360-1385(98)01235-7)

Scott GR, Schulte PM, Egginton S, Scott AL, Richards JG, Milsom WK. 2011 Molecular evolution of cytochrome C oxidase underlies high-altitude adaptation in the bar-headed goose. *Mol. Biol. Evol*. **28**:351-363. (doi:10.1093/molbev/msq205)

Shoffner JM, Lott MT, Lezza AM, Seibel P, Ballinger SW, Wallace DC. 1990. Myoclonic epilepsy and ragged-red fiber disease (MERRF) is associated with a mitochondrial DNA *tRNA(Lys)* mutation. *Cell.* **61**:931-937. (doi:10.1016/009-8674(90)90059-N)

Stewart JB, Chinnery PF. 2015. The dynamics of mitochondrial DNA heteroplasmy: implications for human health and disease. *Nat. Rev. Genet*. **16**:530-542. (doi:10.1038/nrg3966)

Tang Y, Manfredi G, Hirano M, Schon EA. 2000. Maintenance of human rearranged mitochondrial DNAs in long-term cultured transmitochondrial cell lines. *Mol. Biol. Cell*. **11**:2349-2358. (doi:10.1091/mbc.11.7.2349)

Taylor DR, Zeyl C, Cooke E. 2002. Conflicting levels of selection in the accumulation of mitochondrial defects in *Saccharomyces cerevisiae*. *Proc. Natl Acad. Sci. USA.* **99**:3690-3694. (doi:10.1073/pnas.072660299)

Telschow A, Gadau J, Werren JH, Kobayashi Y. 2019. Genetic incompatibilities between mitochondria and nuclear genes: effect on gene flow and speciation. *Front. Genet*. **10**:62. (doi:10.3389/fgene.2019.00062)

Tsang WY, Lemire BD. 2002. Stable heteroplasmy but differential inheritance of a large mitochondrial DNA deletion in nematodes. *Biochem. Cell Biol*. **80**:645-654. (doi:10.1139/o02-135)

Wallace DC. 1982. Structure and evolution of organelle genomes. *Microbiol. Rev*. **46**:208-240. (doi:10.1128/mr.46.2.208-240.1982)

Wallace DC. 1992. Mitochondrial genetics: a paradigm for aging and degenerative diseases. *Science*. **256**:628-632. (doi:10.1126/science.1533953)

Wallace DC. 1999. Mitochondrial diseases in man and mouse. *Science.* **283**:1482-1488. (doi:10.1126/science.283.5407.1482)

Wallace DC, Chalkia D. 2013. Mitochondrial DNA genetics and the heteroplasmy conundrum in evolution and disease. *Cold Spring Harb. Perspect. Biol.* **5**:a021220. (doi:10.1101/cshperspect.a021220)

Zeviani M, Antozzi C. 1997. Mitochondrial disorders. *Mol. Hum. Reprod*. **3**:133-148. (doi:10.1093/molehr/3.2.133)

CHAPTER III

DISSECTING THE SEQUENTIAL EVOLUTION OF A SELFISH MITOCHONDRIAL GENOME IN *CAENORHABDITIS ELEGANS*

Introduction

Mitochondria are essential components of all eukaryotic cells, having originated through the endosymbiosis of an ancient prokaryote into an archaebacterium (Martin and Müller 1998) or basal eukaryote (Margulis 1970; Doolittle 1981). While the two main competing hypotheses regarding mitochondrial origin differ with respect to the nature of the host (Martin et al. 2001; Koonin 2010; Gray 2012), many of the cellular processes of this ancient prokaryote have been taken over by its host during more than one billion years of evolution. As such, mitochondria have greatly reduced genomes and primarily exist to produce energy for their host cells (Lang et al. 1997). Within the animal kingdom, with very few exceptions, all mitochondrial genomes contain the same limited set of components: 13 protein, two rRNA, and 22 tRNA encoding regions (Kairo et al. 1994). This drastic reduction of the mitochondrial genome dictates its reliance on the nuclear gene products of eukaryotic cells. The eukaryotic nuclear genome not only controls functions like translation, transcription, and replication for mitochondria (Burton et al. 2013), but also produces most proteins that interact with mtDNA-encoded proteins to create the complexes involved in the electron transport chain (ETC). This mitonuclear interaction has resulted in tight coevolution between mitochondrial and nuclear-encoded subunits and is reflected in cases of “mitonuclear mismatch” where

hybrids with incompatible nuclear and mitochondrial genomes show reduced fitness and ETC efficiency (Pinto and Moraes 2015).

The population dynamics of mitochondrial genes differ in notable aspects from that of nuclear genes which, in turn, can facilitate an increase in the frequency of deleterious mitochondrial variants. First, the predominantly uniparental inheritance of mitochondria can result in cytonuclear conflict (Cosmides and Tooby 1981, Havird et al. 2019). Classic examples of cytonuclear conflict include cytoplasmic male sterility in flowering plants and Mother's curse (Gemmell et al. 2004; Fujii et al. 2011). Second, a single cell contains multiple copies of the mitochondrial chromosome, thereby engendering competition between different mitochondrial genotypes (mitotypes) (Eberhard 1980; Cosmides and Tooby 1981). Deleterious mitochondrial DNA (mtDNA) mutations can occasionally increase in frequency by taking advantage of some form of transmission or replicative advantage (Eberhard 1980; Clark et al. 2012; Havird et al. 2019; Dubie et al. 2020). The biased transmission of deleterious mutations is the hallmark of selfish DNA and the mechanisms that favor them in mtDNA are poorly understood (Havird et al. 2019). Some of the best studied examples of selfish mtDNA mutations are deletions in yeast, *Drosophila melanogaster* and *Caenorhabditis* nematodes (MacAlpine et al. 2001; Taylor et al. 2002; Tsang and Lemire 2002; Clark et al. 2012; Lin et al. 2016; Ma and O'Farrell 2016; Dubie et al. 2020). The simplest explanation for a replicative advantage of deleterious mtDNA deletions is that smaller mtDNA molecules can replicate faster than a full-length mtDNA molecule, referred to as the "small genome hypothesis" (Wallace 1992). However, mtDNA point mutations and

small deletions can sometimes expand clonally at a rate that is similar to large mtDNA deletions (Campbell et al. 2013). Furthermore, experiments in *Caenorhabditis elegans* have failed to find support for the "small genome hypothesis" (Gitschlag et al. 2016). In yeast mtDNA petite mutants, an expansion of replication origins appears to play a large role for their replicative advantage (MacAlpine et al. 2001). Experiments in *Drosophila* and *Caenorhabditis* suggest that an increase in mtDNA copy-number and changes in mitochondrial fusion-fission cycles can favor mtDNA mutants (Tam et al. 2013). Unfortunately, mitochondrial genomes are challenging to engineer, and mtDNA mutations are initially heteroplasmic in very low frequencies, impeding both their detection and analyses of their consequences (Tsang and Lemire 2002; Gitschlag et al. 2016; Klucnika and Ma 2019).

Much of the initial work on selfish mtDNA deletions in *C. elegans* has been performed on *uaDF5*, a 3-kb deletion which encompasses four protein-coding genes (*nd1*, *atp6*, *nd2*, and *cytb*) and seven tRNA genes (Tsang and Lemire 2002). This deletion was formed between two 9 bp repeats and is inherited as a stable heteroplasmy in laboratory populations (Tsang and Lemire 2002; Liau et al. 2007; Gitschlag et al. 2016). The *uaDF5* deletion adversely affects fitness-related traits including productivity, longevity, and sperm motility, and yet exhibits a biased replication/transmission which increases the intracellular frequency of the deletion (Tsang and Lemire 2002; Liau et al. 2007; Gitschlag et al. 2016). Additionally, several natural isolates of the congeneric *Caenorhabditis briggsae* harbor selfish mtDNA deletions in *nd5* (*nad5*Δ) (Clark et al. 2012). The *C. briggsae nad5*Δ deletions are

detrimental for fitness and appear to persist due to a transmission bias (Estes et al. 2011; Clark et al. 2012). The severity of fitness effects and transmission/replication bias of *nad5*Δ vary with genetic background, either due to preexisting natural variation for controlling selfish mtDNA mutations or compensatory mutations (Sullins et al. 2019).

We have previously described a 499 bp deletion in the *C. elegans* mitochondrial *cytochrome b(1)* gene (Δ*ctb-1*) that arose spontaneously during a spontaneous mutation accumulation (MA) experiment (Katju et al. 2015, 2018; Konrad et al. 2017). The Δ*ctb-1* mutation also causes a frameshift resulting in a shortened polypeptide, from 370 amino acids in the normal gene to 118 amino acids in the deletion bearing lines. This deletion rapidly rose to high frequency within this *C. elegans* MA line, has strong deleterious fitness effects and a replicative or transmission advantage over the wild-type (WT) mtDNA molecule (Dubie et al. 2020). However, at the end of the MA experiment, the *ctb-1* deletion was also linked to four additional mutations: three in *ND5*, and another low frequency mutation in *tRNA-Asn.* The regular cryopreservation of the original MA experimental line has allowed us to dissect the sequential origin of each mutation and to test their effects on host fitness and on the replicative/transmission advantage of the Δ*ctb-1* mitotype. The additional missense and frameshift mutations might either be neutral, detrimental, or compensatory. The compensatory effects of two mutations that affect mitochondrial function was, for example, observed in *ctb-1*/*isp-1* double mutants in *C. elegans* where a mutation in *ctb-1* suppressed the slow development of a line bearing a nuclear *isp-1* mutation without improving complex III function (Suthammarak et al. 2010). Herein, we test how additional mutations linked to this

ΔmtDNA mitotype affect fitness and if they contribute to the selfish dynamics of the Δ*ctb-1* deletion or alternatively, act in a compensatory manner to ameliorate the fitness cost associated with the Δ*ctb-1* deletion.

Methods

Experimental strains used in this study

The lines used in this study are derived from a long-term spontaneous MA experiment in which populations of *C. elegans* were propagated in bottlenecked populations of varying sizes (Katju et al. 2015, 2018; Konrad et al. 2016). Illumina paired-end sequencing revealed that the mtDNA of MA line 1G harbored five heteroplasmic mtDNA mutations relative to the ancestral control: a 499 bp frameshift deletion in the *ctb-1* gene (frequency 96%), a single T insertion in a homopolymeric run within the *nd5* gene [$(T)_8 \rightarrow (T)_9$; frequency 3%], a C → T nonsynonymous substitution (Thr → Ile) in the nd5 gene (frequency 94%), a sybsequent insertion of another T in the homopolymeric run within the *nd5* gene [$(T)_8 \rightarrow (T)_{10}$; frequency 70%], and a G → T substitution in the *tRNA-Asn* gene (frequency 13%). Line 1G was bottlenecked to a single self-fertilizing hermaphrodite every generation for 346 generations. Additionally, 1G was cryopreserved at generations 25, 51, 72, 96, 137, 157, 221, 300 and 346. *C. elegans'* ability to survive cryogenic storage at -80°C allowed for nematodes to be thawed from stocks preserved throughout the original MA experiment. A stock of WT PreMA Bristol (N2) nematodes was also thawed to act as a WT control and for further line new line generation (see below). Thawed stocks were propagated at 20°C on

nematode growth media (NGM) plates seeded with *Escherichia coli* OP50 (Steiernagle 2006) for two generations to remove grandmaternal effects of freezing prior to any experimental manipulation.

Generation of obligately outcrossing lines

Obligately outcrossing *C. elegans* were needed to facilitate the sequestration of mutant bearing mtDNA in a WT nuclear background (see below). To generate obligately outcrossing *C. elegans*, *fog-2* deletion-bearing lines (Δ*fog-2* henceforth) were created using InVivo Biosystems's (formerly NemaMetrix) *C. elegans* CRISPR knockout service. Mutations resulting in a loss of function in *fog-2* inhibit hermaphrodite sperm production and convert the facultatively outcrossing nematode into an obligately outcrossing one (Schedl and Kimble 1988). However, gene conversion events between *fog-2* and *fog-2* homolog *ftr-1* have been known to restore hermaphrodite sperm production (Katju et al. 2008; Rane et al. 2010). To prevent gene conversion by *ftr-1*, the engineered *fog-2* deletion encompassed most of *fog*-2, spanning 76 bp of intron 1 through the first 13 bp of exon 5 for a total 1,106 bp of *fog-2*'s 1,212 bp (Chr. V:20199390..20200491; version WS282; www.wormbase.org). After lines were received from InVivo Biosystems, they were allowed to produce progeny before the parent worms were collected for single worm DNA extraction in worm lysis buffer (90 µl 10×PCR buffer + 10 µl 10 mg ml^{-1} proteinase K). The deletion was verified by PCR. First single worm lysates were used in a PCR reaction with primers 5'-CAA AGC TTC GCT TCA TGC TC-3' and 5'-CAG TGA TCA TGC CAA TTT ATC-3'which would

generate a 1,475 bp product in WT lines, a 369 bp product in homozygous deletion-bearing lines, or both products in heterozygous lines. Lysates from lines that appeared homozygous deletion-bearing were then further screened by PCR using primers 5'-CAA AGC TTC GCT TCA TGC TC-3' and 5'-TCT CCA TTG GCA TGT CAG AG-3', which would generate a 334 bp product in heterozygous lines and no product in homozygous deletion-bearing lines. In homozygous deletion-bearing lines the location of the deletion was confirmed by Sanger sequencing using the 369 bp amplified PCR product.

Sequestering each mtDNA mutation combination in a wild-type background

In order to measure the fitness consequences of each subsequent mtDNA mutation in combination with the preceding mutations, lines were generated that contained a high frequency of each mutation-combination isolated from nuclear mutations that had arisen during the original MA experiment (Katju et al. 2015). Dubie et al. (2020) identified MA generations in which each subsequent mtDNA mutation had risen to a high intracellular frequency but did not contain subsequent mtDNA mutations (table III-1). From each of these generations (71, 96, 221, 350) a few nematodes were recovered from cryopreservation. These nematodes were backcrossed to WT *C. elegans* males for 17 generations. Backcrossing to WT males transfers the MA mtDNA to the progeny while reducing the nuclear mutational load by half with each cross.

First, a single L4 hermaphrodite from each generation was picked onto an individual 35mm NGM plate seeded with OP50 along with three young adult male Δ*fog*-

2 C. elegans. From each plate ten random F1 progeny were picked and transferred individually to new 35mm NGM plates along with three young adult male Δ*fog-2 C. elegans*. Hermaphroditic *C. elegans* preferentially self-fertilize, so mating was confirmed by observing a high frequency of males among the progeny (Anderson et al. 2010), and a single F2 born on the 2nd or 3rd day of laying were transferred from each plate to a new plate along with three young adult male Δ*fog-2 C. elegans*. Selecting the progeny produced later gives a higher chance that they derive their parentage from outcrossing rather than self-fertilization. From each of the ten F2 backcrosses, ten F3 progeny were picked onto individual 35mm NGM plates seeded with OP50. Two young adult male Δ*fog-2* were added to each of the F3s that did not produce any progeny via self-fertilization within 24h of reaching adulthood,. From each of the F3 backcrosses, a single F4, L4 hermaphrodite was transferred to a new 35mm NGM plate seeded with OP50 along with three young adult male Δ*fog-2 C. elegans*. Every four days, a single L4 nematode was picked to a new plate along with three young adult male Δ*fog-2 C. elegans* for an additional 11 generations. An F15 L4 nematode was then transferred to a new plate with 2 young adult N2 males. From this cross, a single F16 L4 was again backcrossed to N2 males to generate an facultatively outcrossing line which contained the MA mtDNA, and predominately WT nDNA. After 17 generations of backcrossing, the proportion of nDNA remaining from MA is estimated to be 0.5^{17}, effectively removing all nuclear mutations from the original MA experiment. Several lines became infertile during the process of backcrossing. In total four fertile lines were created from backcrossed nematodes derived from generation 71 (G71.A, G71.B, G71.C, and G71.D),

five from generation 96 (G96.A, G96.B, G96.C, G96.D, and G96.D), four from generation 221 (G221.A, G221.B, G221.C, and G221.D), and six from generation 350 (G350.C, G350.L, G350.M, G350.N, G350.T, and G350.U).

Fitness assays

Phenotypic assays for four fitness-related traits (productivity, developmental rate, longevity, and survivorship) were performed to determine the consequences of bearing each mutation combination. All fitness assays were performed using backcrossed G71, G96, G221 lines and a WT N2 control concurrently at 20̲°C (Katju et al. 2015, 2018; Lee 2016; Dubie et al. 2020) with 15 replicates per line (total of 210).

For each replicate, a single L4 was picked to a new 35mm NGM plate seeded with OP50 prior to the line being cryopreserved using standard *C. elegans* procedures (Steiernagle 2006). The nematode was then allowed to lay eggs overnight. The next day, 10 L1 nematodes were transferred to a single 60mm NGM plate seeded with OP50. These nematodes were used to measure survivorship. Next, a single L1 nematode was picked from among the remaining progeny and transferred singly to a new 35mm NGM plate seeded with OP50. This nematode was used for the developmental rate, productivity, and longevity assays.

For the survivorship assay, the 10 L1s were incubated for 48h, and then the number of nematodes that had survived to adulthood were counted. The quotient of the count and 10 was then calculated to assign a survivorship score to each replicate from 0

to 1. This was then normalized by dividing the calculated survivorship score by the mean survivorship score of the N2 control prior to further analysis.

Developmental rate was measured using the single transferred L1. After incubating for 30 hours , the nematode was visually inspected under a dissecting microscope every 2 hours to determine the number of hours to adulthood. At the time that a nematode had developed its first egg, and that egg had migrated into the nematode's uterus, it was scored as having reached adulthood. The mean number of hours from L1 to adulthood of the N2 control was then divided by the observed number of hours from L1 to adulthood for the replicate to get a relative rate of development.

24 hours after the nematode used in the previous assay had reached adulthood, and every 24 hours thereafter for eight days, the adult nematode was transferred to a new plate. The plate from which the nematode had been transferred was then incubated for an additional 24 hours before being transferred into a 4°C incubator for 30 days. After 30 days, the plates were stained with 200µl of 1% toluidine blue solution and the number of nematodes present was recorded. The total count between all eight plates was recorded as the raw productivity which was then normalized by dividing by the mean raw productivity of the N2 control.

Longevity was measured by further transferring the nematode used above to a new plate as a nine-day adult worm. The worm was then inspected every day to determine if it still survived. A nematode that no longer moved and did not have any apparent pharyngeal pumping was then gently prodded with a worming pick. The day a nematode did not respond to prodding was recorded as its day of death. Raw longevity

was calculated as the number of days between plating the L1 for the time to adulthood assay and the day of death. A relative longevity score was then calculated by dividing the raw longevity by the mean raw longevity of the N2 control.

Data reported for G350 lines has been previously published in Dubie et al. (2020) and has been reanalyzed here.

Mutation accumulation "replay" experiment

To determine if each of the mutations increased in frequency during MA because of selfish drive, mutation-bearing nematodes were propagated in populations with reduced interindividual selection (mirroring the original MA experiment) while tracking the intraindividual dynamics of each mutation over time. To this end, cryopreserved nematodes from the original MA experiment were recovered from generations in which the heteroplasmic frequency of a mutation of interest was low, and previous mtDNA mutations were near fixation (table III-1). Recovered nematodes from each of these generations (G71, G96, G221, and G350) were then propagated in bottlenecked populations ($N = 1$) for three generations to remove grandmaternal effects of freezing. From each generation, a single L4 hermaphrodite was transferred to a new 35mm NGM plate seeded with OP50 as the parental generation (P0) for the "replay" experiment. After 48h, the P0 hermaphrodite was collected, and DNA was extracted by single worm lysis using the Sigma Extract-N Amp kit (catalog #: XNAT2-1KT). The F1 generation was given an additional 48h to develop at which point 25 L4 F1 hermaphrodites were transferred individually to new plates. Every four days thereafter, a single L4

hermaphrodite was transferred from each plate to a new plate to propagate the population for a total of 10 generations. The F5 and F10 progenitor worms were also collected, and DNA was extracted by single worm lysis as day two adults.

Calculation of the frequency of heteroplasmic mutations

The heteroplasmic frequency of Δ*ctb-1* mutations were determined by digital droplet PCR (ddPCR) using previously established methods (Dubie et al. 2020). Each multiplexed reaction was run with 2.2µL of single worm lysate diluted 1:100 with molecular grade water, 11µL Bio-Rad ddPCR supermix for probes (No dUTP) (catalog #: 1863024), 1.1µL Bio-Rad custom ddPCR copy number assay with a 6-carboxyfluorescein (FAM) fluorophore targeting a region within the *ctb-1* deletion (assay ID: dCNS821148280), 1.1µL Bio-Rad custom ddPCR copy number assay with a 5'-Hexachlorofluorescein phosphoramidite (HEX) fluorophore targeting a conserved region of *cox-1* (assay ID: dCNS484374227), and 6.6 µL molecular grade water. The FAM assay used hybridizes to the deleted region of *ctb-1* and so should only fluoresce in droplets when bound to WT mtDNA templates. The HEX assay, which hybridizes with *cox-1*, will fluoresce in droplets with any mtDNA templates, regardless of whether the deletion is present. For each reaction, droplet separation thresholds and concentration of each template were calculated automatically by Quantisoft (Bio-Rad Laboratories) and the heteroplasmic frequency of the deletion was calculated as:

$$f(\Delta\text{mtDNA}) = \frac{cox\ 1\ \text{concentration} - ctb\ 1\ \text{concentration}}{cox\ 1\ \text{concentration}}$$

The heteroplasmic frequency of the *nd5* mutations were determined by examining relative fluorescence in chromatograms generated by Sanger sequencing as described in Dubie et al. (2020). Three independent PCR products were generated from each single worm lysate using standard PCR protocols and primers designed to amplify a region of the *C. elegans nd5* locus which contained all three mutations (forward primer: 5′-TCATCTTCATCTTGGGAGGATTT-3′; reverse primer: 5′-GTGTCCTCAAGGCTACCACC-3′). PCR samples were then sequenced by Eton Biosciences using the forward primer for the *nd5* frameshift mutations and the reverse primer for the *nd5* missense mutation. The generated .ab1 chromatogram files were then visualized in Chromas to generate images that could be processed in FIJI to calculate the heteroplasmic frequency of each mutation.

To measure the heteroplasmic frequency of the $T_8 \rightarrow T_9$ frameshift mutation, the peak heights at the first and second double peak after the poly-T run at mtDNA:11778 were measured in FIJI and substituted into the following formula:

$$f(T_8 \rightarrow T_9) = \frac{((T_9/(A_1 + T_9)) + (A_2/(A_2 + G_1)))}{2}$$

Where A_1 and T_9 are the heights of overlapping peaks at the ninth position of the poly-T run and A_2 and G_1 are the heights of overlapping peaks just after the poly-T run.

The heteroplasmic frequency of the further $T_9 \rightarrow T_{10}$ frameshift mutation was calculated using measurements at the first triple peak after the poly-T run at mtDNA:11778 using the following formulas:

$$f(T_8 \rightarrow T_9) = \frac{A}{A + G + T_{10}}$$

and

$$f(T_9 \rightarrow T_{10}) = \frac{A}{A + G + T_{10}}$$

Finally, the heteroplasmic frequency of the *nd5* missense mutation was determined using measurements of the double peak at mtDNA:12304 and the following formula:

$$f(missense) = \frac{T}{T + C}$$

In each case the calculated frequency from the three sequenced PCR reactions were then averaged to yield a final estimate of the heteroplasmic mutation frequency of each sample. Variation between PCR reactions was low, with an average *CV* = 0.059.

Calculation of mitochondrial copy number

Average mtDNA copy number per cell was measured using ddPCR. In all cases, nematodes were recovered from cryopreserved stocks and replated onto fresh 60mm NGM plates seeded with OP50. DNA from single worms was extracted using the Sigma Extract-N Amp kit (catalog #: XNAT2-1KT). ddPCR was performed as above except that single worm lysates were diluted 1:50 in molecular grade water and the ddPCR copy number assay with a FAM fluorophore targeted a region within the nuclear gene *actin-2* (assay ID: dCNS440514568). The FAM fluorophore fluoresces in droplets that contain *actin-2* nDNA template, and was used as a proxy for nuclear templates found in each sample. The gene *actin-2* was chosen to facilitate comparisons in mtDNA copy number between the current study and those of Dubie et al. (2020) and Gitschlag et al. (2015).

As above, reaction droplet separation thresholds and concentration of each template were calculated automatically by Quantisoft (Bio-Rad Laboratories). mtDNA copy number per cell was calculated as:

$$\frac{2(cox\ 1\ \text{concentration})}{actin\ 2\ \text{concentration}}$$

We measured average mtDNA copy number in the ancestral G71, G96, G135, G221, G300, and G350 lines and in the backcrossed G71, G96, G221, and G350 lines. For the ancestral lines, single-worm DNA was extracted from five randomly selected worms per line. For the backcrossed lines, a single randomly selected worm was used for each of the backcrossed replicate lines (n = 4, 5, 5, and 6 for G71, G96, G221, and G350, respectively).

A few of the ancestral lines appeared to have unusually elevated (G135) or reduced (G221) mtDNA copy number (see results below). It was important to ensure that these changes were actual changes in mtDNA copy number and not variation in the copy number of *actin-2*. To this end, an additional duplexed reaction was performed for three samples each of the ancestral lines. In these reactions the Bio-Rad custom ddPCR copy number assay with a FAM fluorophore was replaced with one targeting a region within the third exon of *daf-3* on the X chromosome (assay ID: dCNS736258201). Otherwise, the reactions were performed as described above. The ancestral mtDNA copy number was multiplied by the number of copies of *actin-2* (*actin-2* concentration per sample/*daf-3* concentration per sample). In all cases, the estimated mtDNA copy number was normalized by the average mtDNA copy number of the WT control from the original MA experiment (Konrad et al. 2017).

Results

Significant decline in fitness with the addition of subsequent mitochondrial mutations.

The productivity, developmental rate, longevity, and survivorship of backcrossed, mitochondrial mutation-bearing lines were compared to each other and a cryopreserved N2 ancestor (pre-MA) of the original mutation accumulation experiment (Katju et al. 2015, 2018). For each fitness trait, nested ANOVA finds a significant variance component for productivity ($F_s' = 55.12$; $P < 0.0001$), developmental rate ($F_s' = 19.42$; $p < 0.0001$), longevity ($F_s' = 2.65$; $p = 0.0298$), and survivorship ($F_s' = 17.04$; $p < 0.0001$) among treatments (table III-2). There is no significant among-line divergence within treatments for productivity, developmental rate, and longevity, but there was for survivorship ($F_s' = 36.5$; $p < 0.0001$) (table III-2).

The backcrossed lines decrease in mean productivity with the addition of each subsequent mutation (figure III-1), with G71, G96, G221, and G350 derived lines producing 247, 234, 165, and 131 progeny on average, respectively. The productivity of all backcrossed lines are significantly reduced compared to the mean pre-MA productivity of 334 progeny (table III-3). Despite the apparent decline in mean fitness, the 5% decline in productivity from G71 to G96 due to the addition of a *nd5* frameshift mutation does not appear significant in pairwise comparisons (table III-3). However, there is a significant decline in fitness from G96 to G221 and from G221 to G350. It is not clear if there would be a greater effect of the first *nd5* frameshift if it were at a higher frequency within individual nematodes.

Developmental rate shows the same pattern as productivity (figure III-1). The backcrossed lines take 0.8%, 4.3%, 8.9%, and 11.7% longer than WT to reach adulthood for G71, G96, G221, and G350, respectively. Despite this trend, only G221 and G350 take significantly longer than the ancestral control (pre-MA) average of 46.2 hours to reach adulthood (table III-3). There is no significant difference between G71 and G96, between G96 and G221, or between G221 and G350. Despite the lack of significance, the trend is for slower development with the addition of each mutation.

Despite the ANOVA analyses suggesting that mitochondrial background had a significant effect on longevity (table III-2), no pairwise comparison shows any significant difference between mutant-bearing lines or pre-MA longevity (table III-3).

Survivorship initially decreases with the addition of each mutation (figure III-1), reducing to 92.8% of pre-MA in G71, 85.3% of pre-MA in G96, and 79.5% of pre-MA in G221. Survivorship appears to increase back to 91.3% in G350. The mean survivorship of all backcrossed lines, apart from G71, are significantly reduced compared to pre-MA (table III-3). When performing comparisons between backcrossed lines from a common ancestor, there are no significant differences between any G71 backcrossed lines. Within G96, there is a significant difference between the line with the highest survivorship, G96.E at 91%, and the line with the lowest survivorship, G96.A with 75% (table III-4). Within the G221 backcrossed lines, both G221.A and G221.D have significantly greater survivorship (89.2% and 87.3%, respectively) than G221.C (table III-4) which had a survivorship of 65.3%. In G350 backcrossed lines, there are significant differences between line G350.N and lines G350.L, G350.M, G350.T, and

G350.U (table III-4). The survivorship of G350 backcrossed lines varied from 97.3% in G350.M to 76% in G350.N.

Selfish drive explains some but not all high frequency mutations.

Ancestral lines, those recovered from the original MA experiment without backcrossing, were propagated in bottlenecked populations for ten generations to remove interindividual competition and reveal intraindividual evolutionary dynamics. For each combination of mutations, a single L4 was selected to begin the experiment. 25 L4 progenies from this generation zero parent nematode were randomly selected to begin 25 replicate, bottlenecked populations. Heteroplasmic frequency was measured in second day adult parent nematodes from generations 0, 5, and 10.

Line G71, in which only the *ctb-1* deletion has arisen in, shows a steady increase in its heteroplasmic frequency of the deletion (figure III-2) likely due to selfish genetic drive. Pairwise comparisons show that there is a significant difference between the means of each generation (figure III-2). The mean percent increase in the heteroplasmic frequency of the deletion across G71 replicates is positive over the course of the entire experiment (figure III-3).

Line G96, in which the *ctb-1* deletion is near fixation but the first *nd5* frameshift mutation is still at a low frequency, does not show any clear evidence of selfish genetic drive. There is no significant difference between the mean heteroplasmic frequency of the frameshift at any generation (figure III-2). While there does appear to be a significant

positive increase in heteroplasmic frequency from generations 0 to 5, there is no such evidence from generations 5 to 10 or from 0 to 10 (figure III-3).

Line G135, in which the *ctb-1* deletion and the first *nd5* frameshift are near fixation but the *nd5* missense mutation is still at a low frequency, shows a steady increase in the heteroplasmic frequency of the missense mutation (figure III-2). Like G71, generation has a significant impact on the mean heteroplasmic frequency. Unlike G71, there is not a significant difference between the mean heteroplasmic frequency at generations 5 and 10. However, there is a significant positive mean percent increase between all generations (figure III-3).

Line G300, in which the *ctb-1* deletion, the first *nd5* frameshift, and the *nd5* missense mutation are near fixation but the second *nd5* frameshift mutation is still at a low frequency, also shows some evidence for selfish genetic drive. Comparisons between generations reveal that there is no significant change from generations 0 to 5 (figure III-2). This is also reflected in the mean percent change from generations 0 to 5 which is not significantly positive (figure III-3). However, when comparing generations 5 to 10 or generations 0 to 10, the pairwise comparisons and the mean percent change in heteroplasmic frequency show a significant positive increase in frequency.

mtDNA copy number in backcrossed and ancestral lines

In the backcrossed lines used for the fitness experiments, all lines had increased mtDNA copy number relative to the WT ancestral control (pre-MA N2) (figure III-4).

G71 had a further increased copy number relative to all other mutation-bearing backcrossed lines (table III-5).

mtDNA copy number in the ancestral lines, in which both nuclear and mitochondrial mutations from the original MA experiment are present, varies more than the backcrossed lines. Only G135 and G221 have significantly different mean mtDNA copy number relative to WT pre-MA (table III-6). G135 is especially noteworthy, having an increase in mtDNA copy number significantly greater than all other ancestral lines. Interestingly, G221 has extremely reduced copy number relative to WT (figure III-5) with an average 19.2% of WT mtDNA copy number. The only differences between G135 and G221 are the frequency of the nd5 missense mutation and the nuclear mutational load. Since mtDNA copy number would not be expected to decrease as the frequency of deleterious mtDNA increased, the low mtDNA copy number found in G221 likely results from some mtDNA copy number controlling nDNA mutation acquired during MA.

The reduced mtDNA copy number in the ancestral G221 lines has been confirmed by ddPCR using DNA extracted from two worm tissue samples preserved in TEN during the original MA experiment. Though there is a significant difference in the mean mtDNA copy number of each sample (ANOVA, $F = 45.72$, $p < 0.0001$), all are significantly lower than WT, ranging from 16.78% of WT (Student's t, $t = 14.62$, $p < 0.0001$) to 32.84% of WT (Student's t, $t = 10.36$, $p < 0.0001$).

To ensure that the differences between samples were due to changes in mtDNA copy number and not due to changes in the concentration of nuclear templates in the

ddPCR samples the samples, a duplexed ddPCR reaction with *daf-3* and *actin-2* probes was performed. This revealed that there is a significant increase of 29.8% *actin-2* templates in ancestral G96 lines and a significant reduction of 40% *actin-2* templates in ancestral G135 lines (table III-7). When correcting for *actin-2* template in each sample (figure 6), G135 is no longer significantly elevated relative to WT (table III-6). The amount of *actin-2* template does not explain the low mtDNA copy number of G211.

When comparing ancestral lines to their corresponding backcrossed lines, both G71 and G221 have significant increases in mitochondrial copy number in the backcrossed lines relative to their corresponding ancestral lines (unpaired t-tests $p = 0.0028$ and $p < 0.0001$ respectively). This difference suggests that some mitochondrial-interacting nuclear element present in generation 71 and 221 of MA was lost during backcrossing. However, whatever these elements were, they were likely lost stochastically throughout the original experimental evolution, as backcrossing seems to have had no effect on mtDNA copy number in either G96 or G350 backcrossed lines.

Discussion

In this study we used populations of *C. elegans* that had been cryopreserved regularly throughout 350 generations of experimental evolution to dissect the impact that subsequent mitochondrial mutations had on a previously identified selfish mitotype. Using nematodes recovered from the original MA experiment (Katju et al. 2015, 2018), we found no evidence for mtDNA mutations that compensated for the deleterious effects of the preceding mutations. We also observed, in the intracellular environment in which they arose, that several different classes of mutations can exhibit a selfish genetic drive.

Even though the mean fitness appears to go down with the addition of each mutation in most of the traits measured, there was little significant difference between G71 and G96 which represents the addition of a *nd5* frameshift mutation to the same mtDNA molecule as the *ctb-1* deletion. This is unexpected since the *nd5* frameshift is expected to reduce the length of the ND5 polypeptide to 41 amino acids from 527. One potential explanation is that in an already dysfunctional mtDNA, the effect of another mitochondrial mutation is masked. This explanation may seem to have some support from the subsequent *nd5* frameshift in G350 which also does not appear to have any further impact on productivity, developmental rate, or longevity than the preceding *nd5* missense mutation in G221. However, the difference in predicted polypeptide sequence between G350 and G96 suggest that there may not be much difference between the fitness phenotype of lines bearing these mutations. Interestingly, the *nd5* missense mutation in G221 does have a significant effect on fitness compared to the *nd5* frameshift mutation that preceded it in G96. In G221, considering the 78.49% and

88.14% heteroplasmic frequencies of the *nd5* frameshift and missense mutations, respectively, nearly every missense mutation must cooccur on the same mtDNA as the frameshift, which is predicted to have no effect on the polypeptide that is translated. The differences in fitness that were measured between G96 and G221 may instead be due to an increase in heteroplasmic frequency of the frameshift mutation from 27.21% to 78.49%. This may be possible to distinguish, but it would require extensive selection and sequencing to create a line in which the frameshift present in G96 is at a high intracellular frequency without the missense mutation present in G221.

An alternative hypothesis is that there may be some anomalous translation within the *nd5* gene, downstream of the premature stop codons introduced by each of the frameshift mutations. There are numerous other potential start codons, both in and out of frame, upstream of the missense mutation and downstream of the premature stop codon. Therefore, it would not be surprising if a new truncated protein was translated from the remaining mRNA transcript. If this were the case then the missense mutation could have a measurable effect on this new protein.

Survivorship appears to vary greatly between backcrossed lines sharing a common mitotype. Despite the mean survivorship being lower, on average, in the backcrossed lines, some backcrossed lines have near WT mean survivorship whereas other exhibit reduced mean survivorship from each mitotype. It is clear that the mitochondrial ~~the~~ mutations in *nd5* do significantly impact survivorship in *C. elegans*, and that there is a mean increase in the survivorship with the addition of a subsequent frameshift mutation between G221 and G350. However, given the high within-mitotype

variance present in the backcrossed lines, there is not enough evidence to support the hypothesis that this increase is due to the compensatory effects of a subsequent mitochondrial mutation.

We found that three of the four mutations had some evidence for intraindividual advantage. The deletion in *ctb-1* has a clear selfish phenotype. This is unsurprising based on our previous study and those done with mtDNA deletions in *C. elegans*, *C. briggsae*, and humans (Estes et al. 2011; Gitschlag et al. 2016; Dubie et al. 2020). G96 is interesting because it does not have a clear sign of selfish drive. In the original MA experiment, its frequency rapidly rose to near fixation and was maintained at this level for almost 100 generations. It is therefore surprising that in our experiment, despite a mostly positive initial change in average heteroplasmic frequency from generation 0 to 5, there was no significant change in average frequency of the *nd5* missense mutation. Why the first frameshift mutation likely rose to high frequency due to drift and the second though selfish genetic drive is unclear at this time and will require more experimental manipulation to uncover.

In our previous study we found that the mtDNA copy number of the G350 lines were, on average, elevated relative to WT pre-MA lines. It has been predicted that increased replication of mitochondria in response to reduced ETC efficiency could be taken advantage of by selfish mtDNA (Chinnery and Samuels 1999; Capps et al. 2003; Gitschlag et al. 2016). As deleterious mtDNA are replicated, the bioenergetic needs of the host cell continue to not be met and further rounds of replication are signaled to meet these needs. With each round of replication, the frequency of the deleterious mtDNA

would increase, making replicating those same mtDNA more likely and driving up mtDNA copy number. In the backcrossed lines, we observed that all lines but G96 had increased mtDNA copy number relative to the WT pre-MA control. Despite the increased frequency of the deletion, and the addition of the subsequent *nd5* frameshift mutation, G96 backcrossed lines have near WT mitochondrial copy number. The subsequent mutation-bearing lines also all seem to have similar mtDNA copy number, though these are all elevated compared to N2. Since most, if not all the mutations are linked in these backcrossed lines, it makes sense that mitochondrial copy number would be similar across each of these backcrossed lines. It is unclear why the *ctb-1* deletion alone has elevated mtDNA copy number relative to the other mutation combinations. One possible explanation could be that at a lower frequency of heteroplasmy, or with fewer mutations present in G71, the cell is less efficient at recognizing deleterious mitochondria and removing them from the cell. Another possible explanation is that the greater cooccurrence of the deletion-bearing mtDNA in mitochondrion also bearing a healthy mtDNA could prevent the host cell from recognizing the selfishly acting mtDNA and targeting them for degradation.

The mitochondrial copy number of the ancestral, non-backcrossed lines is less clear. G71, G96, and G300 are not significantly different than the pre-MA with respect to copy number, though they are also not significantly different from each other or G350 which is significantly greater than the pre-MA. In contrast, G135 and G221 have extremely elevated and reduced mitochondrial copy number, respectively. When comparing the ancestral lines to the backcrossed lines, we see an increase in mtDNA

copy number and, except for G71, the mtDNA copy number remains constant across these lines. This suggests that the difference between copy number is consistent, and that the differences observed (i) between the ancestral and backcrossed lines, and (ii) between ancestral lines are due to some nuclear factor that controls mtDNA copy number. It is interesting to note that the decrease in mtDNA copy number seen in G221 is not observed in backcrossed lines of MA lines from later generations. This suggests that the reduction in ancestral mtDNA copy number may be due to nuclear mtDNA copy number controlling mutations that may have been lost or compensated for by nuclear mutations during MA.

While this study has added to our understanding of subsequent mitochondrial mutations in a shared background, we are unable to analyze the effects of each of these mutations separately. It is possible that the selfishness of the *nd5* missense mutation and frameshift mutation might not appear independent of the original deletion. Instead, each subsequent mutation might contribute more to the selfish drive seen in the original deletion-bearing mtDNA. Until mitochondrial gene engineering improves or the subsequent mtDNA mutations are discovered as isolated, heteroplasmic mtDNA, it will not be possible to fully disentangle the selfish drive of the *ctb-1* deletion from that of the subsequent mutations.

Understanding the intracellular dynamics of mitochondrial mutations is essential to understand mitochondrial diseases and the evolutionary fate of any new mitochondrial mutation. Our study has shown the effect of multiple mitochondrial mutations on a single mtDNA, and on host fitness. We found that the mtDNA mutations that arose

during MA did not compensate for the fitness of previous mutations, nor did they induce subsequently higher mtDNA copy number. Despite this, several of the mtDNA mutations used in this study appear to have selfish genetic drive in combination with the other mtDNA mutations. Furthermore, mutations not predicted to have a phenotypic consequence, such as the missense mutation and the small frameshift mutations, may still have selfish drive like phenotypes.

Tables

Table III-1: Ancestral frequency of each subsequent mtDNA mutation during mutation accumulation. A horizontal bar "-" represents that the mutation had not arisen by that generation. Generations 71, 96, 221, and 350 were selected to be backcrossed for fitness assays. Generations 71, 96, 135, and 300 were selected to test for selfish genetic drive.

Frequency of mutation

	Δctb-1	*nd5 frame shift ($T_8 \rightarrow T_9$)*	*nd5 missense*	*nd5 frame shift ($T_9 \rightarrow T_{10}$)*
pre-MA	-	-	-	-
G71	38.39%	-	-	-
G96	89.59%	27.21%	-	-
G135	80.87%	80.58%	37.79%	-
G221	98.49%	78.49%	88.14%	-
G300	93.58%	60.05%	89.65%	25.94%
G350	87.37%	14.36%	91.15%	77.84%

Table III-2. Two-level nested ANOVA for productivity, developmental rate, longevity, and survivorship to adulthood of ancestral control and backcrossed MA lines of *C. elegans* bearing mtDNA mutations.

Source of variation	df	SS	MS	F_s	F_s'
Productivity					
Among groups	4	18.067	4.517	51.92	55.12****
Among lines	18	1.559	0.087	1.06(n.s.)	
Within lines (error)	307	25.157	0.082		
Total	329	44.724			
Developmental Rate					
Among groups	4	0.720	0.180	10.43	19.42****
Among lines	18	0.311	0.017	1.86(n.s.)	
Within lines (error)	306	2.837	0.009		
Total	328	3.866			
Longevity					
Among groups	4	1.447	0.362	1.82	2.65*
Among lines	18	3.585	0.199	1.46(n.s.)	
Within lines (error)	302	41.216	0.136		
Total	324	46.272			
Survivorship					
Among groups	4	1.328	0.332	4.67	17.04****
Among lines	18	1.281	0.0711	3.65****	
Within lines (error)	313	6.099	0.019		
Total	335	8.787			

*$p < 0.05$
****$p < 0.0001$

Table III-3. Tukey-Kramer HSD method of multiple comparisons among pairs of means in productivity, developmental rate, longevity, and survivorship assays of pre-MA N2 controls and three sets of backcrossed *C. elegans* lines at various generations (71, 96, 221, and 350) with MA mtDNA and pre-MA N2 nDNA.

Productivity

	pre-MA	G71	G96	G221	G350
pre-MA	-	0.144	0.138	0.148	0.132
G71	0.207*	-	0.139	0.149	0.133
G96	0.315*	0.108	-	0.143	0.126
G221	0.547*	0.34*	0.232*	-	0.137
G350	0.641*	0.433*	0.325*	0.093	-

Developmental Rate

	pre-MA	G71	G96	G221	G350
pre-MA	-	0.05	0.048	0.051	0.045
G71	0.008	-	0.048	0.051	0.046
G96	0.043	0.036	-	0.049	0.043
G221	0.089*	0.081*	0.045	-	0.047
G350	0.117*	0.109*	0.074*	0.029	-

Longevity

	pre-MA	G71	G96	G221	G350
pre-MA	-	0.187	0.182	0.172	0.198
G71	0.058	-	0.182	0.172	0.198
G96	0.022	0.036	-	0.166	0.192
G221	0.157	0.099	0.135	-	0.183
G350	0.16	0.102	0.138	0.003	-

Survivorship

	pre-MA	G71	G96	G221	G350
pre-MA	-	0.076	0.073	0.077	0.07
G71	0.066	-	0.071	0.075	0.068
G96	0.142*	0.076*	-	0.072	0.064
G221	0.2*	0.134*	0.058	-	0.069
G350	0.088*	0.022	0.054	0.112*	-

Absolute differences between all pairs listed below the diagonal. Critical HSD values are listed above the diagonal. Comparisons are significant ($\alpha = 0.05$) if their absolute differences are greater than their critical HSD (indicated with an asterisk).

Table III-4. Tukey-Kramer HSD method of multiple comparisons among mean survivorship of backcrossed *C. elegans* lines from a common ancestral population at various generations (71, 96, 221, and 350) with MA mtDNA and pre-MA N2 nDNA.

G71

	A	B	C	D
A	-	0.114	0.114	0.114
B	0.033	-	0.114	0.114
C	0.033	0	-	0.114
D	0.007	0.04	0.04	-

G96

	A	B	C	D	E
A	-	0.147	0.147	0.15	0.147
B	0.087	-	0.147	0.15	0.147
C	0.14	0.053	-	0.15	0.147
D	0.111	0.024	0.029	-	0.15
E	0.16*	0.073	0.02	0.049	-

G221

	A	B	C	D
A	-	0.188	0.188	0.2
B	0.093	-	0.188	0.2
C	0.22*	0.127	-	0.2
D	0.018	0.112	0.238*	-

G350

	M	L	T	U	C	N
M	-	0.159	0.159	0.159	0.159	0.159
L	0.007	-	0.159	0.159	0.159	0.159
T	0.019	0.013	-	0.159	0.159	0.159
U	0.019	0.013	0	-	0.159	0.159
C	0.099	0.093	0.08	0.08	-	0.159
N	0.213*	0.206*	0.193*	0.193*	0.113	-

Absolute differences between all pairs listed below the diagonal. Critical HSD values are listed above the diagonal. Comparisons are significant ($\alpha = 0.05$) if their absolute differences are greater than their critical HSD (indicated with an asterisk).

Table III-5. Multiple comparisons among mean mtDNA copy number in backcrossed *C. elegans* lines from a common ancestral population at various generations (71, 96, 221, and 350) with MA mtDNA and pre-MA N2 nDNA. Means were compared using student's t-test. T ratios are reported with significance indicated by asterisks (*$p < 0.05$, **$p < 0.01$, ***$p < 0.001$). Bold indicates significant t-tests at a family wise $\alpha = 0.05$ corrected by Holm-Bonferroni method.

	backcrossed lines			
	pre-MA	1G71	1G96	1G221
G71	**6.86*** **	-	-	-
G96	3.14*	**4.47** **	-	-
G221	**4.95** **	3.73**	1.41	-
G350	2.78*	3.20*	0.45	0.58

Table III-6. Multiple comparisons among mean mtDNA copy number in ancestral *C. elegans* lines from a mutation accumulation experiment at various generations (71, 96, 135, 221, 300, and 350). Means were compared using student's t-test. T ratios are reported with significance indicated by asterisks (*$p < 0.05$, **$p < 0.01$, ***$p < 0.001$, ****$p < 0.0001$). Bold indicates significant t-tests at a family wise $\alpha = 0.05$ corrected by Holm-Bonferroni method. T ratios above the diagonal were performed using mtDNA copy number normalized by *actin-1* targets per sample. T ratios reported below the diagonal were performed using mtDNA copy number normalized by *daf-3* targets per sample.

	ancestral lines						
	pre-MA	G71	G96	G135	G221	G300	G350
pre-MA	-	2.59*	2.45*	**14.39****	**15.24****	2.20	3.32**
G71	3.22*	-	0.57	**8.33*****	**17.44****	0.57	1.37
G96	**3.88** **	2.26*	-	**5.64*****	**13.83****	1.02	0.72
G135	**4.76** **	0.32	2.06	-	**51.92****	**9.73*****	**5.49*****
G221	**14.39****	**17.45****	**14.40****	**30.21****	-	**17.81****	**16.52****
G300	2.70*	0.80	2.72*	0.55	**17.65****	-	1.83
G350	3.57**	0.94	1.50	1.13	**16.34****	1.64	-

Table III-7. Multiple comparisons among mean *actin-1* templates per *daf-3* template in ancestral *C. elegans* lines from a mutation accumulation experiment at various generations (71, 96, 135, 221, 300, and 350). Means were compared using student's t-test. T ratios are reported with significance indicated by asterisks (*$p < 0.05$, **$p < 0.01$, ***$p < 0.001$, ****$p < 0.0001$). Bold indicates significant t-tests at a family wise $\alpha = 0.05$ corrected by Holm-Bonferroni method.

actin-1 copies per daf-3

	pre-MA	G71	G96	G135	G221	G300
G71	1.41	-	-	-	-	-
G96	**8.44****	3.42*	-	-	-	-
G135	**9.38*****	**7.11****	**14.05*****	-	-	-
G221	2.07	0.01	4.67**	**9.19*****	-	-
G300	1.17	0.32	4.25*	**7.50****	0.38	-
G350	1.50	0.74	**7.21****	**10.13*****	1.07	0.40

Figures

Figure III-1. Decrease in relative fitness of mutant mtDNA with the addition of each subsequent mutation. Relative trait means of backcrossed *C. elegans* lines with MA mtDNA from various generations (71, 96, 221, and 350) and pre-MA N2 nDNA and the pre-MA *N2* control. Mean fitness values for each of the four traits were measured across four G generation 71 derived lines (orange), each with 15 replicates where possible (n = 59-60), five G generation 96 derived lines (grey), each with 15 replicates where possible (n = 68-74), four G generation 221 derived lines (yellow), each with 15 replicates where possible (n = 49-57), six G generation 350 derived lines (dark blue), each with 15 replicates where possible (n = 87-90), and four pre-MA *N2* control lines (light blue), each with 15 replicates where possible (n = 55-60). Phenotypic assays were conducted for four fitness-related traits, namely productivity, developmental rate, longevity, and survivorship to adulthood. For simplicity, the mean relative fitness value for each of the four traits in the control was scaled to a value of 1. All mtDNA mutation-bearing lines perform worse than the wild-type control and the subsequent effect of each mutation results in sequentially worse performance overall.

Figure III-2. Distribution of the heteroplasmic frequency of mitochondrial mutations during 10 generations of experimental evolution. In each case only the frequency of the most recent mtDNA mutation is reported as all other mutations present are near fixation. 25 replicates were propagated in bottlenecked populations, all originating from a single generation 0 parent who's heteroplasmic frequency is reported as a single bar in generation 0 with error bars representing 95% confidence intervals for the estimation of the parents' frequency. One sample t-tests, using the heteroplasmic frequency at generation 0 as the null hypothesis, were used to determine if the heteroplasmic frequency of generations 5 and 10 were significantly different than generation 0. Paired sample t-tests were performed to compare the mean heteroplasmic frequency of each

mutation at generations 5 and 10. Significant comparisons are indicated by asterisks (n.s. $p > 0.05$, *$p < 0.05$, **$p < 0.01$, ***$p < 0.001$, ****$p < 0.0001$).

Figure III-3. Histograms of percent change in heteroplasmic frequency between generations 0 and 5, 5 and 10, and 0 and 10. In each case, the difference in frequency of the most recent mtDNA mutation between the later and former generation is divided by the former. 25 replicates from each line were propagated in bottlenecked populations, all originating from a single generation 0 parent. A horizontal dashed line is placed at a 0% change representing the expected mean if these mutations are evolving under drift. The mean percent change is reported above each graph along with whether this is significantly different from 0% via a one-sample t-test (n.s. $p > 0.05$, *$p < 0.05$, **$p < 0.01$, ***$p < 0.001$, ****$p < 0.0001$).

Figure III-4. A boxplot of mtDNA copy number in backcrossed mutant mitochondria-bearing lines relative to wild-type pre-MA N2. There is an average increase in mtDNA copy number of 89.2%, 34.1%, 47.4%, and 40.0% relative to wild-type pre-MA N2 in backcrossed lines G71, G96, G221, and G3350 respectively.

Figure III-5. A boxplot of mtDNA copy number in ancestral mutant-mitochondria bearing lines relative to wild-type pre-MA N2. There is an average increase in mtDNA copy number of 33.2%, 41.2%, 133.6%, 26.5%, and 51.5% relative to wild-type pre-MA N2 in ancestral lines G71, G96, G135, G300, and G3350 respectively and an average 80.9% decrease in mtDNA copy number relative to wild-type pre-MA N2 in line G221.

Figure III-6. A boxplot of mtDNA copy number in ancestral mutant-mitochondria bearing lines relative to wild-type Pre-MA N2, normalized by *actin-1* copy number. There is an average increase in mtDNA copy number of 44.12%, 83.3%, 40%, 33.9%, and 57.4% relative to wild-type pre-MA N2 in ancestral lines G71, G96, G135, G300, and G3350 respectively and an average 75.6% decrease in mtDNA copy number relative to wild-type pre-MA N2 in line G221.

Figure III-1. Decrease in relative fitness of mutant mtDNA with the addition of each subsequent mutation**.**

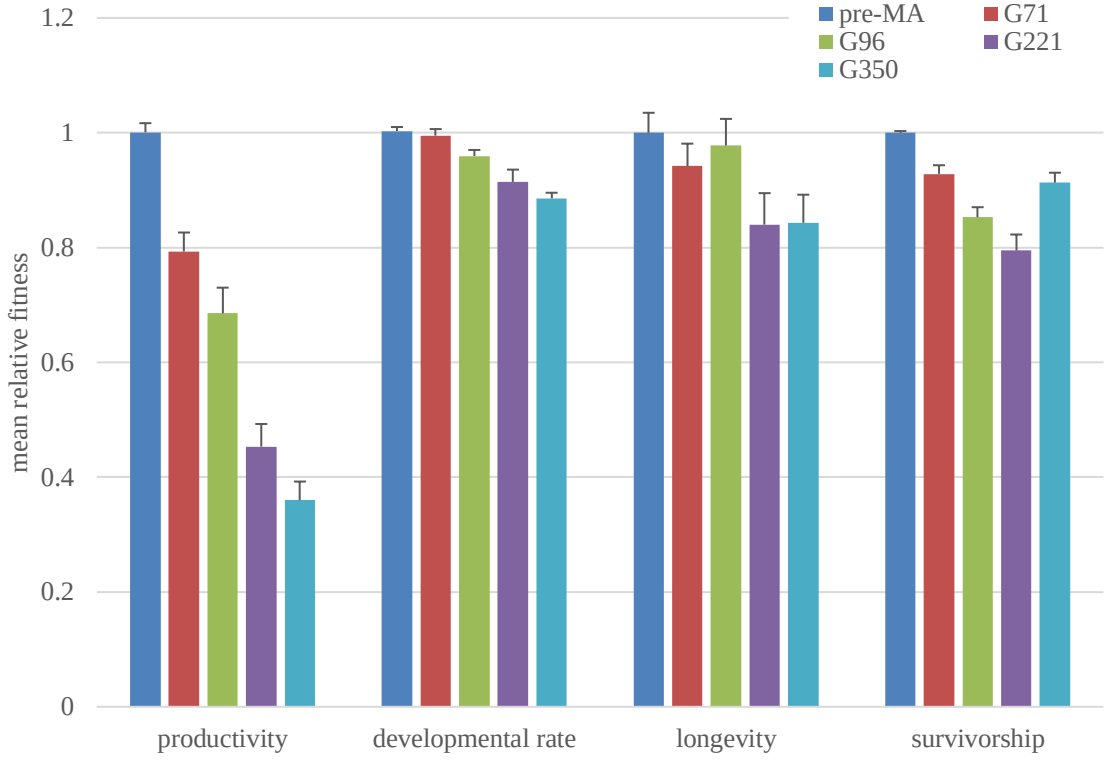

Figure III-2. Distribution of the heteroplasmic frequency of mitochondrial mutations during 10 generations of experimental evolution.

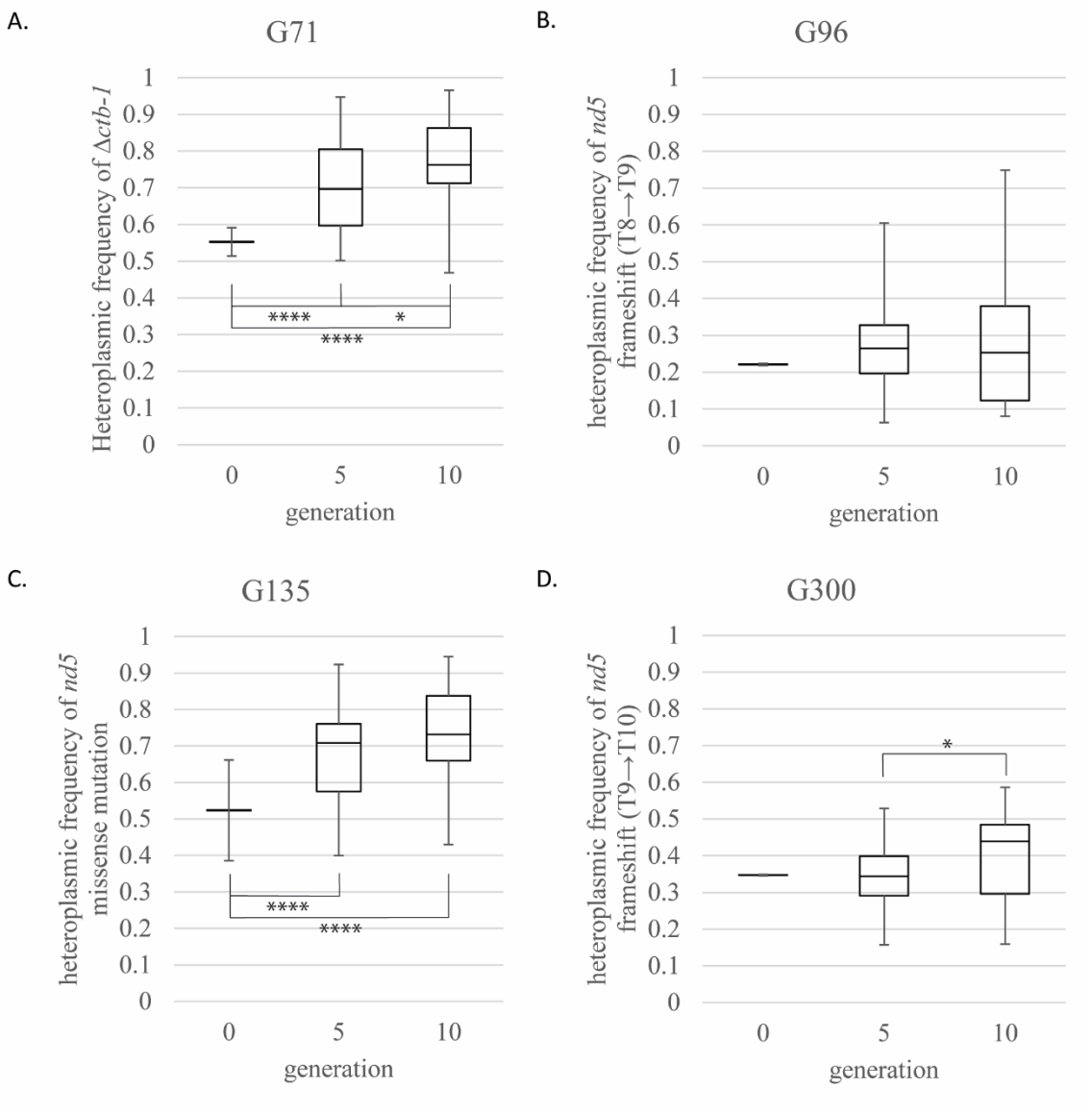

Figure III-3. Histograms of percent change in heteroplasmic frequency between generations 0 and 5, 5 and 10, and 0 and 10.

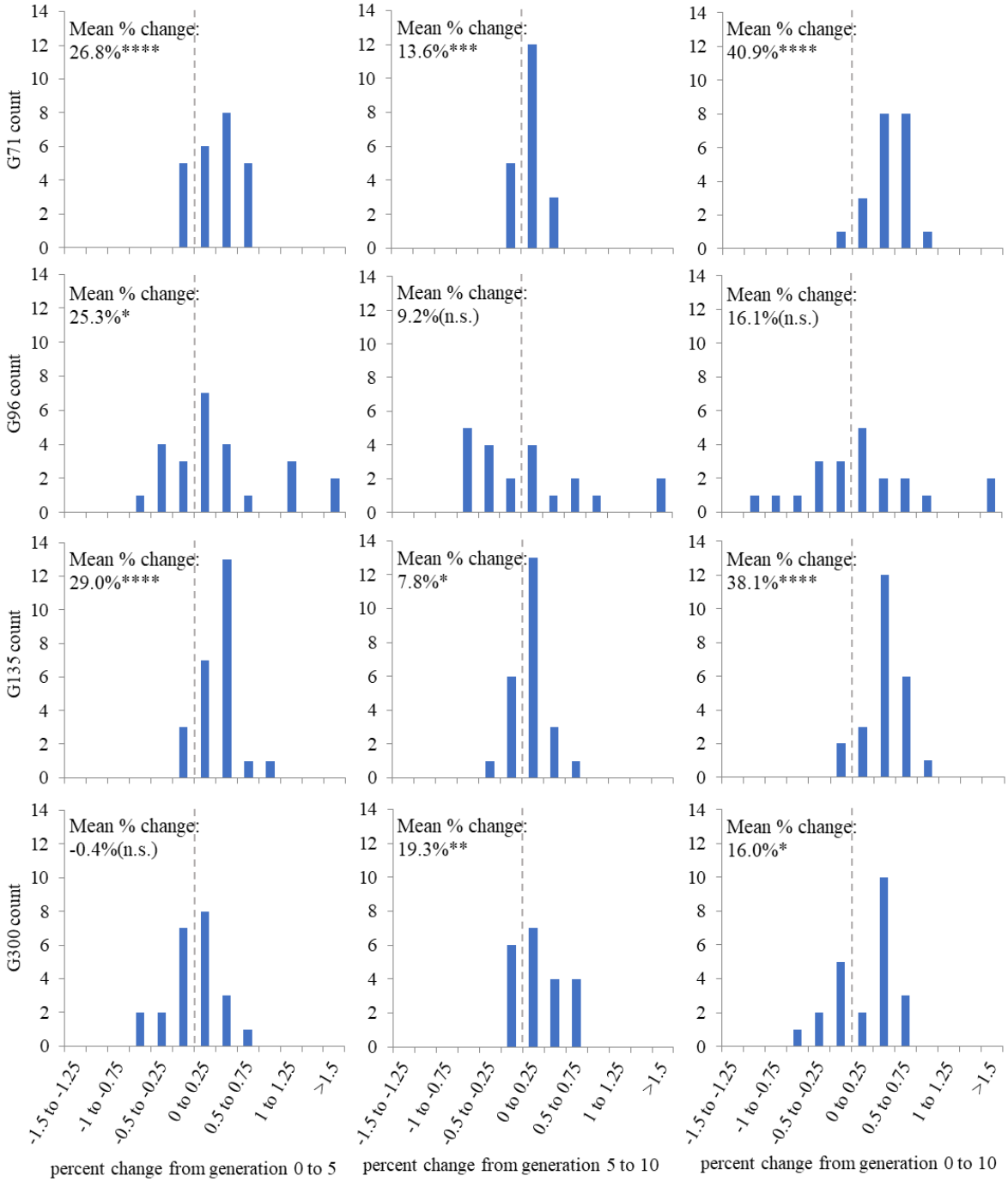

Figure III-4. A boxplot of mtDNA copy number in backcrossed mutant-mitochondria bearing lines relative to wild-type pre-MA N2.

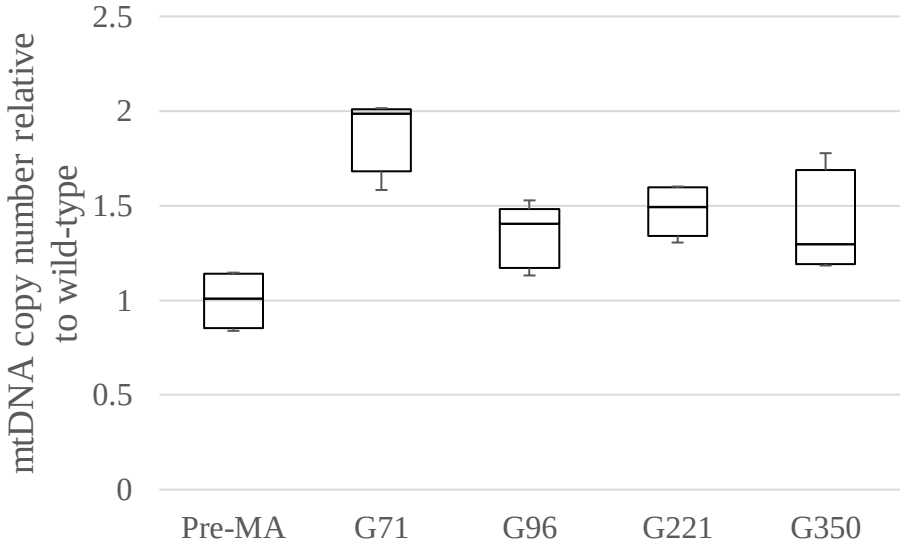

Figure III-5. A boxplot of mtDNA copy number in ancestral mutant-mitochondria bearing lines relative to wild-type pre-MA N2.

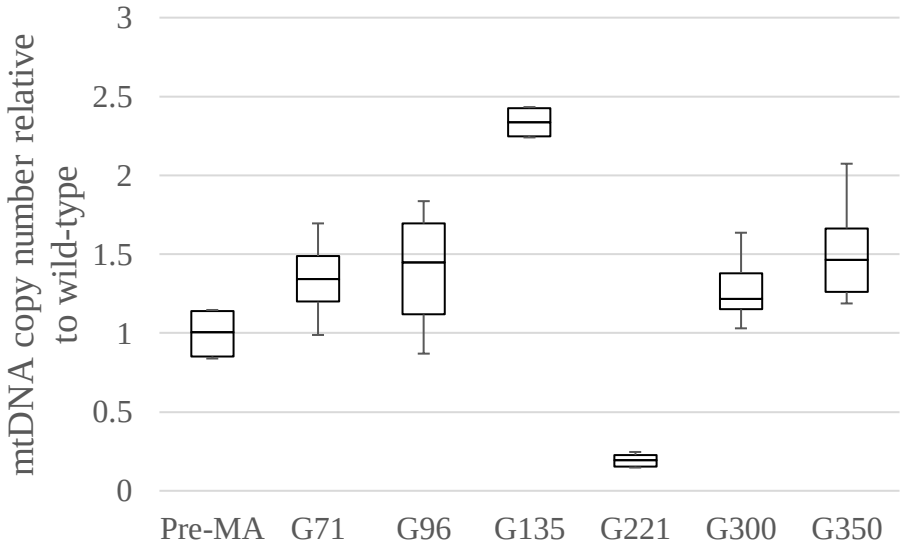

Figure III-6. A boxplot of mtDNA copy number in ancestral mutant-mitochondria bearing lines relative to wild-type Pre-MA N2, normalized by *actin-1* copy number.

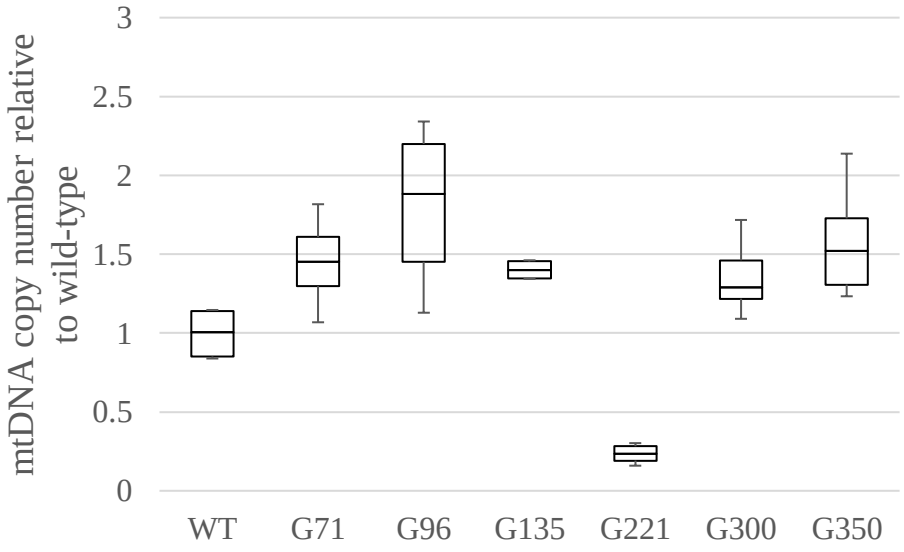

References

Anderson JL, Morran LT, Phillips PC. 2010. Outcrossing and the maintenance of males within C. elegans populations. *J Hered*. **101**(Suppl 1):S62-74. (doi:10.1093/jhered/esq003)

Burton RS, Pereira RJ, Barreto FS. 2013. Cytonuclear genomic interactions and hybrid breakdown. *Annu. Rev. Ecol. Evol. Syst*. **44**:281-302. (doi:10.1146/annurev-ecolsys-110512-135758)

Campbell GR, Reeve AK, Ziabreva I, Reynolds R, Turnbull DM, Mahad DJ. 2013. No excess of mitochondrial DNA deletions within muscle in progressive multiple sclerosis. *Mult Scler*. **19**(14):1858-66. (doi:10.1177/1352458513490547)

Capps GJ, Samuels DC, Chinnery PF. 2003. A Model of the nuclear control of mitochondrial DNA replication. *J. theor. Biol.* **221**:565-583. (doi:10.1006/jtbi.2003.3207)

Chinnery PF, Samuels DC. 1999. Relaxed replication of mtDNA: A model with implications for the expression of disease. *Am. J. Hum. Genet.* **64**:1158-1165. (doi:10.1086/302311)

Clark KA, Howe DK, Gafner K, Kusuma D, Ping S, Estes S, Denver DR. 2012. Selfish little circles: transmission bias and evolution of large deletion-bearing mitochondrial DNA in *Caenorhabditis briggsae* nematodes. *PLoS One*. **7**:e41433. (doi:10.1371/journal.pone.0041433)

Cosmides LM, Tooby J. 1981. Cytoplasmic inheritance and intragenomic conflict. *J Theor Biol*. **89**(1):83-129. (doi:10.1016/0022-5193(81)90181-8)

Doolittle RF. 1981. Similar amino acid sequences: chance or common ancestry? *Science*. **214**(4517):149-59. (doi:10.1126/science.7280687)

Dubie JJ, Caraway AR, Stout MM, Katju V, Bergthorsson U. 2020. The conflict within: origin, proliferation and persistence of a spontaneously arising selfish mitochondrial genome. *Phil. Trans. R. Soc. B*. **375**:20190174. (doi:10.1098/rstb.2019.0174)

Eberhard WG. 1980. Evolutionary consequences of intracellular organelle competition. *Q. Rev. Biol.* **55**:231-249. (doi:10.1086/411855)

Estes S, Coleman-Hulbert AL, Hicks KA, de Haan G, Martha SR, Knapp JB, Smith SW, Stein KC, Denver DR. 2011. Natural variation in life history and aging phenotypes is associated with mitochondrial DNA deletion frequency in *Caenorhabditis briggsae*. *BMC Evol Biol.* **11**:11. (doi:10.1186/1471-2148-11-11)

Fujii S, Bond CS, Small ID. 2011. Selection patterns on restorer-like genes reveal a conflict between nuclear and mitochondrial genomes throughout angiosperm evolution. *Proc Natl Acad Sci U S A*. **108**(4):1723-8. (doi:10.1073/pnas.1007667108)

Gemmell NJ, Metcalf VJ, Allendorf FW. 2004. Mother's curse: the effect of mtDNA on individual fitness and population viability. *Trends Ecol Evol*. **19**(5):238-44. (doi:10.1016/j.tree.2004.02.002)

Gitschlag BL, Kirby CS, Samuels DC, Gangula RD, Mallal SA, Patel MR. 2016. Homeostatic responses regulate selfish mitochondrial genome dynamics in *C. elegans*. *Cell Metab*. **24**:91-103. (doi:10.1016/j.cmet.2016.06.008)

Gray MW. 2012. Mitochondrial evolution. *Cold Spring Harb Perspect Biol*. **4**(9):a011403. (doi:10.1101/cshperspect.a011403)

Havird JC, Forsythe ES, Williams AM, Werren JH, Dowling DK, Sloan DB. 2019. Selfish mitonuclear conflict. *Curr Biol*. **29**(11):R496-R511. (doi:10.1016/j.cub.2019.03.020)

Kairo A, Fairlamb AH, Gobright E, Nene V. 1994. A 7.1 kb linear DNA molecule of Theileria parva has scrambled rDNA sequences and open reading frames for mitochondrially encoded proteins. *EMBO J*. **13**: 898-905. (doi:10.1002/j.1460-2075.1994.tb06333.x)

Katju V, Packard LB, Bu L, Keightley PD, Bergthorsson U. 2015 Fitness decline in spontaneous mutation accumulation lines of *Caenorhabditis elegans* with varying effective population sizes. *Evolution* **69**:104-116. (doi:10.1111/evo.12554)

Katju V, Packard LB, Keightley PD. 2018 Fitness decline under osmotic stress in *Caenorhabditis elegans* populations subjected to spontaneous mutation accumulation at varying population sizes. *Evolution* **72**:1000-1008. (doi:10.1111/evo.13463)

Klucnika A, Ma H. 2019. Mapping and editing animal mitochondrial genomes: can we overcome the challenges? *Phil. Trans. R. Soc. B*. **375**:20190187. (doi:10.1098/rstb.2019.0187)

Konrad A, Thompson O, Waterston RH, Moerman DG, Keightley PD, Bergthorsson U, Katju V. 2017. Mitochondrial mutation rate, spectrum and heteroplasmy in *Caenorhabditis elegans* spontaneous mutation accumulation lines of differing population size. *Mol. Biol. Evol.* **34**:1319-1334. (doi:10.1093/molbev/msx051)

Koonin EV. 2010. The origin and early evolution of eukaryotes in the light of phylogenomics. *Genome Biol.* **11**(5):209. (doi:10.1186/gb-2010-11-5-209)

Lang BF, Burger G, O'Kelly CJ, Cedergren R, Golding GB, Lemieux C, Sankoff D, Turmel M, Gray MW. 1997. An ancestral mitochondrial DNA resembling a eubacterial genome in miniature. *Nature*. **387**:493-497. (doi:10.1038/387493a0)

Lee Y, Hwang W, Jung J, Park S, Cabatbat JJ, Kim PJ, Lee SJ. 2016. Inverse correlation between longevity and developmental rate among wild *C. elegans* strains. *Aging* **8**:986-999. (doi:10.18632/aging.100960)

Liau WS, Gonzalez-Serricchio AS, Deshommes C, Chin K, LaMunyon CW. 2007. A persistent mitochondrial deletion reduces fitness and sperm performance in heteroplasmic populations of *C. elegans*. *BMC Genet*. **29**:8:8. (doi:10.1186/1471-2156-8-8)

Lin YF, Schulz AM, Pellegrino MW, Lu Y, Shaham S, Haynes CM. 2016. Maintenance and propagation of a deleterious mitochondrial genome by the mitochondrial unfolded protein response. *Nature*. **533**(7603):416-9. (doi:10.1038/nature17989)

Ma H, O'Farrell PH. 2016. Selfish drive can trump function when animal mitochondrial genomes compete. *Nat Genet*. **48**(7):798-802. (doi:10.1038/ng.3587)

MacAlpine DM, Kolesar J, Okamoto K, Butow RA, Perlman PS. 2001. Replication and preferential inheritance of hypersuppressive petite mitochondrial DNA. *EMBO J.* **20**(7):1807-17. (doi:10.1093/emboj/20.7.1807)

Margulis L. 1970. Origin of eukaryotic cells. New Haven, CT: Yale University Press; 1970.

Martin W, Müller M. 1998. The hydrogen hypothesis for the first eukaryote. *Nature.* **392**(6671):37-41. (doi:10.1038/32096)

Martin W, Hoffmeister M, Rotte C, Henze K. 2001. An overview of endosymbiotic models for the origins of eukaryotes, their ATP-producing organelles (mitochondria and hydrogenosomes), and their heterotrophic lifestyle. *Biol Chem*. **382**(11):1521-39. (doi:10.1515/BC.2001.187)

Pinto M, Moraes CT. 2015. Mechanisms linking mtDNA damage and aging. *Free Radic. Biol. Med.* **85**:250-258. (doi:10.1016/j.freeradbiomed.2015.05.005)

Stiernagle T. 2006. Maintenance of *Caenorhabditis elegans. WormBook*. 1-11. (doi:10.1895/wormbook.1.101.1)

Sullins JA, Coleman-Hulbert AL, Gallegos A, Howe DK, Denver DR, Estes S. 2019. Complex transmission patterns and age-related dynamics of a selfish mtDNA deletion. *Integr Comp Biol*. **59**(4):983-993. (doi:10.1093/icb/icz128)

Suthammarak W, Morgan PG, Sedensky MM. 2010. Mutations in mitochondrial complex III uniquely affect complex I in *Caenorhabditis elegans*. *J Biol Chem*. **285**(52):40724-40731. (doi:10.1074/jbc.M110.159608)

Tam ZY, Gruber J, Halliwell B, Gunawan R. 2013. Mathematical modeling of the role of mitochondrial fusion and fission in mitochondrial DNA maintenance. *PLoS One*. **8**(10):e76230. (doi:10.1371/journal.pone.0076230)

Taylor DR, Zeyl C, Cooke E. 2002. Conflicting levels of selection in the accumulation of mitochondrial defects in *Saccharomyces cerevisiae*. *Proc Natl Acad Sci U S A*. **99**(6):3690-4. (doi:10.1073/pnas.072660299)

Tsang WY, Lemire BD. 2002. Stable heteroplasmy but differential inheritance of a large mitochondrial DNA deletion in nematodes. *Biochem Cell Biol*. **80**(5):645-54. (doi:10.1139/o02-135)

Wallace DC. 1992. Mitochondrial genetics: a paradigm for aging and degenerative diseases? *Science*. **256**:628-32. (doi:10.1126/science.1533953)

CHAPTER IV

SELFISH BEHAVIOR OF A *COI* DELETION-BEARING MITOTYPE IN *CAENORHABDITIS ELEGANS*

Introduction

Mitochondria are small, nearly ubiquitous, energy-producing organelles found in eukaryotes that formed due to an endosymbiosis event billions of years ago (Martin et al. 2015). Since then, many of their cellular processes have been taken over by the eukaryotic host cell, leaving them with greatly reduced genomes (Lang et al. 1999) that contain only a few components essential for their energy production and replication. However, despite the control exerted by host cells, mitochondria remain highly dynamic structures (Westermann 2010) that replicate independent of the cell cycle (Fontana and Gahlon 2020). Because of their independence, selection acts on mitochondria differently depending on the level of organization, transitioning from organismal fitness at the population level through transmission advantage and replicative advantage at the level of individual mitochondrial genomes (mtDNA) (Birky 1973; Rand 2001; Ma et al. 2016). In addition, the high number of mitochondria within individual cells (Shmookler and Goldstein 1983; Tsang and Lemire 2002; Bianconi et al. 2013) dilutes the phenotypic consequences of any individual mitochondrial mutations (Rossignol et al. 2003; Haig 2016), reducing the strength of natural selection for cellular function and favoring mtDNA replication. These factors together create opportunities for selfish mitotypes, which have an intracellular advantage over wild-type (WT) mitotypes

and increase in frequency, despite the deleterious effects that selfish mitotypes may have on their host's fitness (Hurst and Werren 2001; Clark et al. 2012; Ma and O'Farrell 2016).

The phenomenon of mitotypes behaving selfishly is well documented (Havird et al. 2019) and has been implicated in diseases caused by mtDNA mutations (Taylor and Turnbull 2005; Wallace 2005; Sharpley et al. 2012; Wallace and Chalkia 2013; Stewart and Chinnery 2015), but much experimental work needs to be done to determine why some mitotypes are selfish and others are not. The "moral hazard hypothesis" contends that a cellular response to poorly performing mitochondria is to increase mitochondrial replication without discriminating between healthy and deleterious mtDNA. Replicating poorly performing mitochondria results in positive feedback by creating more deleterious copies without meeting the cell's bioenergetic needs. This positive feedback loop results in further mitochondrial biogenesis with a greater probability of replicating deleterious mtDNA (Kowald and Kirkwood 2014, 2018). There is some evidence for this phenomenon in *Caenorhabditis elegans* with the *uaDf5* deletion (Gitschlag et al. 2016), in *C. briggsae* with the *nd5*Δ mitotype (Clark et al. 2012), and in modeling studies (Capps et al. 2003). However, more detailed experimental studies are needed with a variety of different mitotypes to determine the conditions under which the moral hazard hypothesis is applicable.

Another hypothesis is that selfishness can arise when a deleterious mitotype replicates faster than the WT (Wallace 1989; Lawless et al. 2020). This hypothesis originates from the observation that many of the known selfish mitotypes are deletions,

such as the “petite” mutation in yeast (Chen and Clark-Walker 2000), an *nd5* deletion in *C. briggsae* (Clark et al. 2012), and the large deletion-bearing *uaDf5* mitotype in *C. elegans* (Gitschlag et al. 2016). The deletions in “petite” yeast create pseudo-*ori* sequences, which promote the recruitment of polymerases and increase the rate of replication (MacAlpine et al. 2001; Chen and Clark-Walker 2018). While the creation of new origins of replication has not been seen in *Caenorhabditis* species, the mechanism by which they replicate their mtDNA may support the faster replication of mtDNA deletions. In *C. elegans*, mtDNA is replicated as a single multimeric molecule via a rolling circle mechanism like that seen in bacteriophages (Lewis et al. 2015). As a result, deletion-bearing mitotypes may have a replicative advantage in producing a greater number of mtDNA copies per DNA multimer during a single instance of replication.

To robustly test these hypotheses and better understand mitochondrial biology, it is essential that we have a large catalog of mutant mitotypes to examine. Unfortunately, despite the many recent increases in our capacity to engineer and manipulate nuclear genomes (nDNA) in many varied organisms (Carroll 2017), it remains difficult and unreliable to engineer mtDNA (Klucnika and Ma 2019). The difficulties in engineering mtDNA are due predominately to its many copies and infrequent recombination.

Bypassing the need to engineer mtDNA mutations, Katju et al. (2015, 2018) spontaneously generated new mutant-bearing mitotypes in *C. elegans* through mutation accumulation experiments (MA) over 409 generations. Following the termination of the MA experiment and whole-genome sequencing of extant MA lines, Konrad et al. (2017) identified several mitotypes that appeared to be good candidates for selfishness. These

selfish mitotype candidates contained large, high frequency, heteroplasmic mtDNA deletions. Previously, we showed that a mitotype bearing a 499 bp deletion in the *cytochrome b(1)* gene (Δ*ctb-1*), had both a deleterious effect on host fitness and a transmission advantage over WT mitotypes (Dubie et al. 2020).

In this study, we examine the fitness consequences and evolutionary dynamics of a mitotype bearing a 1185 bp deletion within the Cytochrome c oxidase subunit 1 encoding gene, *COI*. We then experimentally manipulated populations of *C. elegans* to determine how the heteroplasmic frequency of the deletion-bearing mitotype (Δ*COI*) was impacted by varying the amount of interindividual selection. Finally, we discuss the similarities and differences between the selfish behavior of Δ*COI* and Δ*ctb-1*.

Methods

Worms and culture methods

A 1185 bp deletion in the mitochondrial *COI* gene originated in one replicate line (10C) of a long-term *C. elegans* spontaneous MA experiment with varying population sizes conducted over 409 consecutive generations (Katju et al. 2015; Konrad et al. 2017; Katju et al. 2018). Line 10C was propagated in populations of hermaphrodites bottlenecked to ten individuals each generation ($N = 10$). After 409 generations of MA, whole-genome sequencing of all MA lines and their ancestral pre-MA control was conducted via Illumina paired-ends sequencing and all mtDNA mutations across the 35 MA lines were identified (Konrad et al. 2017). Two mtDNA mutations were found in MA line 10C: (i) a 1185 bp in-frame deletion within the mitochondrial *COI* gene

(frequency 82%), and (ii) a single T insertion in a homopolymeric run within the *nd1* gene [(T)8 → (T)9; frequency 2%]. During the spontaneous MA experiment, *C. elegans* from line 10C were cryogenically preserved at -86°C and tissue samples were collected and preserved in TEN (20mM Tris, 50mM EDTA, 100mM NaCl) at generations 25, 55, 77, 100, 133, 150, 172, 251, 300, 350, and 408. *C. elegans* can survive long term storage at temperatures below -80°C, permitting the recovery of live worms from various points throughout the original MA experiment. In cases where worms were recovered from cryopreserved stocks, recovered worms were propagated for two generations prior to experimental manipulation to remove grandmaternal effects of freezing (Hu et al. 2015; Vita-More and Barranco 2015; Stastna et al. 2020).

To sequester the Δ*COI* mtDNA in lines with WT nDNA, seven backcrossed lines (10C.B, D, F, H, I, J, and M) were generated using previously published methods (Dubie et al. 2020; chapters II and III). Briefly, 10C hermaphrodites thawed from cryopreserved generation 408 stocks were crossed to *fog-2*(*lf*) worms for 13 generations. These lines were then backcrossed to WT N2 males for an additional 2 generations. In each generation, the 10C derived hermaphrodites transferred their Δ*COI* mtDNA to their progeny while outcrossing with a male *fog-2*(*lf*) produces obligately outcrossing progeny (Schedl and Kimble 1988; Hu et al. 2019) with a lower nDNA mutational load from the MA experiment. The final 2 generations of backcrossing to WT N2 males converted the progeny back into facultatively outcrossing hermaphrodites with Δ*COI* mtDNA and approximately 3.05×10^{-3} percent of the MA nDNA mutational load.

Calculation of heteroplasmic frequency and mtDNA copy number by ddPCR

Heteroplasmic frequency of Δ*COI* mtDNA and mtDNA copy number within worms was measured via ddPCR using Bio-Rad's QX100 Droplet Digital PCR system. In each case, DNA samples were diluted in molecular-grade water. A 10-fold dilution was used for single-worm DNA extracts. DNA extracted from frozen tissues was diluted to concentration 0.05ng/µl. All ddPCR was performed as multiplexed reactions using previously published reaction parameters (Dubie et al. 2020). To determine the heteroplasmic frequency of Δ*COI* in a sample, an assay targeting a region within the *COI* deletion (assay ID: dCNS200119854) was used to quantify the concentration of WT templates. In the same reaction, an assay targeting a WT *ctb-1* region of mtDNA (assay ID: dCNS141090989) was used to quantify the total concentration of mtDNA templates. The heteroplasmic frequency of Δ*COI* was defined as:

$$f(\Delta COI) = \frac{\text{total mtDNA concentration} - \text{WT mtDNA concentration}}{\text{total mtDNA concentration}}$$

To determine mtDNA copy number in a sample, we utilized the previously mentioned assay targeting WT *ctb-1*. This assay was used alongside another assay targeting *actin-1* (assay ID: dCNS257340490) to quantify the concentration of nDNA templates present in the sample. The copy number of mtDNA in a sample was calculated by dividing the concentration of WT *ctb-1* templates (total mtDNA) by half of the concentration of *actin-1* templates (total nDNA) in the sample.

Trajectory of ΔCOI during mutation accumulation

Over the course of a long-term *C. elegans* spontaneous MA experiment with varying population sizes (Katju et al. 2015, 2018), a 1185 bp deletion within *COI* arose in population 10C (named for its bottlenecked population size, $N = 10$, and replicate line C). Konrad et al. (2017) detected the mutation in the 10C line via Illumina HiSeq of DNA extracted worms recovered from cryopreserved stocks of the 10C line after 409generations of MA. Using this method, they estimated the heteroplasmic frequency of Δ*COI* to be 82% within the 10C lines at the end of the MA experiment.

To determine the origin and trajectory of Δ*COI* during MA, DNA was extracted from worm tissues frozen in TEN from generations 25, 55, 77, 100, 133, 150, 172, 251, 300, 350, and 408 of the original MA experiment (Konrad et al. 2017) using the Qiagen Puregene Genomic DNA Tissue Kit (cat. No. 158622). The presence of the mutation was detected by PCR across the deletion using primers 5'-TAA TGT GCT AAT AAT TAT GTT-3' and 5'-AAC TCA AGG GTA TGA ACC TTA C-3'. These primers flank the deletion, producing a 1736 bp product when amplifying WT template and a 551 bp product when amplifying Δ*COI* template. The heteroplasmic frequency of Δ*COI* was then determined using DNA from each generation in which the deletion was detected (MA generations 350 and 408) and the preceding generation (MA generation 300) by multiplexed ddPCR reactions as described above.

Fitness assays

The first criterion of selfishness is that a mitotype must either be neutral or engender some cost to the overall fitness of its host. To determine if there is a fitness cost to bearing Δ*COI* mtDNA, four fitness-related traits, namely (i) productivity, (ii) developmental rate, (iii) longevity, and (iv) survivorship to adulthood were measured using standard *C. elegans* procedures with previously published modifications (Dubie et al. 2020). Briefly, from seven lines generated by backcrossing MA generation 409 10C lines (10C.B, D, F, H, I, J, and M) and an N2 control, a population of worms was recovered from cryogenically preserved stocks. From each of these populations, 25 individual L4 hermaphrodites were transferred singly onto NGM plates to lay eggs for 48h. From each of these 25 plates, a single L1 was transferred by picking to a new NGM plate for the developmental rate, productivity, and longevity assays. An additional 10 L1 siblings from each plate were transferred to a single plate for the survivorship assay.

Time to adulthood (or developmental rate) was measured by physically inspecting the worms every 2 hours and recording how many hours it took for them to reach adulthood. Worms were said to have reached adulthood when their first egg had developed and migrated into their uterus. These worms were allowed to lay eggs for 24 hours and were then transferred to a new NGM plate every subsequent 24 hours for eight days. The plate from the previous day was incubated for an additional 24 hours to allow eggs to hatch before being transferred to 4°C for 30 days. To these plates, 300µL of 0.075% Toluidine blue was added to increase contrast between progeny and the plate, assisting the ease of counting the number of progenies present on each plate.

Productivity was scored as the sum of progeny produced by each worm over the course of the eight days.

After the worm had been transferred for eight days, it was inspected daily. If a worm appeared immobile and/or failed to respond to gentle prodding, it was determined to have died. Longevity was then scored as the number of days from when the original L1 was transferred for the developmental rate assay to death.

Using the plates with 10 L1 siblings, survivorship was scored as the proportion of worms that survived to adulthood on a scale from 0 to 1. Time to adulthood was converted into developmental rate by dividing each worm's time to adulthood by the mean time to adulthood for the N2 controls. All analyses were done using raw fitness measurements.

Experimental evolution with reduced interindividual selection

The second criterion of selfishness is that a mitotype must have some intraindividual advantage, either transmissive or replicative, over other mitotypes present within the host. To observe intraindividual dynamics of Δ*COI*, populations of worms were propagated by bottlenecking ($N = 1$) to reduce the efficacy of interindividual selection. Worms were recovered from cryopreserved MA generation 350 and a population of worms backcrossed from generation 350 (see methods above). From the recovered worms, five L4 hermaphrodites were transferred individually to NGM plates for both MA and backcrossed worms. From the progeny of these generation 0 worms, five L4s were randomly selected as the progenitors of the bottlenecked populations.

Generation 1 worms were allowed to lay eggs for 24h and then were collected for single-worm DNA extraction (total of 50, 25 MA background and 25 WT background) using the InVivo Biosystems *C. elegans* Lysis/DNA Extraction Kit (Cat No: PCR101). The next day, an L4 hermaphrodite was transferred singly to a new plate and allowed to lay eggs. Every three days thereafter, a single L4 hermaphrodite was transferred from among the progeny to a new plate to propagate the population. Parent worms were collected for single-worm DNA extraction as day two adults at the 5^{th} and 10^{th} generations. Single-worm DNA extracts were used to quantify heteroplasmic frequency of Δ*COI* via ddPCR.

Experimental evolution with interindividual selection

The effect of interindividual selection on the intraindividual heteroplasmic frequency of Δ*COI* was determined by propagating large populations of backcrossed worms with a high heteroplasmic frequency of Δ*COI*. Backcrossed worms were recovered from cryopreserved stocks. From the recovered worms, 100 L4 hermaphrodites were transferred to large 100mm NGM plates in benign conditions with abundant food (1ml OP50) to establish seven large populations. Each population was synchronized and transferred to a new 100mm NGM plate with abundant food by bleaching (Stiernagle 2006) every four days to prevent overlapping generations for a total of 75 generations. From each population, single-worm DNA extractions were performed with 30 L4 worms each from generations 0, 30, and 75. Δ*COI* frequency and

mtDNA copy number were measured in eight randomly selected single-worm extracts from each population at each generation.

Results

Origin of the COI deletion in the 10C Mutation Accumulation line.

Over the course of a previous MA experiment (Katju et al. 2015, 2018), in which *C. elegans* were kept in bottlenecked populations (N = 10) for 409 generations, an in-frame 1185 bp deletion within *COI* spontaneously arose in MA line 10C (Konrad et al. 2017). While in frame, the deletion removes 84.9% of the total *COI* coding sequence, leaving only the first 93 and the last 324 bases. This is predicted to result in a truncation of the original COI protein, to only 130 amino acids from the original 525.

Throughout the course of MA experiment, the 10C line was cryopreserved (both tissue and live worms) every 25-50 generations (Katju et al. 2015, 2018). We screened these previous generations by PCR to confirm the presence of Δ*COI*. We further performed ddPCR on preserved worm tissue to determine the average heteroplasmic frequency of Δ*COI* within worms at each generation available. Δ*COI* is first detected in generation 350 of MA, suggesting that it arose sometime between the preceding cryopreserved generation, 300, and generation 350. At generation 350, Δ*COI* had an average heteroplasmic frequency of 24.5%. By the end of the experiment at MA generation 409, this frequency had increased to 68.8%. While this is less than the 82% reported previously for this mutation (Konrad et al. 2017), this difference could be explained by fluctuations in heteroplasmic frequency during cryopreservation. In fact,

the original 82% reported by Konrad et al. (2017) is closer to what is observed when the frequency of individual worms recovered from cryopreservation is tested (see below). This suggests that though the 82% estimate may not reflect generation 409 as closely, it is more similar to the frequency of Δ*COI* within worms that can be recovered from cryopreservation.

There is an additional mtDNA mutation detected in the original MA experiment. A single base pair frameshift in mitochondrially encoded NADH:ubiquinone oxidoreductase core subunit 1 gene (*ND1*) was detected at a heteroplasmic frequency of 2% by Konrad et al. (2017). We were unable to confirm the presence of this mutation. Its location in a poly-thymine run makes it a poor target for differentially binding probes, like in ddPCR applications, and its low frequency prevented us from detecting it by Sanger sequencing.

Significant fitness decline in Δ*COI-bearing lines.*

To determine whether the Δ*COI* mitotype is selfish, it is important to first establish whether there are any fitness costs associated with bearing the Δ*COI* mitotype. Lines bearing the Δ*COI* mitotype were first backcrossed into worms bearing WT nDNA. This backcrossing removed the nuclear mutational load that had accumulated during MA so that the fitness consequences of Δ*COI* could be more directly measured. Productivity, developmental rate, survivorship, and longevity were assayed in seven backcrossed lines (10C.B, 10C.D, 10C.F, 10C.H, 10C.I, 10C.J, and 10C.M) and the WT N2 ancestor used for the backcrossing, with 15 replicates of each.

The Δ*COI*-bearing lines have significantly lower productivity than WT N2 (figure IV-1; Wilcoxon rank sum, $\chi^2 = 17.031$, d.f. = 1, $p < 0.0001$), producing on average 28.5% fewer progeny (table IV-1). Mean productivity ranges from 59.5% of WT (10C.I) to 93.2% of WT (10C.B). There is a significant difference between the mean productivity of the Δ*COI*-bearing lines (Kruskal-Wallis test, $\chi^2 = 17.742$, d.f. = 6, $p = 0.0069$). However, the only lines with significantly different mean productivity are 10C.B and 10C.I (table IV-1; Tukey-Kramer HSD, $p = 0.0314$).

Developmental rate is also significantly reduced in Δ*COI*-bearing lines compared to WT (figure IV-1; Wilcoxon rank sum, $\chi^2 = 24.771$, d.f. = 1, $p < 0.0001$). Δ*COI*-bearing lines take 10.9% more time, on average, to reach adulthood than N2. There is a significant difference in mean developmental rate within the Δ*COI*-bearing lines (Kruskal-Wallis test, $\chi^2 = 22.894$, d.f. = 6, $p = 0.0008$) with mean time to adulthood ranging from 46 hours (10C.J) to 52.4 hours (10C.F) compared to N2's 44.6 hours (table IV-1).

There is no significant difference between WT and Δ*COI* line in longevity (figure IV-1; Wilcoxon rank sum, $\chi^2 = 2.698$, d.f. = 1, $p = 0.1005$). While the mean longevity of Δ*COI*-bearing lines ranges between 72% (10C.D) and 99.3% (10C.M) of WT longevity (table IV-1), there is no significant difference in mean longevity between Δ*COI*-bearing lines (Kruskal-Wallis test, $\chi^2 = 8.056$, d.f. = 6, $p = 0.2340$).

Δ*COI*-bearing lines have significantly lower survivorship than WT N2 (figure IV-1; Wilcoxon rank sum, $\chi^2 = 3.946$, d.f. = 1, $p < 0.0470$), with progeny of WT worms 7.6% more likely to survive to adulthood than Δ*COI*-bearing progeny (table IV-1). Mean

survivorship of Δ*COI*-bearing lines ranges from 82.8% of WT (10C.H) to 97.8% of WT (10C.B) with no significant difference between any Δ*COI*-bearing lines (Kruskal-Wallis test, $\chi^2 = 5.734$, d.f. = 6, $p = 0.4536$).

ΔCOI has a competitive advantage when interindividual selection is reduced.

To determine if the Δ*COI* mitotype has an intraindividual advantage over WT mitotypes, Δ*COI* mitotype-bearing *C. elegans* were propagated in bottlenecked populations ($N = 1$) for 10 generations. Bottlenecking in this way reduces interindividual selection so that intraindividual selection and drift are the main forces acting upon mtDNA. The heteroplasmic frequency of the Δ*COI* mitotype was measured in day 2 adult worms at generations 1, 5, and 10. If Δ*COI* is selfishly acting, then pairwise comparisons between generations 1, 5, and 10 should reveal an increase in the frequency of the Δ*COI* mitotype and a decrease in the WT mitotype within individual worms. Independent bottlenecking experiments were performed using lines bearing the Δ*COI* mitotype in both the MA nuclear background and in the WT N2 nuclear background. For both backgrounds, five worms were used to establish the parental generation 0 (A-E), and five progeny from each of the parental generation where then used to start generation 1 (A.1-5, B.1-5, C.1-5, D.1-5, and E.1-5) for a total of 25 replicate populations.

The bottlenecked populations in the MA nuclear background show clear signs of selfish drive. The mean frequency of Δ*COI* mtDNA increases significantly in each generation (figure IV-2), from 76.13% at generation 1, to 82.43% in generation 5, and to

84.98% by generation 10 (table IV-2). Moreover, the increase was consistent across all the lines tested. Despite pairwise comparisons between generations being significant, comparisons of the mean heteroplasmic frequency between lines derived from each generation 0 parent were not significant at generation 1 (Kruskal-Wallis test, $\chi^2 = 6.905$, d.f. = 4, $p = 0.1410$), generation 5 (Kruskal-Wallis test, $\chi^2 = 5.697$, d.f. = 4, $p = 0.2229$), or generation 10 (Kruskal-Wallis test, $\chi^2 = 7.178$, d.f. = 4, $p = 0.1268$).

There is not clear evidence of selfish drive in the WT N2 background. The mean frequency of Δ*COI* mtDNA across all lines decreases from 79.04% in generation 1 to 77.18% in generation 5, it then goes up to 77.96% in generation 10 (table IV-2), and none of the pairwise comparisons between generations are significant (figure IV-2). In contrast to the MA nuclear background, there is significant differences between mean heteroplasmic frequency of lines derived from a common generation 0 parent at generation 1 (table IV-2; Kruskal-Wallis test, $\chi^2 = 13.651$, d.f. = 4, $p = 0.0085$).

*Δ*COI* decreases in frequency in large populations.*

Seven Δ*COI*-bearing lines with WT N2 nDNA (10C.B, 10C.D, 10C.F, 10C.H, 10C.I, 10C.J, and 10C.M) were maintained at large population sizes for 75 generations. Under these conditions, interindividual selection strongly favors organismal fitness over organellular replication. At generation 0, the mean heteroplasmic frequency of Δ*COI* across all lines is 86.5% (figure IV-3). There is a small but significant difference between means of each line (Kruskal-Wallis test, $\chi^2 = 13.0197$, d.f. = 6, $p = 0.0427$) ranging from 81.5% in 10C.M to 89.6% in 10C.D. Though the mean heteroplasmic

frequency across all lines decreases to 85.4% in generation 30, this change is not significantly different from generation 0 (Tukey-Kramer HSD, $p = 0.8509$). In addition, there is no significant difference between the mean heteroplasmic frequency of each line at generation 30 (Kruskal-Wallis test, $\chi^2 = 7.6718$, d.f. = 6, $p = 0.2631$), which ranged from 82.4% in 10C.D to 88% in 10C.H. The mean heteroplasmic frequency of Δ*COI* in generation 75 is significantly lower than both generation 0 (Tukey-Kramer HSD, $p < 0.0001$) and generation 30 (Tukey-Kramer HSD, $p < 0.0001$), decreasing to 65.5% (figure IV-3). In Generation 75 there is a significant amount of variation in mean heteroplasmic frequency of Δ*COI* (Kruskal-Wallis test, $\chi^2 = 30.2416$, d.f. = 6, $p < 0.0001$), ranging from a mean heteroplasmic frequency of 45.6% in 10C.J to 79.6% in 10C.D.

When looking at the trajectory of the heteroplasmic frequency of Δ*COI* in each line under increased interindividual selection, there is a general trend for non-significant differences between generations 0 and 30 and a significant decline in heteroplasmic frequency by generation 75. However, 10C.B never changes significantly in mean heteroplasmic frequency (table IV-3). 10C.B and 10C.M have the lowest heteroplasmic frequency at generation 0 (83.9% and 81.5% respectively), and are the only lines to show an increase in heteroplasmic frequency from generation 0 to 30 (figure IV-3). However, 10C.M dramatically decreases in frequency by generation 75 whereas 10C.B does not change significantly.

mtDNA copy number in large populations

In the Δ*COI*-bearing lines, there is no initial significant increase in mean mtDNA copy number within individual worms relative to N2 controls (table IV-4). However, there is much variation in the mtDNA copy number within lines (figure IV-4). On the low end of the spectrum, 10C.F worms sampled have relative mtDNA copy numbers ranging from 78.6% to 107.5% of mean WT mtDNA copy number ($\sigma = 0.162$) which is similar to that seen in the WT N2 ($\sigma = 0.143$). MtDNA copy number varies much more widely in other lines like 10C.M with mtDNA copy numbers ranging from 81.9% to 258.3% of WT in worms sampled ($\sigma = 1.422$).

When propagated in large populations very few lines exhibited a change in mtDNA copy number between generations 0 and 30. The only line with a significant change in mean mtDNA copy number is 10C.D with a 49.3% increase in mean mtDNA copy number (table IV-5).

By generation 75, line 10C.D decreases to its starting mean mtDNA copy number (table IV-5) but remains elevated compared to N2 (table IV-4). Lines 10C.B, 10C.I, and 10C.J also exhibit a decrease in generation 75 with a 20.7%, 57.1%, and 71.5% decline in mtDNA copy number from generation 30, respectively. 10C.I and 10C.J both decrease to less than WT mtDNA copy number in generation 75 (table IV-4, figure IV-4).

Discussion

Random genetic drift is often thought of as the major evolutionary force determining the fixation or loss of new mitochondrial variants within a host (Jenuth et al. 1996; Chinnery et al. 2000). However, there is a growing appreciation for the role of selfish genetic drive in determining the within individual evolutionary dynamics of mtDNA (Beziat et al. 1993; Hurst and Werren 2001; MA an O'Farell 2016; Havird et al. 2019). There is evidence that deletion bearing mitotypes can act as selfish genetic elements (Taylor et al. 2002; Tsang and Lemire 2002; Clark et al. 2012; Dubie et al. 2020), having either neutral or deleterious effects on host fitness and having a transmission advantage over other mitotypes.

Previously, we identified a selfish mitotype (Δ*ctb-1*) that had spontaneously arisen during a MA experiment of *C. elegans* (Dubie et al. 2020). This mitotype was characterized by its 499 bp deletion in *ctb-1*, though it also possessed three other linked mutations in *nd5*. We were able to show that the Δ*ctb-1* mitotype reduces the fitness of worms that bear it and has a within-individual advantage over WT mitotypes, satisfying both criteria of selfishness. Having characterized the selfish behavior of this mitotype, we sought to determine if other mitotypes that had arisen during MA had similar characteristics — namely large deletions in mtDNA with a high heteroplasmic frequency — were also selfishly acting.

Line 10C (10 representing the population size bottleneck during MA and C denoting the replicate line name) acquired a 1185 bp deletion in the mitochondrial *COI* gene during MA. Despite the increased interindividual selection in the experimental

populations maintained at $N = 10$ individuals per generation, we found that the Δ*COI* mitotype rapidly increases in frequency (from 24.5% in generation 350 to 68.8% in generation 409) but does not reach fixation during MA. When comparing our results using worm tissues collected at the end of the MA experiment to previously published sequencing results performed using worms recovered from cryopreserved stocks, we found that the heteroplasmic frequency of Δ*COI* had further increased to 82% (Konrad et al. 2017). These results show that the heteroplasmic frequency was continuing to increase in these lines, even after the populations were allowed to expand after MA so that they could be cryopreserved. While Δ*COI* arose much later during MA, its increase in heteroplasmic frequency appears to match the patterns previously observed with Δ*ctb-1*. These factors suggested that, like Δ*ctb-1*, Δ*COI* likely increased heteroplasmic frequency due to selfish drive.

To determine if the Δ*COI* mitotype is selfishly acting, it is important to first establish a fitness cost of bearing the mitotype. We measured productivity, developmental rate, survivorship, and longevity of lines in which the mitotype was isolated from the nuclear mutational load of MA. Among the four fitness traits measured, all traits were lower than WT, but only productivity, developmental rate, and survivorship were significantly so. The fitness burden of bearing the Δ*COI* mitotype was lower than that of the Δ*ctb-1* mitotype. This is especially pronounced with respect to productivity, where Δ*ctb-1* produced 65% less progeny than WT whereas Δ*COI* produced only 29% less progeny than WT. While the previously identified Δ*ctb-1* mitotype arose in drastically bottlenecked populations ($N = 1$ individual per generation),

where selection on individual fitness is largely absent, Δ*COI* arose in an environment where interindividual selection on fitness was present (N = 10 individuals per generation; Konrad et al. 2017). In MA experiments with varying levels of interindividual selection, the efficiency of removing even slightly deleterious mutations is high (Katju et al. 2015, 2018). It is therefore not surprising that the Δ*COI* mitotype confers a lower fitness cost than the Δ*ctb-1* mitotype on its host. However, it is surprising that Δ*COI* increased in frequency at all with this level of selection. In fact, no other nonsynonymous mtDNA mutations increased to a high heteroplasmic frequency (>60%) during 409 generations of MA in population sizes greater than N = 1 (Konrad et al. 2017), and the average fitness in MA lines was indistinguishable from WT in bottlenecked populations of ten individuals (Katju et al. 2025, 2018). All of these factors emphasize the strength of intracellular drift and negative selection in these MA populations that Δ*COI* had to overcome in order to increase in frequency.

Secondly, for a genetic element to be selfishly acting it must have an intraindividual advantage over other mitotypes. To determine if this could be said of Δ*COI*, we examined the intraindividual dynamics of competition between Δ*COI* and WT mitotypes in bottlenecked populations (N = 1). Propagating worms in bottlenecked populations reduced the effect of interindividual selection so that the main evolutionary factors controlling the frequency of Δ*COI* would be genetic drift and intraindividual selection. Since the nDNA of worms in which the Δ*COI* mitotype arose had accumulated a number of mutations during MA, Δ*COI* was propagated in bottlenecked populations with either WT nDNA or MA nDNA to see if there was a background specific difference

in competition between Δ*COI* and WT mitotypes. As expected, the Δ*COI* mitotype had an intraindividual advantage in the MA nDNA background as was observed with Δ*ctb-1* (see chapters II and III). Interestingly, in this study we did not see clear evidence for intraindividual advantage in the WT nDNA background. Initially this would suggest that unlike Δ*ctb-1*, the selfishness of Δ*COI* is specific to the intracellular environment of the late-stage MA line. However, the starting heteroplasmic frequency of Δ*COI* backcrossed lines in the WT background are higher than those in the MA background. Furthermore, there seems to be a density-dependent change in heteroplasmic frequency, with lines with a higher starting frequency of Δ*COI* decreasing each generation and lines with lower starting frequency increasing. Unfortunately, analysis of density dependence is prone to type I error (Freckleton et al. 2006; Kelly and Price 2015), and this study was not designed to directly study density dependence of selfish drive. It is also likely that there is a threshold in heteroplasmic frequency to which a selfish mitotype could increase before resulting in nonviable offspring. Theoretically, increasing above this frequency would leave too few WT mitochondria to meet the bioenergetic needs of a host and result in either death or nonviability. This is one explanation for why selfish deletion-bearing mitotypes are often observed as high frequency heteroplasmies. It could also explain why Δ*ctb-1* was maintained as a high frequency heteroplasmy (96%) for over 200 generations without fixing within individual worms.

The moral hazard hypothesis suggests that one mechanism by which mitotypes can behave selfishly is to trigger indiscriminate biogenesis of mtDNA as a response to the selfish mitochondria disrupting bioenergetic homeostasis (Havird et al. 2019). There

has been support for this phenomenon in *C. elegans* (Gitschlag et al. 2016) where the selfish *uaDf5* mitotype results in hosts with elevated mtDNA copy numbers. With regards to both Δ*COI* and Δ*ctb-1*, the trend is less clear. While some lines bearing these mitotypes have elevated mtDNA copy number, most lines do not. However, the mechanism proposed by the moral hazard hypothesis is indiscriminate, suggesting that there would also be an increase in the range of mtDNA copy numbers observed in selfish mtDNA bearing lines. This matches what is observed in the Δ*COI* mitotype-bearing lines, with even lines that do not have increased mean mtDNA copy number having an increased range of observed mtDNA copy numbers. Within Δ*ctb-1* lines, a correlation between mutant and WT mtDNA quantity within individuals accompanied by an increase in mtDNA copy number variation within lines further supports the idea that there is a nonspecific increase in mtDNA (Dubie et al. 2020). While the increase in mtDNA copy number is not a consistent feature within Δ*COI* and Δ*ctb-1* bearing lines, an indiscriminate increase in mtDNA does appear to be present within these lines, potentially providing a mechanism for a within-individual advantage.

The heteroplasmic frequency of selfish mitotypes is thought to be maintained in populations at an equilibrium where the force of within-individual drive is balanced by the between-individual negative selective pressure favoring organismal fitness (Ma and O'Farrell 2016). Like Δ*ctb-1*, Δ*COI* was able to be maintained in large populations (>100 individuals) for many generations despite its fitness costs. During 75 generations (10 months) of competition in large populations, Δ*COI* decreased from an initial frequency of 86.5% to 65.5%. However, despite selection acting to reduce the frequency

of Δ*COI* in these populations, there was not an appreciable difference in heteroplasmic frequency for at least the first 30 generations. This phenomenon was also observed in the Δ*ctb-1* lines. In both cases the heteroplasmic frequency of deletion-bearing mtDNA was high at the start of the experiment, and that the variation of heteroplasmic frequencies found within progenies produced was therefore likely small. This is due to the small number of WT mtDNA that could be portioned into eggs relative to the deletion-bearing mtDNA. As a result, selection would not have been efficient at selecting between progeny early in competition. As the experiment continued, and the heteroplasmic frequencies within lines increased in variation each generation, selection would become more efficient at lowering the heteroplasmic frequency of ΔmtDNA.

This study has identified a new selfish Δ*COI* mitotype in *C. elegans* and characterized its intraindividual dynamics in both small and large populations. In doing so, we have been able to corroborate many of the findings with both the Δ*ctb-1* and *UaDf5* mitotypes in *C. elegans*. This suggests that the characteristics seen in the current study may be more generally applicable to mtDNA deletions in *C. elegans* — namely their selfish behavior, persistence in large populations despite selection for lower heteroplasmic frequencies, and nonspecific increases in mtDNA copy number. The similarity in both origin and evolutionary dynamics to the previously identified Δ*ctb-1* mitotype provides a new tool to test what aspects of mitochondrial biology affect the fate of new mtDNA mutations and their selfish behavior. Previously, experimental analysis of mitochondrial biology and the mechanism of selfishness has been limited by the inability to efficiently engineer mitochondrial mutations and the few known selfish

mitotypes in experimental models. MA experiments and large collections of *C. elegans* natural isolates (Cook et al. 2017) contain an untapped wellspring of mitotypes that could be used to better understand the complex and dynamic evolutionary biology of mitochondria.

Tables

Table IV-1. Fitness of Δ*COI*-bearing mtDNA in a wild-type nuclear background relative to control worms of the laboratory strain, N2 bearing wild-type mtDNA. Fifteen replicates of the N2 control and each experimental Δ*COI*-bearing (10C.B, 10C.D, 10C.F, 10C.F, 10C.H, 10 C.I, 10C.J, 10C.M) lines were assayed when possible. Estimates of the mean phenotype for four fitness traits are provided for the wild-type N2 control ($\bar{z}_{N2\ control}$; n = 15) and the Δ*COI*-bearing lines ($\bar{z}_{\Delta ctb\text{-}1\ \text{bearing lines}}$; n = 93). Mean fitness values across replicates for individual experimental lines are also provided.

		fitness related trait			
	n	productivity	developmental time (hours)	longevity (days)	survivorship to adulthood
$\bar{z}_{\text{N2-control}}$	15	321.2	44.60	18.27	0.9812
$\bar{z}_{\Delta COI\ \text{bearing lines}}$	93	229.699	49.47	15.34	0.9116
$\bar{z}_{\Delta COI\ \text{bearing lines 10C.B}}$	13	299.308	47.92	17.85	0.9596
$\bar{z}_{\Delta COI\ \text{bearing lines 10C.D}}$	13	201.615	51.15	13.15	0.8790
$\bar{z}_{\Delta COI\ \text{bearing lines 10C.F}}$	15	208.133	52.40	14.60	0.8600
$\bar{z}_{\Delta COI\ \text{bearing lines 10C.H}}$	8	215.875	48.75	14.13	0.8125
$\bar{z}_{\Delta COI\ \text{bearing lines 10C.I}}$	15	191.2	49.67	13.53	0.9533
$\bar{z}_{\Delta COI\ \text{bearing lines 10C.J}}$	14	235.143	46.00	15.50	0.9214
$\bar{z}_{\Delta COI\ \text{bearing lines 10C.M}}$	15	256.067	49.87	18.13	0.9519

Table IV-2. Mean heteroplasmic frequency of Δ*COI* mitotypes in bottlenecked populations ($N = 1$) over time (10 generations).

	MA background				N2 background		
	Generation				generation		
	1	5	10		1	5	10
all	76.13%	82.43%	84.98%	all	79.04%	77.18%	77.96%
A	80.28%	82.83%	82.44%	A	80.66%	73.47%	76.45%
B	68.20%	77.46%	84.36%	B	69.36%	75.12%	80.99%
C	83.11%	86.87%	84.51%	C	80.02%	78.93%	81.64%
D	79.36%	83.34%	87.32%	D	88.70%	81.27%	77.98%
E	69.70%	80.71%	86.73%	E	81.29%	77.11%	70.99%

Table IV-3. Absolute differences in mean heteroplasmic frequency of Δ*COI* in large homogeneous populations at generations 0, 30, and 75. Significant differences as determined by the Tukey-Kramer honestly significant difference test are shown with asterisks (* $p \leq 0.05$, ** $p \leq 0.01$, *** $p \leq 0.001$, **** $p \leq 0.0001$).

comparison	Lines							
	10C.B	10C.D	10C.F	10C.H	10C.I	10C.J	10C.M	Total
0 to 30	0.026	0.072	0.030	0.014	0.002	0.022	0.037	0.011
30 to 75	0.090	0.028	0.123***	0.320****	0.170**	0.377****	0.309****	0.200****
0 to 75	0.064	0.100*	0.152****	0.334****	0.168**	0.399****	0.273****	0.211****

Table IV-4. Tukey-Kramer HSD method and student's t-tests of multiple comparisons among pairs of mean mtDNA copy number within Δ*COI*-bearing lines in large homogeneous populations at generations 0, 30, and 75.

generation 0

generation 0	N2	B	D	F	H	I	J	M
N2	-	13.39	15.46	17.29	15.46	12.74	17.29	17.29
B	6.45	-	17.29	18.94	17.29	14.90	18.94	18.94
D	9.55	3.10	-	20.45	18.94	16.79	20.45	20.45
F	2.13	8.58	11.68	-	20.45	18.48	21.87	21.87
H	2.51	3.95	7.04	4.64	-	16.79	20.45	20.45
I	7.04	0.59	2.51	9.17	4.53	-	18.48	18.48
J	7.44	0.99	2.11	9.58	4.94	0.40	-	21.87
M	8.06	1.60	1.49	10.19	5.55	1.01	0.61	-

generation 30

generation 30	N2	B	D	F	H	I	J	M
N2	-	8.89	9.35	8.89	8.89	8.89	8.89	9.95
B	0.19	-	10.40	10.00	10.00	10.00	10.00	10.95
D	**23.66***	**23.47***	-	10.40	10.40	10.40	10.40	11.32
F	0.93	0.74	**22.73***	-	10.00	10.00	10.00	10.95
H	1.32	1.52	**24.99***	2.25	-	10.00	10.00	10.95
I	1.92	1.72	**21.75***	0.99	3.24	-	10.00	10.95
J	0.53	0.34	**23.13***	0.40	1.85	1.39	-	10.95
M	0.84	1.03	**24.5***	1.77	0.48	2.76	1.37	-

generation 75

generation 75	N2	B	D	F	H	I	J	M
N2	-	7.16	7.52	7.16	8.69	7.16	8.01	8.01
B	3.80	-	8.37	8.04	9.43	8.04	8.81	8.81
D	**8.33***	**12.13***	-	8.37	9.71	8.37	9.11	9.11
F	2.75	1.05	**11.08***	-	9.43	8.04	8.81	8.81
H	0.69	4.49	7.64	3.43	-	9.43	10.09	10.09
I	**10.08***	6.28	**18.41***	7.33	**10.76***	-	8.81	8.81
J	**11.53***	7.73	**19.87***	8.79	**12.22***	1.46	-	9.52
M	1.81	1.99	**10.15***	0.93	2.50	8.26	**9.72***	-

Absolute differences between all pairs listed below the diagonal. Critical HSD values are listed above the diagonal. Comparisons are significant ($\alpha = 0.05$) if their absolute differences are greater than their critical HSD (indicated with an asterisk). Bold indicates significant t-tests at an alpha level corrected by Holm-Bonferroni method.

Table IV-5. Tukey-Kramer HSD method and student's t-tests of multiple comparisons among pairs of mean mtDNA copy number in large homogeneous populations between generations 0, 30, and 75 within Δ*COI*-bearing lines.

10C.B

	0	30	75
0	-	6.37	6.37
30	6.26	-	6.12
75	**10.25***	3.99	-

10C.D

	0	30	75
0	-	11.72	11.72
30	**14.11***	-	10.49
75	1.21	**15.33***	-

10C.F

	0	30	75
0	-	10.93	10.93
30	3.06	-	8.47
75	0.61	3.67	-

10C.H

	0	30	75
0	-	11.03	12.44
30	3.83	-	11.02
75	1.82	2.01	-

10C.I

	0	30	75
0	-	10.21	10.21
30	5.13	-	10.21
75	**17.12***	**11.99***	-

10C.J

	0	30	75
0	-	16.31	17.27
30	6.92	-	13.84
75	**18.98***	12.06	-

10C.M

	0	30	75
0	-	19.14	19.14
30	8.90	-	16.58
75	9.87	0.97	-

Absolute differences between all pairs listed below the diagonal. Critical HSD values are listed above the diagonal. Comparisons are significant ($\alpha = 0.05$) if their absolute differences are greater than their critical HSD (indicated with an asterisk). Bold indicates significant t-tests at an alpha level corrected by Holm-Bonferroni method.

Figures

Figure IV-1. Relative trait means of Δ*COI*-bearing 10C replicate lines and the WT *N2* control. Phenotypic assays were conducted for four fitness-related traits, namely productivity, survivorship to adulthood, developmental rate, and longevity. For simplicity, the mean relative fitness value for each of the four traits in the WT N2 control was scaled to a value of 1. Asterisks represent significantly different means (**** $p < 0.0001$ and * $p < 0.05$). Error bars represent one standard error.

Figure IV-2. Box plots of heteroplasmic frequency of Δ*COI* over time in bottlenecked populations. Asterisks represent significant paired t-tests (*** $p < 0.001$ and * $p < 0.05$). The Holm-Bonferroni method was used to ensure the family wise error rate was lower than $\alpha = 0.05$.

Figure IV-3. Box plot of heteroplasmic frequency of Δ*COI* over time in large homogeneous populations. The average heteroplasmic frequency of Δ*COI* across all populations is 86.5% at generation 0, 85.4% at generation 30, and 65.5% at generation 75.

Figure IV-4. Box plots of mtDNA copy number relative to wild-type N2 mtDNA copy number over time in large homogeneous populations of Δ*COI*-bearing worms.

Figure IV-1. Relative trait means of Δ*COI*-bearing 10C replicate lines and the wild-type *N2* control.

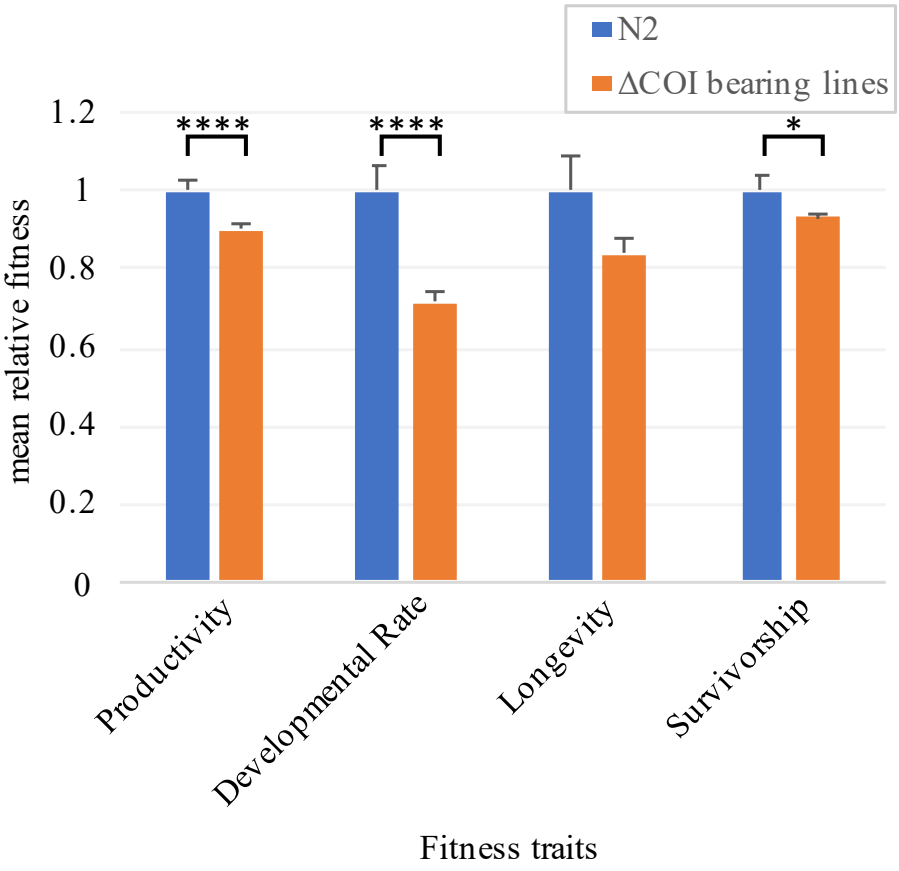

Figure IV-2. Box plots of heteroplasmic frequency of Δ*COI* over time in bottlenecked populations.

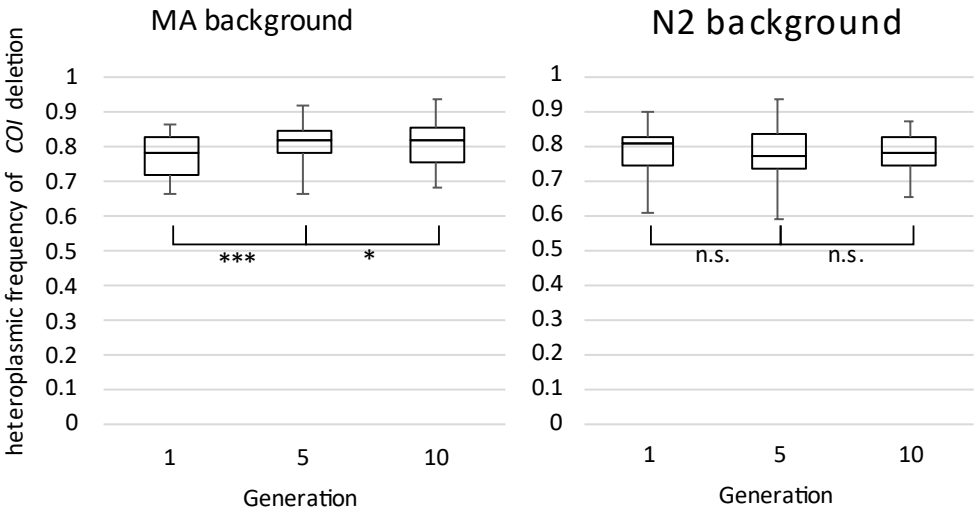

Figure IV-3. Box plot of heteroplasmic frequency of Δ*COI* over time in large homogeneous populations.

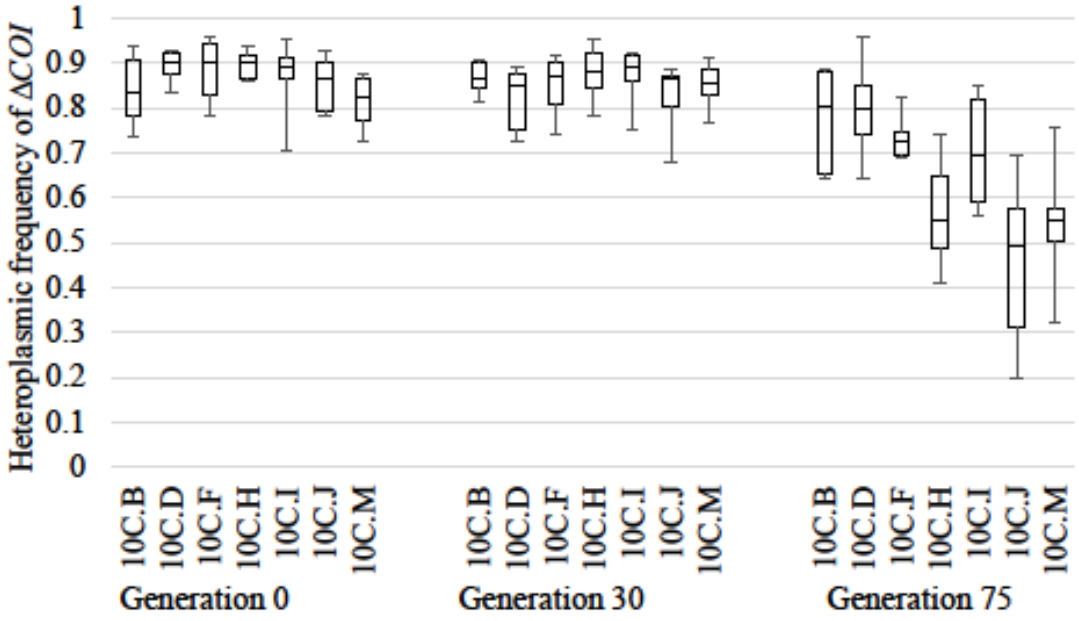

Figure IV-4. Box plots of mtDNA copy number relative to wild-type N2 mtDNA copy number over time in large homogeneous populations of Δ*COI*-bearing worms.

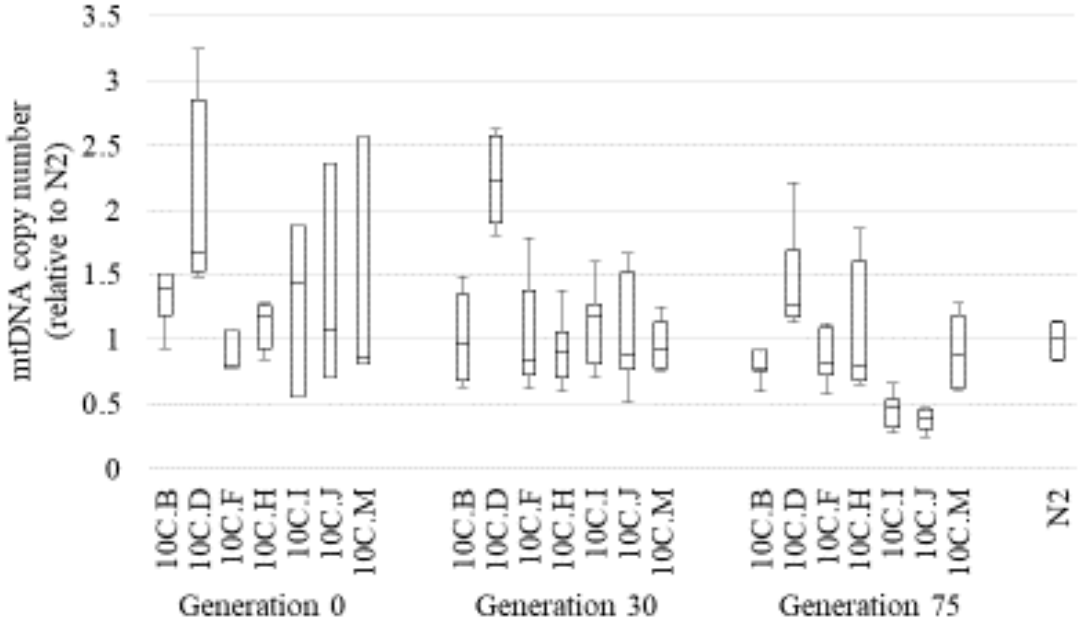

References

Beziat F, Morel F, Volz-Lingenhol A, Saint Paul N, Alziari S. 1993. Mitochondrial genome expression in a mutant strain of *D. subobscura*, an animal model for large scale mtDNA deletion. *Nucleic Acids Res*. **21**(3):387-92. (doi:10.1093/nar/21.3.387)

Bianconi E, Piovesan A, Facchin F, Beraudi A, Casadei R, Frabetti F, Vitale L, Pelleri MC, Tassani S, Piva F, Perez-Amodio S, Strippoli P, Canaider S. 2013. An estimation of the number of cells in the human body. *Ann Hum Biol*. **40**(6):463-71. (doi:10.3109/03014460.2013.807878)

Birky CW Jr. 1973. On the origin of mitochondrial mutants: evidence for intracellular selection of mitochondria in the origin of antibiotic-resistant cells in yeast. *Genetics*. **74**(3):421-32. (doi:10.1093/genetics/74.3.421)

Capps GJ, Samuels DC, Chinnery PF. 2003. A model of the nuclear control of mitochondrial DNA replication. *J. theor. Biol.* **221**:565-583. (doi:10.1006/jtbi.2003.3207)

Carroll D. 2017. Genome editing: past, present, and future. *Yale J Biol Med*. **90**(4):653-659.

Chen XJ, Clark-Walker GD. 2000. The petite mutation in yeasts: 50 years on. Int Rev Cytol. **194**:197-238. (doi:10.1016/s0074-7696(08)62397-9)

Chen XJ, Clark-Walker GD. 2018. Unveiling the mystery of mitochondrial DNA replication in yeasts. Mitochondrion. **38**:17-22. (doi:10.1016/j.mito.2017.07.009)

Chinnery PF, Thorburn DR, Samuels DC, White SL, Dahl HM, Turnbull DM, Lightowlers RN, Howell N. 2000. The inheritance of mitochondrial DNA heteroplasmy: random drift, selection or both? *Trends Genet*. **16**(11):500-5. (doi:10.1016/s0168-9525(00)02120-x)

Clark KA, Howe DK, Gafner K, Kusuma D, Ping S, Estes S, Denver DR. 2012. Selfish little circles: transmission bias and evolution of large deletion-bearing mitochondrial DNA in *Caenorhabditis briggsae* nematodes. *PLoS One*. **7**:e41433. (doi:10.1371/journal.pone.0041433)

Cook DE, Zdraljevic S, Roberts JP, Andersen EC. 2017. CeNDR, the *Caenorhabditis elegans* natural diversity resource. *Nucleic Acids Res*. **45**(D1):D650-D657. (doi:10.1093/nar/gkw893)

Dubie JJ, Caraway AR, Stout MM, Katju V, Bergthorsson U. 2020. The conflict within: origin, proliferation and persistence of a spontaneously arising selfish

mitochondrial genome. *Phil. Trans. R. Soc. B*. **375**:20190174. (doi:10.1098/rstb.2019.0174)

Fontana GA, Gahlon HL. 2020. Mechanisms of replication and repair in mitochondrial DNA deletion formation. *Nucleic Acids Res*. **48**(20):11244-11258. (doi:10.1093/nar/gkaa804)

Freckleton RP, Watkinson AR, Green RE, Sutherland WJ. 2006. Census error and the detection of density dependence. *J Anim* Ecol. **75**(4):837-51. (doi:10.1111/j.1365-2656.2006.01121.x)

Gitschlag BL, Kirby CS, Samuels DC, Gangula RD, Mallal SA, Patel MR. 2016. Homeostatic responses regulate selfish mitochondrial genome dynamics in *C. elegans. Cell Metab*. **24**:91-103. (doi:10.1016/j.cmet.2016.06.008)

Haig D. 2016. Intracellular evolution of mitochondrial DNA (mtDNA) and the tragedy of the cytoplasmic commons. *Bioessays*. **38**(6):549-55. (doi:10.1002/bies.201600003)

Havird JC, Forsythe ES, Williams AM, Werren JH, Dowling DK, Sloan DB. 2019. Selfish mitonuclear conflict. *Curr Biol.* **29**(11):R496-R511. (doi:10.1016/j.cub.2019.03.020)

He F. 2011. Common worm media and buffers. *Bio-101*. e55. (doi:10.21769/BioProtoc.55)

Hu JP, Xu XY, Huang LY, Wang LS, Fang NY. 2015. Freeze-thaw *Caenorhabditis elegans* freeze-thaw stress response is regulated by the insulin/IGF-1 receptor *daf-2*. *BMC Genet.* **16**:139. (doi:10.1186/s12863-015-0298-5)

Hu S, Skelly LE, Kaymak E, Freeberg L, Lo TW, Kuersten S, Ryder SP, Haag ES. 2019. Multi-modal regulation of *C. elegans* hermaphrodite spermatogenesis by the GLD-1-FOG-2 complex. *Dev Biol*. **446**(2):193-205. (doi:10.1016/j.ydbio.2018.11.024)

Hurst GD, Werren JH. 2001. The role of selfish genetic elements in eukaryotic evolution. *Nat. Rev. Genet.* **2**:597-606. (doi:10.1038/35084545)

Jenuth JP, Peterson AC, Fu K, Shoubridge EA. 1996. Random genetic drift in the female germline explains the rapid segregation of mammalian mitochondrial DNA. *Nat Genet*. **14**(2):146-51. (doi:10.1038/ng1096-146)

Katju V, Packard LB, Bu L, Keightley PD, Bergthorsson U. 2015 Fitness decline in spontaneous mutation accumulation lines of *Caenorhabditis elegans* with varying effective population sizes. *Evolution* **69**:104-116. (doi:10.1111/evo.12554)

Katju V, Packard LB, Keightley PD. 2018. Fitness decline under osmotic stress in *Caenorhabditis elegans* populations subjected to spontaneous mutation accumulation at varying population sizes. *Evolution* **72**:1000-1008. (doi:10.1111/evo.13463)

Kelly C, Price TD. 2015. Correcting for regression to the mean in behavior and ecology. *Am Nat.* **166**(6):700-7. (doi:10.1086/497402)

Klucnika A, Ma H. 2019. Mapping and editing animal mitochondrial genomes: can we overcome the challenges? *Phil. Trans. R. Soc. B*. **375**:20190187. (doi:10.1098/rstb.2019.0187)

Konrad A, Thompson O, Waterston RH, Moerman DG, Keightley PD, Bergthorsson U, Katju V. 2017. Mitochondrial mutation rate, spectrum and heteroplasmy in *Caenorhabditis elegans* spontaneous mutation accumulation lines of differing population size. *Mol. Biol. Evol.* **34**:1319-1334. (doi:10.1093/molbev/msx051)

Kowald A, Kirkwood TB. 2014. Transcription could be the key to the selection advantage of mitochondrial deletion mutants in aging. *Proc Natl Acad Sci U S A.* **111**(8):2972-7. (doi:10.1073/pnas.1314970111)

Kowald A, Kirkwood TBL. 2018. Resolving the enigma of the clonal expansion of mtDNA deletions. *Genes (Basel)*. **9**(3):126. (doi:10.3390/genes9030126)

Lang BF, Gray MW, Burger G. 1999. Mitochondrial genome evolution and the origin of eukaryotes. *Annu Rev Genet*. **33**:351-97. (doi:10.1146/annurev.genet.33.1.351)

Lawless C, Greaves L, Reeve AK, Turnbull DM, Vincent AE. 2020. The rise and rise of mitochondrial DNA mutations. *Open Biol*. **10**(5):200061. (doi:10.1098/rsob.200061)

Lewis SC, Joers P, Willcox S, Griffith JD, Jacobs HT, Hyman BC. 2015. A rolling circle replication mechanism produces multimeric lariats of mitochondrial DNA in *Caenorhabditis elegans*. *PLoS Genet*. **11**(2):e1004985. (doi:10.1371/journal.pgen.1004985)

Ma H, Marti Gutierrez N, Morey R, Van Dyken C, Kang E, Hayama T, Lee Y, Li Y, Tippner-Hedges R, Wolf DP, Laurent LC, Mitalipov S. 2016. Incompatibility between nuclear and mitochondrial genomes contributes to an interspecies reproductive barrier. *Cell Metab.* **24**(2):283-94. (doi:10.1016/j.cmet.2016.06.012)

Ma H, O'Farrell PH. 2016. Selfish drive can trump function when animal mitochondrial genomes compete. *Nat Genet*. **48**(7):798-802. (doi:10.1038/ng.3587)

MacAlpine DM, Kolesar J, Okamoto K, Butow RA, Perlman PS. 2001. Replication and preferential inheritance of hypersuppressive petite mitochondrial DNA. *EMBO J.* **20**(7):1807-17. (doi:10.1093/emboj/20.7.1807)

Martin WF, Garg S, Zimorski V. 2015. Endosymbiotic theories for eukaryote origin. *Philos Trans R Soc Lond B Biol Sci*. **370**(1678):20140330. (doi:10.1098/rstb.2014.0330)

Rand DM. 2001. The units of selection on mitochondrial DNA. *Annu. Rev. Ecol. Evol. Syst*. **32**:415-448. (doi:10.1146/annurev.ecolsys.32.081501.114109)

Rossignol R, Faustin B, Rocher C, Malgat M, Mazat JP, Letellier T. 2003. Mitochondrial threshold effects. *Biochem J.* **370**(Pt 3):751-62. (doi:10.1042/BJ20021594)

Schedl T, Kimble J. 1988. *fog-2*, a germ-line-specific sex determination gene required for hermaphrodite spermatogenesis in *Caenorhabditis elegans*. *Genetics*. **119**(1):43-61. (doi:10.1093/genetics/119.1.43)

Sharpley MS, Marciniak C, Eckel-Mahan K, McManus M, Crimi M, Waymire K, Lin CS, Masubuchi S, Friend N, Koike M, Chalkia D, MacGregor G, Sassone-Corsi P, Wallace DC. 2012. Heteroplasmy of mouse mtDNA is genetically unstable and results in altered behavior and cognition. *Cell*. **151**(2):333-343. (doi:10.1016/j.cell.2012.09.004)

Shmookler Reis RJ, Goldstein S. 1983. Mitochondrial DNA in mortal and immortal human cells. Genome number, integrity, and methylation. *J Biol Chem*. **258**(15):9078-85.

Stastna JJ, Yiapanas AD, Mandawala AA, Fowler KE, Harvey SC. 2020. Cryopreservation produces limited long-term effects on the nematode *Caenorhabditis elegans*. *Cryobiology*. **92**:86-91. (doi:10.1016/j.cryobiol.2019.11.039)

Stewart JB, Chinnery PF. 2015. The dynamics of mitochondrial DNA heteroplasmy: implications for human health and disease. *Nat Rev Genet*. **16**(9):530-42. (doi:10.1038/nrg3966)

Stiernagle T. 2006. Maintenance of *C. elegans*. *WormBook*. 1-11. (doi:10.1895/wormbook.1.101.1)

Taylor DR, Zeyl C, Cooke E. 2002. Conflicting levels of selection in the accumulation of mitochondrial defects in *Saccharomyces cerevisiae*. *Proc Natl Acad Sci U S A*. **99**(6):3690-4. (doi:10.1073/pnas.072660299)

Taylor R., Turnbull D. 2005. Mitochondrial DNA mutations in human disease. *Nat Rev Genet*. **6**:389-402. (doi:10.1038/nrg1606)

Tsang WY, Lemire BD. 2002. Mitochondrial genome content is regulated during nematode development. *Biochem Biophys Res Commun*. **291**(1):8-16. (doi:10.1006/bbrc.2002.6394)

Vita-More N, Barranco D. 2015. Persistence of long-term memory in vitrified and revived *Caenorhabditis elegans*. *Rejuvenation Res*. **18**(5):458-63. (doi:10.1089/rej.2014.1636)

Wallace DC. 1989. Mitochondrial DNA mutations and neuromuscular disease. *Trends Genet*. **5**:9-13. (doi:10.1016/0168-9525(89)90005-X)

Wallace DC. 2005. A mitochondrial paradigm of metabolic and degenerative diseases, aging, and cancer: a dawn for evolutionary medicine. *Annu Rev Genet.* **39**:359-407. (doi:10.1146/annurev.genet.39.110304.095751)

Wallace DC, Chalkia D. 2013. Mitochondrial DNA genetics and the heteroplasmy conundrum in evolution and disease. *Cold Spring Harb Perspect Biol*. **5**(11):a021220. (doi:10.1101/cshperspect.a021220)

Westermann B. 2010. Mitochondrial fusion and fission in cell life and death. *Nat Rev Mol Cell Biol.* **11**(12):872-84. (doi:10.1038/nrm3013)

CHAPTER V

COMPARING THE FITNESS AND RESPIRTATION OF ELECTON TRANSPORT CHAIN MUTATIONS IN THREE SEX SYSTEMS

Introduction

Mitochondria are an essential component of all eukaryotic cells. These organelles are believed to have been formed through the endosymbiosis of an ancient prokaryote into the ancestor of eukaryotes. Since then, many of the cellular processes of that ancient prokaryote have been taken over by its eukaryotic host, such that mitochondria have a greatly reduced genome and primarily exist to produce energy for their host cell (Lang et al. 1999). Because the mitochondrial genome (mtDNA) has been so greatly reduced, it is reliant on nuclear gene products of the host. The nuclear genome controls functions like translation, transcription, and replication of mitochondria (Burton et al. 2013) and produces most of the proteins that interact with mtDNA-encoded proteins in the electron transport chain (ETC; Lemire 2005). This interaction has resulted in a tight coevolution between mitochondrial and nuclear-encoded subunits (Azevedo et al. 2009; Osada and Akashi 2012) and is reflected in cases of mitonuclear mismatch, where hybrids with incompatible nuclear and mitochondrial genomes show reduced fitness and ETC efficiency (Sackton et al. 2003; Morales et al. 2018).

Within most animals, mtDNA does not have the same level of DNA repair or recombination as nuclear DNA (nDNA; Ballard and Whitlock 2004). Mitochondria also contain highly reactive intermediates of cellular respiration, which can interact with

DNA and cause damage (Ballard and Whitlock 2004). These factors contribute to an increased mutation rate in the mtDNA of animals compared to that of nDNA (Lynch 1996; Konrad et al. 2017). The accumulation of deleterious new mutations in mtDNA is thought to be inhibited by characteristics of mitochondrial biology, such as lifecycles involving fusion, fission, and autophagy (Rand 2008), uniparental inheritance (Radzvilavicius et al. 2017), and germline selection (Radzvilavicius et al. 2016; Zaidi et al. 2019).

While uniparental inheritance helps to purge deleterious mtDNA mutations that are incompatible with the nuclear genome, it does so only for the parent transferring its mitochondria to the next generation (the female, in the case of most eukaryotes). This means that selection for mutations that benefit the female will be favored, even at the expense of male fitness, a phenomenon referred to as the mother's curse (Gemmel et al. 2004). Mother's curse also diminishes the benefit of nDNA driven compensation for mtDNA mutations in males (Immonen et al. 2016).

There are certain biological traits that have been shown to lessen the effect of the mother's curse (Hill 2015). For example, in mammals, where males are the heterogametic sex, there is a paucity of mtDNA interacting genes on the X-chromosome relative to autosomes, which is believed to be caused by an increase in selective pressure to resolve sexual conflict (Drown et al. 2012). Aves, in which females are the heterogametic sex, have mtDNA interacting genes distributed randomly between their sex chromosomes and autosomes (Drown et al. 2012). Since Aves have an equal chance

inheriting either sex chromosome along with the mother's mtDNA there is less potential for maternally driven genetic conflict (Hill 2014).

Another factor limiting the effects of the mother's curse is inbreeding. In order for a variant that benefits females and harms males to increase in frequency within a population, the benefit to females must be greater than the relatedness of her mate (Wade 2014). The mother's curse can also be limited by kin selection. When the fitness of females is dependent on the fitness of their male brood mates, there is greater selection to resolve genetic conflict (Wade 2014; Keaney et al. 2020).

A synthesis of mother's curse and the nuclear compensatory hypothesis has led to the development of the mitonuclear sex hypothesis (Havird et al. 2015), which proposes that sex is maintained because it allows new combinations of nuclear alleles to interact with mtDNA mutations, increasing the rate of compensation. It also predicts that in facultative outcrossing lineages, sex should be the favored mode in the presence of mitonuclear mismatch. Molecular studies have been inconsistent in showing this relationship when comparing sexual lineages and asexual lineages (Paland and Lynch 2006; Nieman et al. 2010; Xu et al. 2012), and studies of selfing versus outcrossing lineages have not shown any differences in the accumulation of deleterious mutations (Cutter and Payseur 2003). However, all these studies assume mitochondrial mutations with sex-specific effects. While some evidence exists for male-bias in the detrimental effects of mitochondrial mutations (Aw et al. 2017; Wolff et al. 2016; Nagarajan-Radha et al. 2020), many studies do not find this bias (Mossman et al. 2016, 2017; Đorđević et al. 2017; Hoekstra et al. 2018).

Building on previous work (Wernick et al. 2016; Christy et al. 2017), we explored the effect of ETC mutations in different sexes of *Caenorhabditis elegans* under different reproductive systems. We selected two nuclear mutations and two homoplasmic mtDNA mutations known to affect ETC components by a single nonsynonymous substitution of an amino acid (Feng et al. 2001; Carroll et al. 2006; Dingley et al. 2014). The first is the nuclear *gas-1(fc21)* mutation, which disrupts a core subunit of ETC complex I and results in highly reduced complex I-dependent metabolism (Kayser et al. 2004). A second nuclear ETC mutation, *isp-1(qm150),* is believed to distort the head domain of the mitochondrial Cytochrome b-c1 complex Rieske subunit and reduce its redox potential (Jafari et al. 2015).

The final two mutations are both mitochondrial in origin. The first is *ctb-1(189),* which alters a site in Cytochrome b near the binding site of Cytochrome b-c1 complex Rieske subunit. The *ctb-1(189)* mutation is known to suppress *isp-1(qm150)* (Dingley et al. 2014), but it also reduces complex III activity. The second mutation, *cox-1(chpIR),* is a substitution in the *cox-1* gene isolated from a wild *C. elegans* strain, CB4856(Hawaii) (Suthammarak et al. 2009). While *cox-1(chpIR)* appears beneficial at CB4856's native temperature of 25˚C, at standard lab temperatures of 20˚C it seems to have a variety of detrimental effects (Dingley et al. 2014). Each of these lines were isolated in three nuclear backgrounds for the purpose of evaluating the effects, if any, of the reproductive system: N2 wild type (facultative outcrossing), *xol-1* (obligate selfing; Hargitai et al. 2009), and *fog-2* (obligate outcrossing; Schedl and Kimble 1988; Katju et al. 2008).

In this study we sought to determine if the effect of ETC mutations in *C. elegans* had measurable, phenotypic effects in different sexes and reproductive systems. To this end, we measured fitness traits of lines for each ETC/reproductive system combination, along with mitochondrial respiration in hermaphrodites from the obligately selfing and facultatively outcrossing lines, and in males and females from the obligately outcrossing lines.

Methods

ETC mutant line generation

In total, 17 lines were used in this project, each with a unique combination of reproductive system and ETC mutation. Of the 17 lines, 7 were facultatively outcrossing lines, 5 were obligately outcrossing, and 5 were obligately selfing. Lines used in these experiments are referred to herein with a capital letter (N, X, or F) denoting their reproductive strategy, a lowercase letter denoting female or male (f or m) where appropriate, and a subscript denoting their ETC mutations (Table V-1).

Four lines bearing ETC mutations in a facultatively outcrossing background were provided by the Estes laboratory at Portland State University: CW153 which bears *gas-1(fc21)* (N_{gas}), MQ887 which bears *isp-1(qm150)* (N_{isp}), the double mutant line MQ989 which bears both *isp-1(qm150)* and *ctb-1(189)* ($N_{ctb/isp}$), and CB4856 which is a Hawaiian strain bearing *cox-1(chpIR)* (N_{cox}). To generate a line bearing the *ctb-1(189)* alone, MQ989 hermaphrodites were backcrossed to N2 males to transfer mitochondrial genomes (mtDNA) bearing *ctb-1(189)* into worms with wild-type nuclear DNA (N_{ctb}). A

wild-type (WT) N2 lab strain (N_{wt}) was used as a control for the facultatively outcrossing lines. In addition, another WT N2 strain from the Estes Lab at Portland State University (N_{se}) was used to see if there was any significant difference between our WT laboratory strains.

To generate obligately outcrossing *C. elegans*, *fog-2* deletion-bearing lines (Δ*fog-2*) were generated using InVivo Biosystems's (formerly NemaMetrix) *C. elegans* CRISPR knockout service. Loss-of-function mutations in *fog-2* inhibit hermaphrodite sperm production and convert the facultatively outcrossing strain into an obligately outcrossing one comprising females and males (Schedl and Kimble 1988). However, gene conversion events between *fog-2* and *ftr-1* have been known to restore hermaphrodite sperm production (Katju et al. 2008; Rane et al. 2010). To prevent gene conversion, the engineered *fog-2* deletion encompassed most of *fog*-2, spanning the last 76 bp of intron 1 through the first 13 bp of exon 5 for a total 1,106 bp of *fog-2*'s 1,212 bp open reading frame (Chr. V:20199387..20200495). After lines were received from InVivo Biosystems, they were allowed to produce progeny before the parent worms were collected for single worm DNA extraction in worm lysis buffer (90 µl 10×PCR buffer + 10 µl 10 mg ml^{-1} proteinase K). The deletion was verified by PCR across the deleted region (table V-2). First, single worm lysates were used in a PCR reaction with primers Fog-2.F1 and Fog-2.R1 which was expected to generate a 1,475 bp product in WT lines, a 369 bp product in homozygous deletion-bearing lines, or both products in heterozygous lines. Lysates from lines that appeared homozygous deletion-bearing were then further screened by PCR using Fog-2.F1 and Fog-2.R2, which would generate a

334 bp product in heterozygous lines and no product in homozygous deletion-bearing lines. In homozygous deletion-bearing lines, the location of the deletion was confirmed by Sanger sequencing using the 369 bp amplified PCR product. The homozygous Δ*fog-2* lines were used as a WT control for the obligately outcrossing lines.

Obligately selfing lines were generated by deleting the majority of the open reading frame of *xol-1* (Δ*xol-1*). In the *C. elegans* sex-determining pathway, *xol-1* (XO lethal) is a key factor in X chromosome dosage compensation and its inhibition prevents the formation of males (Hargitai et al. 2009). InVivo Biosystems's *C. elegans* CRISPR knockout service was employed to generate a 3,057 bp deletion that spanned from 93 bp upstream of the *xol-1* coding sequence to the first 196 bp of exon 7 (Chr. X:8041234..8044290). Upon receipt of candidate lines from InVivo Biosystems, they were allowed to produce progeny before the parent worms were collected for single worm DNA extraction in worm lysis buffer. The deletion was verified by PCR across the deleted region in much the same way as described above for Δ*fog-2*. First, single worm lysates were used in a PCR reaction with primers Xol-1.F1 and Xol-1.R1 (table V-2) which would generate a 3,570 bp product in WT lines, a 514 bp product in homozygous deletion-bearing lines, or both products in heterozygous lines. Lysates from lines that appeared homozygous deletion-bearing were then further screened by PCR using primers Xol-1.F1 and Xol-1.R2 (table V-2), which generate a 203 bp product in heterozygous lines and no product in homozygous deletion-bearing lines. In homozygous deletion-bearing lines, the location of the deletion was confirmed by

Sanger sequencing of the 514 bp amplified PCR product. The homozygous Δ*xol-1* lines were used as a WT control for the obligately outcrossing lines.

Δ*fog-2* was also backcrossed to each of our ETC mutant strains to generate obligately outcrossing ETC mutant lines. The presence of Δ*fog-2* after backcrossing was screened by PCR as stated above. The presence of each ETC mutation after backcrossing was confirmed by Sanger sequencing PCR products generated using primers flanking each ETC mutation (table V-2). Obligately selfing ETC mutant-bearing lines were generated by InVivo Biosystems via engineering the *xol-1* deletion in each of the ETC mutant lines. Presence of Δ*xol-1* was confirmed using the methods above.

Fitness assays

The phenotypic effect of each ETC mutation in the different nuclear backgrounds was assayed, along with the *xol-1* and *fog-2* deletion-bearing control lines, an N2 control line from both the Katju lab at Texas A&M University and from the Estes lab at Portland State University, and the double mutant line MQ989, for a total of 17 lines. Each line was recovered from cryogenically preserved stocks using standard *C. elegans* procedures (Steiernagle 2006) and propagated for three generations to remove any maternal and grandmaternal effects of freezing. For the N2 and Δ*xol-1* based lines, a single third-generation L4 larva was transferred to a 60mm nematode growth media (NGM) plate seeded with *Escherichia coli* OP50 to establish the worm populations that could be used for fitness assays. For each of the Δ*fog-2* based lines, a L4 female and three young adult

males were transferred to a 60mm NGM plate seeded with OP50 to establish the worm populations that could be used for fitness assays.

Fitness traits were measured in four runs, and the number of replicates for each assay used in each run is reported in Table V-3. In each run, the N2 line from the Katju lab (N_{wt}) was used as an environmental control. In the first three runs, productivity, time to adulthood, longevity, and survivorship were measured using standard *C. elegans* procedures (Katju et al. 2015, 2018; Lee 2016; Dubie et al. 2020). In the fourth run, only productivity was measured.

For each replicate of the time to adulthood assay, a single L1 nematode was transferred by picking from the established populations to a new 35mm NGM plate seeded with OP50 and incubated at 20°C. After 30h, each worm was visually inspected under a dissecting microscope every two hours to determine the number of hours to adulthood. At the time that a nematode had developed its first egg, and that egg had migrated into the nematode's uterus, it was scored as having reached adulthood.

Once a worm had reached adulthood it was then transferred every 24h to a new 35mm NGM plate seeded with OP50 and incubated at 20°C for eight days. For F_{ctb}, F_{cox}, F_{gas}, and F_{isp}, if the nematode used in the time to adulthood assay developed into an adult female, two young adult male siblings were added to the plate and transferred daily with their sister. Alternatively, if the nematode used in the time to adulthood assay developed into an adult male, a young adult male sibling and a L4 female sibling were added to the plate and transferred daily. For F_{wt}, the productivity assay was performed separate from the other 3 assays. At the start of the assay a single L4 female and two sibling males

were added to a single 35mm NGM plate seeded with OP50 and incubated at 20°C for eight days with daily transfers. Plates from which the adult worms had been transferred were incubated for an additional 24h at 20°C and then transferred to 4°C for 30 days. The plates were then stained with 200µl of 1% toluidine blue solution to count progeny.

Nematodes previously used in the time to adulthood assay were also inspected every day to determine if they still survived. Nematodes that no longer moved and did not have any apparent pharyngeal pumping were then gently prodded with a worming pick. The day a nematode did not respond to prodding was recorded as its day of death. Longevity was calculated as the number of days between plating the L1 for the time to adulthood assay and the day of death.

Survivorship was measured by plating 10 L1 siblings of the original nematode used in the time to adulthood assay onto a separate 60mm NGM plate seeded with OP50. After their sibling used in the time to adulthood assay had reached adulthood, the 10 nematodes were screened to see how many survived to adulthood. Survivorship was recorded as the proportion of nematodes that survived to adulthood out of the total plated, with a possible minimum of 0 and a maximum of 1.

In all four assays, the value of each fitness trait was normalized by dividing the observed value of the trait by the mean of the N_{vk} nematodes used for that trait in that run. All statistical analysis was performed in JMP.

Seahorse Respiration Assay

Mitochondrial oxygen consumption rate (OCR) is dependent on a series of reactions within mitochondria specific to the ETC (Chance and Williams 1955; Wu et al. 2007; Gerencser et al. 2009). As a result, measuring OCR at the ETC level has emerged as an indicator for mitochondrial dysfunction (Will et al. 2006). To determine OCR in each of the ETC mutant bearing lines, respiration assays were performed using a modified version of previously published protocols (Koopman et al. 2016).

Nematodes were thawed from cryogenically preserved stocks and populations were cultured for three generations on NGM plates seeded with OP50 and incubated at 20°C. All lines were transferred to new plates every three days by chunk transfer to ensure abundant food and space. Populations were then synchronized by dissolution (Lewis and Fleming 1995) so that the worms would be day 1 adults at the time of the respiration assay (140h for the lines bearing *isp-1(qm150)* and 48 hours for all other lines).

24 hours prior to performing each assay, a Seahorse XFe sensor cartridge was hydrated using the included hydration solution and incubated at 30°C. Stock solutions of 100µM carbonyl cyanide 4-(trifluoromethoxy)phenylhydrazone (FCCP) and 400 mM sodium azide were also prepared 24 hours in advance. In addition, the Bioscience Seahorse XFe96 Flux Analyzer's heater was turned off 24 hours before running the assay to prevent it from operating outside of the normal incubation temperatures of *C. elegans.*

On the day of the assay, 100 day one adults were picked into 1.5 ml of M9 buffered solution (Koopman et al. 2016) in a 1.75ml tube for each line. These nematodes were left in the buffer solution for an hour to allow them to release bacteria from their guts into the M9, at which time the worms were gently pelleted at 500 × g for 2 minutes and the supernatant was replaced with fresh M9 three times. A final pelleting was then performed, and the supernatant was drawn off, leaving 100µl of M9 with the nematodes in the tube. Nematodes where then resuspended by aspiration and the worm suspension was pipetted into three wells (20µl each) of the Seahorse Cell Culture microplates using a 200µl wide bore pipet tip that had been coated in 1x PBS + 0.05% Triton-X100 (Koopman et al. 2016). All wells were then topped up to 200µl with M9 and allowed to settle for 10 minutes.

The assay was run using 22µl of FCCP stock in port A and 24µl of sodium azide in port B of the sensor cartridge. The cell culture microplate and sensor cartridge were then loaded into the XFe96 Analyzer and the following protocol was run:

1. Calibrate
2. Equilibrate
3. Loop 5 times
    a. Mix 2 minutes
    b. Wait 30 seconds
    c. Measure 2 minutes
4. Inject from port A
5. Loop 7 times
    a. Mix 2 minutes
    b. Wait 30 seconds
    c. Measure 2 minutes
6. Inject from port B
7. Loop 5 times
    a. Mix 2 minutes
    b. Wait 30 seconds

c. Measure 2 minutes

The mean OCR measured in step 3 represents the baseline OCR in unstressed worms. FCCP acts to uncouple OCR from oxidative phosphorylation by permeabilizing mitochondrial membranes and allowing the free transfer of protons across this barrier (Benz and McLaughlin 1983). The average of the measurements in step 5 therefore measures the maximum OCR possible due to oxidative phosphorylation. Sodium azide inhibits complex IV activity (Tsubaki 1993), stopping oxidative phosphorylation so that only non-mitochondrial OCR can be measured in step 7. Basal respiration is then measured as the difference between the OCR measured in steps 3 and 7, maximal respiration is the difference between OCR measured in steps 5 and 7, and spare capacity is the difference in OCR measured in steps 3 and 5.

Immediately after the assay was run, every well in the cell culture plate was imaged using an AXIO Zoom V16. These images were used to count the nematodes present in each well and to calculate the average size of worms in each well (see below). All OCR data was first normalized by the number of nematodes present in each well and then further by dividing the OCR/worm by the average length, volume, or surface area of nematodes within each well (see below).

Calculation of average nematode dimensions in ImageJ

Images of each well were captured using an AXIO Zoom V16 in a single session without changing settings along with a single image of a mm ruler placed over an empty well. For each well, three representative nematodes were selected from the image. The nematodes had to be linearly aligned with their mouths and tails at the most extreme

points along the X-axis. In some cases, where enough horizontally aligned nematodes could not be found, a vertically aligned nematode was instead selected and rotated 90°. Using FIJI (Schindelin et al. 2012), two lines were drawn around the perimeter of the nematode's profile using the segmented line drawing tool. The upper line was denoted as line A and the lower line B, with both lines connecting at the nematode's mouth and the tip of its tail. The coordinates of each line segment were then extracted from the image in FIJI and exported to Excel. From these coordinates the length, volume, and surface area of the representative nematode were calculated using methods adapted from Moore et al. (2013) and Andrews (2019). Briefly, the worm was divided into 100 segments of equal width (h) from the mouth to the tip of the tail. For each of these segments the difference between the Y coordinates were calculated along line A and B for each segment (Y_A and Y_B respectively) and used to determine the radius of the worm at each end of the segment (r_n and r_{n-1}). The following formulae were then used to determine the volume and surface areas of each worm.

$$Volume = \sum_{n=1}^{100} \frac{\pi(r_n^2 + r_n r_{n-1} + r_{n-1}^2)(x_n - x_{n-1})}{3}$$

$$where\ r_n = \frac{y_{An} - y_{Bn}}{2}$$

$$Surface\ Area = \sum_{n=1}^{100} \pi(r_n + r_{n-1})\sqrt{(r_n - r_{n-1})^2 + (x_n - x_{n-1})^2}$$

The length was determined by first finding the midpoint between each line segment $(y_{Bn} + \frac{1}{2}y_{An}, x_n)$ and summing the distance between each sequential midpoint. The

average volume, surface area, and length were then calculated using the three representative worms from each well.

Results

Fitness traits of electron transport chain mutation-bearing lines

There was no significant difference in time to adulthood, longevity, or survivorship between the control strains (N_{wt}, X_{wt}, F_{wt}). The Δ*fog-2* control lines had greatly increased productivity compared to N2 and Δ*xol-1* control lines, with a 61.23% and 59.08% increase respectively (all Tukey-Kramer honestly significant difference (TK HSD) comparisons have *p*-values < 0.0001). Healthy, obligately outcrossing *C. elegans* typically have increased productivity owing to the increased amount of sperm produced by males and greater investment in egg production by females (Schedl and Kimble 1988). However, these outcrossing lines can also be more sensitive to environmental perturbations (Plesnar-Bielak et al. 2017). In comparing the two different N2 strains, there are no significant difference in time to adulthood, longevity, or survivorship. There is a significant (16.83%) decrease in productivity in N_{se} compared to N_{wt} (TK HSD, $p = 0.0009$).

All nuclear ETC mutation-bearing lines have decreased productivity (figure V-1.A). Within the selfing lines (N2 and Δ*xol-1*), the decreases in productivity range from 73.14% in N_{gas} (TK HSD, $p < 0.0001$) to 86.70% in X_{gas} (TK HSD, $p < 0.0001$) with no significant difference observed between *isp-1(qm150)* and *gas-1(fc21)* mutations. In the obligately outcrossing lines (Δ*fog-2*), the nuclear ETC mutations result in near infertility,

with raw mean productivities of 0.5 offspring produced by F_{gas} and 16.16 by F_{isp} (a 99.91% and 96.71% decrease, respectively). Furthermore, many F_{gas} and F_{isp} nematodes did not produce any progeny at all (66.67% and 26.32%, respectively). Interestingly, *cox-1* mutant-bearing lines produce significantly more offspring in the N2 and fewer progeny in the Δ*xol-1* background than their respective WT controls (TK HSD, $p < 0.0001$ and $p = 0.0015$, respectively). C*tb-1(189)*-bearing lines also produce more progeny in the N2 background (TK HSD, $p < 0.0001$).

All *isp-1(qm150)* mutant-bearing lines have dramatically increased time to adulthood relative to their wild-type controls (figure V-1.B), ranging from a 100.19% increase in X_{isp} (TK HSD, $p < 0.0001$) to a 176.72% increase in F_{isp} (TK HSD, $p < 0.0001$). *Gas-1(fc21)*-bearing lines also show an increase in time to adulthood, though the increase is only significant in N_{gas} (37.26% increase; TK HSD, $p = 0.0047$) and X_{gas} (28.01% increase; TK HSD *p value* < 0.0001) (figure V-1.B). Neither of the mitochondrial ETC mutations had any significant effect on time to adulthood.

In terms of longevity, the N2 and Δ*xol-1* lines are affected similarly by the ETC mutations (figure V-1.C). In both the N2 and Δ*xol-1* backgrounds, only *gas-1(fc21)* has any significant effect on longevity. N_{gas} has a 42.19% reduction in longevity relative to N_{wt} (TK HSD, $p = 0.0160$), and X_{gas} has a 49.98% reduction relative to X_{wt} (TK HSD, $p = 0.0001$). In the Δ*fog-2* lines F_{wt} has a 36.11% reduction in longevity compared to N_{wt} and a 46.63% reduction compared to X_{wt} (TK HSD, $p = 0.0114$ and 0.0131 respectively). F_{ctb}, F_{gas}, and F_{isp} all have significantly increased longevity compared to F_{wt} (TK HSD, $p = 0.0199$, 0.0203, and <0.0001, respectively).

Most of the ETC mutant-bearing lines have no effect on survivorship (figure V-1.D). Only *isp-1(qm150)*-bearing lines reliably show a significant reduction in survivorship. N_{isp}, X_{isp}, and F_{isp} have survivorships 10.75%, 14.44%, 9.54% lower than their WT controls, with *p values* < 0.0001 for TK HSD comparisons to their respective WT controls. *Gas-1(fc21)* only has a significant effect in the Δ*fog-2* background (TK HSD, $p < 0.0001$) with a 19.59% reduction in survivorship.

When comparing the double mutant line (N_{ctb}/N_{isp}) to its related single mutant lines (N_{ctb} and N_{isp}), there was a common trend in which N_{ctb} was always the most fit, N_{isp} was least fit, and N_{ctb}/N_{isp} displayed an intermediate level of fitness regardless of the fitness trait measured (Figure V-2). In terms of productivity, all three lines were significantly different from one another and from WT (TK HSD *p value*<0.0001 for all comparisons). N_{ctb} produces 113% as may progeny as WT, while N*isp* produces only 12.5% as many progeny as WT N2. $N_{ctb}/N_{isp,}$ which bears both *ctb-1(189)* and *isp-1(qm150)* mutations, has increased productivity relative to N_{isp}, producing 49.6% as many progeny as WT. Developmental rate showed a similar pattern. Developmental rate was reduced to 68.4% of WT, from N_{ctb} to N_{ctb}/N_{isp} with the addition of *isp-1(qm150)* (TK HSD, $p = 0.0016$), but was further reduced to 41.7% of WT in N_{isp} (TK HSD, $p < 0.0001$ in both comparisons).

The only ETC mutation in the N2 background to have reduced survivorship was *isp-1(qm150)* (see above). While N_{ctb}/N_{isp} did not have significantly different survivorship from N_{ctb} or N_{isp}, the difference between N_{ctb} and N_{isp} is significant (TK

HSD p-value = 0.0007) suggesting that the double mutant had intermediate survivorship between N_{ctb} and N_{isp}.

Respiration

All respiration data was first normalized by organism count, as is standard in Seahorse respiration assays. However, male (Fm_{wt}) and female (Ff_{wt}) nematodes are significantly different in terms of volume (Student's t, $t = 2.06$, $p = 0.0290$), surface area (Student's t, $t = 2.06$, $p = 0.0492$), and length (Student's t, $t = 2.06$, $p = 0.0345$). It is known that metabolic rate scales with size (Glazier 2005; Burger et al. 2019), so correlations between average nematode size measurements per well and normalized OCR measurements in WT N2 nematodes were calculated (table V-4). All measurements explain a significant amount of the variation in basal and maximal respiration. The measurement that explains the greatest amount of the variation in OCR is volume ($r^2 = 0.3$ and 0.319 for basal and maximal respiration respectively). All further analysis was done on data normalized by nematode count per well, N_{wt} mean basal OCR per plate, and average nematode volume per well.

In the WT controls, Fm_{wt} had elevated basal respiration compared to N_{wt} and X_{wt} (figure V-3). Fm_{wt} also had elevated maximum respiration compared to all other WT controls, resulting in greater spare capacity than both N_{wt} and WT Ff_{wt} (figure V-3). No other comparisons between the WT controls are significant.

In the facultatively outcrossing background (N2), there is no significant difference between any ETC mutant line's basal or maximal respiration. Despite its lack

of significance, N_{isp} does appear to have greatly reduced maximal respiration capacity compared to all other ETC mutant-bearing lines (figure V-4), with an OCR 26.7% lower than WT. This decrease in maximum respiration does result in a significant decrease in the spare capacity of N_{isp} compared to N_{cox} (Student's t, $p = 0.0384$), with a 68.1% decrease in spare capacity, and compared to N_{cox}/N_{isp} (Student's t, $p = 0.0315$), with a 66.1% decrease in spare capacity (figure V-4). Despite no ETC mutation-bearing line being significantly different from WT in terms of OCR, it is also interesting to note that N_{ctb} and N_{ctb}/N_{isp} both have spare capacities more similar to N_{wt} than to N_{isp} (figure V-4), further supporting the idea that *ctb-1(189)* compensates for the deleterious effects of *isp-1(qm150)*.

In the obligately selfing background (Δ*xol-1*), the ETC mutations seem to have had a different effect on basal OCR. In this background, both nuclear ETC mutations result in increases in OCR compared to X_{wt}, with a 118.87% increase in X_{isp} (Student's t, $p = 0.0909$) and a 179.13% increase in X_{gas} (Student's t, $p = 0.0010$). However, there are no significant differences in maximal respiration or spare capacity, partially due to the large amount of variation in X_{wt} ($\bar{x} = 4.568$, $\sigma = 4.301$). Despite the lack of significant differences, the trends in the spare capacity of Δ*xol-1* lines reflect those seen in the N2 lines (figure V-5), with the wild-type and mitochondrial ETC mutations having increased spare capacity relative to the nuclear ETC mutations.

The obligately outcrossing (Δ*fog-2*) background shares the trends seen in the previous two backgrounds (figure V-6). In the female Δ*fog-2* lines, there are no significant differences in basal respiration or in in maximal respiration despite Ff_{isp}

having a 63.35% decrease in maximal respiration compared to Ff_{wt}. The decrease in maximal respiration of Ff_{isp} results in significantly lower spare capacity, with Ff_{isp} having a 84.8% decline in mean spare capacity relative to Ff_{wt} (Student's t, $p = 0.0193$). Though not significant, Ff_{gas} also has lower spare capacity, with a 51.5% reduction compared to Ff_{wt}.

Males from the Δ*fog-2* lines do not show any significant differences in OCR resulting from either of the nDNA ETC mutations or from *ctb(189)*. There is a significant effect of *cox-1(chpIR)* (figure V-6), resulting in a 164.1% increase in maximal respiration (Student's t, $p = 0.0483$) and a 180.9% increase in spare capacity (Student's t, $p = 0.0252$) in Fm_{cox} relative to Fm_{wt}.

Despite the sex specific differences in OCR found in wild-type Δ*fog-2* lines, only *cox-1(chpIR)* and *isp-1(qm150)*-bearing lines have any significant differences between the OCR of males and females. Fm_{cox} has a 75.1% increase in maximal respiration (Student's t, $p = 0.0401$) and a 93.7% increase in spare capacity (Student's t, $p = 0.0285$) relative to Ff_{cox}. Similarly, Fm_{isp} has a 52.6% increase in spare capacity relative to Ff_{isp} (Student's t, $p = 0.0181$).

Discussion

In this study we sought to determine if the effect of ETC mutations in *C. elegans* had measurable, phenotypic effects in different sexes and reproductive systems. To this end, we created 13 lines containing one of four ETC mutations (two nuclear and two mitochondrial) and a mutation in the sex determining pathway of *C. elegans* (either WT N2, Δ*xol-1*, or Δ*fog*-2). We then compared the overall fitness and mitochondrial respiration of each of these lines to that of WT controls that possess the sex determining mutations but not ETC mutations.

To determine if there was a clear reproductive system specific decline in fitness caused by these ETC mutations, we examined four fitness phenotypic traits: productivity, developmental rate, longevity, and survivorship. Overall, there is very little measurable effect of either *ctb-1(189)* or *cox-1(chpIR)* regardless of sex system. Bearing either *cox-1(chpIR)* or *ctb-1(189)* results in a slight, but significant increase in productivity in the facultatively outcrossing lines. In contrast, bearing *cox-1(chpIR)* results in a slight but significant decrease in the productivity of obligately selfing lines. Neither mtDNA mutation has any effect on the other three fitness traits or on the obligately outcrossing line. Initially, this seems to suggest that the mitochondrial ETC mutations do not have much, if any, significant fitness consequences in any background. However, mitochondria are very dynamic organelles whose phenotypes tend to be context-dependent (Rand and Mossman 2020). Furthermore, past studies with *C. elegans* have shown that benign laboratory conditions, as were used in this study, can

underestimate the phenotypic consequences of new mutations which would be under greater stress in a more natural environment (Katju et al. 2018).

The nuclear ETC mutations have much more dramatic effects on fitness. All lines bearing i*sp-1(qm150)* have significant decreases in productivity, developmental rate, and survivorship. Similarly, bearing *gas-1(fc21)* results in reduced productivity, developmental rate, and longevity, regardless of the reproductive system. In terms of reproductive system specific effects, the outcrossing lines appear to be especially susceptible to infertility caused by the nuclear ETC mutations. F_{gas} and F_{isp} have 66.67% and 26.32% reduction in productivity, respectively. In addition, both lines have greater than 90% reductions in productivity compared to F_{wt}.

Sex is thought to be a major player in keeping pace with mitochondrial mutation accumulation by increasing nDNA recombination, and providing the genetic variation necessary for compensatory nuclear coadaptation (Havird et al. 2015). However, the present study suggests another role for sex. Since i*sp-1(qm150)* and *gas-1(fc21)* result in greater fitness decline in outcrossing lines than selfing lines, selection against these mutations will be stronger in outcrossing populations than in selfing populations. The sensitivity of outcrossing *C. elegans* to environmental perturbation such as thermal stress (Plesnar-Bielak et al. 2017) and the notoriously poor mating performance of male *C. elegans* (Garcia et al. 2007) have both been implicated in the low proportion of males, and evolution towards selfing, in natural *C. elegans* populations (Cutter et al. 2019). Furthermore, the reproductive assurance that comes from selfing is thought to have contributed to the transition from an outcrossing species to an androdiecious species in

C. elegans (Theologidis et al. 2014; Cutter et al. 2019). Additionally, the lower productivity of outcrossing i*sp-1(qm150)* and *gas-1(fc21)* bearing lines relative to selfing lines could lead to selection against outcrossing in androdiecious populations of *C. elegans.*

While measurements of organismal fitness are informative, we sought to measure the effect of each of the ETC mutations on mitochondrial dysfunction. Using OCR as a proxy for mitochondrial function, we found that the lines bearing i*sp-1(qm150)* have significantly decreased spare capacity regardless of sex system. Lines bearing *gas-1(fc21)* also reliably have slightly reduced spare capacity. Spare capacity is a measure of an organism's ability to meet its bioenergetic needs under stress (Pfleger et al. 2015), and lower spare capacity is associated with cell death and mitochondrial disease (Yadava and Nicholls 2007; Nickens et al. 2013). Thus, the lower spare capacity in these lines supports the fitness data in suggesting that both i*sp-1(qm150)* and *gas-1(fc2)* result in mitochondrial dysfunction. However, there is no evidence for line-specific effects of the nDNA ETC mutations.

Of the seven different lines bearing mtDNA ETC mutations, only male F_{cox} worms have significantly increased spare capacity. No other changes in OCR from the mtDNA mutations are detected. This supports the trend (or lack thereof) seen with the four fitness phenotypes. Without a significant reduction in spare capacity of the mtDNA ETC mutation-bearing lines, there is no reason to suspect that they would perform differently under stress than the WT control lines.

We found few sex-specific effects of any of the tested ETC mutations. Males have slightly higher OCRs, with Fm_{cox} and Fm_{wt} as extreme examples. The increase in spare capacity of males bearing *cox-1(chpIR)* is the only observed case of a differential effect of our ETC mutations.

Both the fitness and respiration assays confirm the compensatory effect of *ctb-1(189)* for *isp-1(qm150)*. In all the fitness traits, the double mutant N_{ctb}/N_{isp} has an intermediate phenotype between N_{ctb} and N_{isp}. However, the double mutant results in a full recovery of spare capacity to WT levels from that of N_{isp}. The difference between these two results suggests that there is some level of mitochondrial dysfunction not captured by the respiration assay.

In summary, we found that both nuclear ETC mutations cause some mitochondrial dysfunction. Conversely, we found little evidence for mitochondrial dysfunction in either of the mitochondrial ETC mutations. We also found little evidence for sex-specific effects of any of our ETC mutations. We did, however, find some evidence for sex-system specific differences in the deleterious effects of ETC mutations. Obligately outcrossing *C. elegans* have especially lower developmental rate and productivity when bearing either of our nuclear ETC mutants. Further study is required to determine how these differences between reproductive systems will result in differences in mitonuclear coevolution, but this study establishes several constructed genotypes that could be used to pursue these questions.

Tables

Table V-1. *C. elegans* strains used in this study. Strain names are reported for hermaphrodites, females, and males when appropriate. Each line's reproductive strategy is reported as FO (facultatively outcrossing), OO (obligately outcrossing), or OS (obligately selfing). The source of each mutation is reported in the last column, with lines either from the lab of Suzanne Estes at Portland State University (E), from the lab of Vaishali Katju (K), generated via CRISPR-Cas9 by InVivo Biosystems (I), or generated through a combination of CRISPR-Cas9 by InVivo Biosystems and backcross by the Katju lab (I,K).

Strain name ♂/♀	♂	reproductive system	nDNA mutations	mtDNA mutations	source
N_{wt}	-	FO	-	-	K
N_{se}	-	FO	-	-	E
N_{ctb}	-	FO	-	*ctb-1(189)*	E
N_{cox}	-	FO	-	*cox-1(chpIR*)	E
N_{gas}	-	FO	*gas-1(fc21)*	-	E
N_{isp}	-	FO	*isp-1(qm150)*	-	E
$N_{ctb/isp}$	-	FO	*isp-1(qm150)*	*ctb-1(189)*	E
F_{wt}/Ff_{wt}	Fm_{wt}	OO	Δ*fog-1*	-	I
F_{ctb}/Ff_{ctb}	Fm_{ctb}	OO	Δ*fog-1*	*ctb-1(189)*	I,K
F_{cox}/Ff_{cox}	Fm_{cox}	OO	Δ*fog-1*	*cox-1(chpIR*)	I,K
F_{gas}/Ff_{gas}	Fm_{gas}	OO	Δ*fog-1*; *gas-1(fc21)*	-	I,K
F_{isp}/Ff_{isp}	Fm_{isp}	OO	Δ*fog-2; isp-1(qm150)*	-	I,K
X_{wt}	-	OS	Δ*xol-1*	-	I
X_{ctb}	-	OS	Δ*xol-1*	*ctb-1(189)*	I
X_{cox}	-	OS	Δ*xol-1*	*cox-1(chpIR*)	I
X_{gas}	-	OS	Δ*xol-1*; *gas-1(fc21)*	-	I
X_{isp}	-	OS	Δ*xol-1; isp-1(qm150)*	-	I

Table V-2. Primers used to screen electron transport chain mutations and deletions**.**

Δ*fog-2*	
Fog-2.F1	5’-CAA AGC TTC GCT TCA TGC TC-3’
Fog-2.R1	5’-CAG TGA TCA TGC CAA TTT ATC-3’
Fog-2.R2	5’-TCT CCA TTG GCA TGT CAG AG-3’
Δ*xol-1*	
Xol-1.F1	5’-CCT GTA AGA CCA CAC ACG AC-3’
Xol-1.R1	5’-CAT TTG AAG TAG CCG TCC TC-3’
Xol-1.R2	5’-CTC AGA ATT TGC TTC AAC CTG-3’
gas-1(fc21)	
gas-1.F	5'-ATC TCT TCA ATA CGG CAC AAG-3'
gas-1.R	5'-ATC GTC TCG ATT ACG TCT CCA-3'
isp-1(qm150)	
isp-1.F	5'-GAC GAA GAC TGG CTT TCC AC-3'
isp-1.R	5'-ACT ACG ACG CTT CTG GAC GT-3'
ctb-1(qm189)	
ctb-1.F	5'-AAT GGG ATG TTG GTG ACA TT-3'
ctb-1.R	5'-GCA CGC AAA ATT GCA TAA G-3'
cox-1(chpIR)	
cox-1.F	5'-AGG GTT TTC AGC ACC ATT AGT CT-3'
cox-1.R	5'-CAG GGT GCC CCA TTG TTC TT-3'

Table V-3. The number of replicate worms used in each of the four fitness assays. Replicates are reported by the number of worms from each run followed by the total number of replicates in bold.

	Number of Replicates			
Line	Productivity	Time to Adulthood	Longevity	Survivorship
N_{wt}	10/10/15/30/**65**	10/10/15/0/**35**	10/10/15/0/**35**	10/10/15/0/**35**
N_{se}	10/10/0/0/**20**	10/10/0/0/**20**	9/10/0/0/**19**	10/10/0/0/**20**
N_{ctb}	19/0/0/0/**19**	19/0/0/0/**19**	19/0/0/0/**19**	20/0/0/0/**20**
N_{cox}	20/0/0/0/**20**	20/0/0/0/**20**	19/0/0/0/**19**	20/0/0/0/**20**
N_{gas}	20/0/0/0/**20**	20/0/0/0/**20**	20/0/0/0/**20**	14/0/0/0/**14**
N_{isp}	19/7/0/0/**26**	19/7/0/0/**26**	18/6/0/0/**24**	20/10/0/0/**30**
X_{wt}	10/10/0/0/**20**	10/10/0/0/**20**	10/10/0/0/**20**	10/10/0/0/**20**
X_{ctb}	0/19/0/0/**19**	0/19/0/0/**19**	0/19/0/0/**19**	0/20/0/0/**20**
X_{cox}	0/18/0/0/**18**	0/19/0/0/**19**	0/18/0/0/**18**	0/20/0/0/**20**
X_{gas}	0/17/0/0/**17**	0/19/0/0/**19**	0/19/0/0/**19**	0/20/0/0/**20**
X_{isp}	0/20/0/0/**20**	0/20/0/0/**20**	0/18/0/0/**18**	0/20/0/0/**20**
F_{wt}	0/0/0/53/**53**	10/2/0/0/**12**	10/9/0/0/**19**	10/10/0/0/**20**
F_{ctb}	19/0/0/0/**19**	20/0/0/0/**20**	19/0/0/0/**19**	20/0/0/0/**20**
F_{cox}	20/0/0/0/**20**	19/0/0/0/**19**	20/0/0/0/**20**	20/0/0/0/**20**
F_{gas}	0/12/0/0/**12**	0/6/0/0/**6**	0/11/0/0/**11**	0/5/0/0/**5**
F_{isp}	0/19/0/0/**19**	0/9/0/0/**9**	0/19/0/0/**19**	0/18/0/0/**18**
N_{ctb}/N_{isp}	0/0/15/0/**15**	0/0/15/0/**15**	0/0/13/0/**13**	0/0/15/0/**15**

Table V-4. Correlations between wild-type N2 *C. elegans* Oxygen Consumption Rates normalized by nematode count per well and measurements of nematode size. *$p < 0.05$, **$p < 0.01$, ***$p < 0.001$

Correlation	r^2	r^2 adjusted	F-test
Basal Respiration/Count x Length	0.128	0.103	5.00*
Basal Respiration/Count x Volume	0.300	0.279	14.54***
Basal Respiration/Count x SA	0.268	0.246	12.42**
Basal Respiration/Count x SA/V	0.116	0.090	4.46*
Maximum Respiration/Count x Length	0.153	0.128	6.12*
Maximum Respiration/Count x Volume	0.319	0.299	15.95***
Maximum Respiration/Count x SA	0.302	0.281	14.69**
Maximum Respiration/Count x SA/V	0.130	0.105	5.10*

Figures

Figure V-1: Fitness trait means for electron transport chain mutation-bearing lines relative to N_{wt}. Phenotypic assays were performed for four fitness traits: productivity (A), time to adulthood (B), longevity (C), and survivorship to adulthood (D). Each bar represents the mean of a fitness trait of a ETC mutation-bearing line in each background normalized by the mean of that trait in N_{wt} nematodes. Error bars represent one standard error. Significant differences from wild-type nematodes in each line's respective background shown above bars: $*p < 0.05$, $**p < 0.01$, $***p < 0.001$, $****p < 0.0001$.

Figure V-2: Fitness trait means for N_{ctb}, N_{isp}, and N_{ctb}/N_{isp} double mutants. Phenotypic assays were performed for four fitness traits: productivity, time to adulthood, longevity, and survivorship to adulthood. Each bar represents the mean of a fitness normalized by the mean of that trait in N_{wt} nematodes used as a control. Error bars represent one standard error. Significant comparisons shown above bars: $**p < 0.01$, $***p < 0.001$, $****p < 0.0001$, and n.s. = not significant.

Figure V-3: Relative mean oxygen consumption rate (OCR) in wild-type control lines. All OCR means have been normalized to the mean of N_{wt} basal respiration rate = 1. Error bars represent one standard error. Student's t-tests were performed between each line and significant comparisons are represented with bars connecting pairs and asterisks representing p-values: $*p < 0.05$ and $**p < 0.01$.

Figure V-4: Relative mean oxygen consumption rate (OCR) in facultatively outcrossing (N2) electron transport chain mutant-bearing lines. All OCR means have been normalized to the mean of N_{wt} basal respiration rate = 1. Error bars represent one standard error.

Figure V-5: Relative mean oxygen consumption rate (OCR) in obligately selfing (Δ*xol-1*) electron transport chain mutant-bearing lines. All OCR means have been normalized to the mean of X_{wt} basal respiration rate = 1. Error bars represent one standard error.

Figure V-6: Relative mean oxygen consumption rate (OCR) in obligately outcrossing (Δ*fog-2*) electron transport chain mutant-bearing lines. All female OCR means have been normalized to the mean of Ff_{wt} basal respiration rate = 1 and male OCR have been normalized to the mean of Fm_{wt} basal respiration rate = 1. Error bars represent one standard error.

Figure V-1. Fitness trait means for electron transport chain mutation-bearing lines relative to N_{wt}.

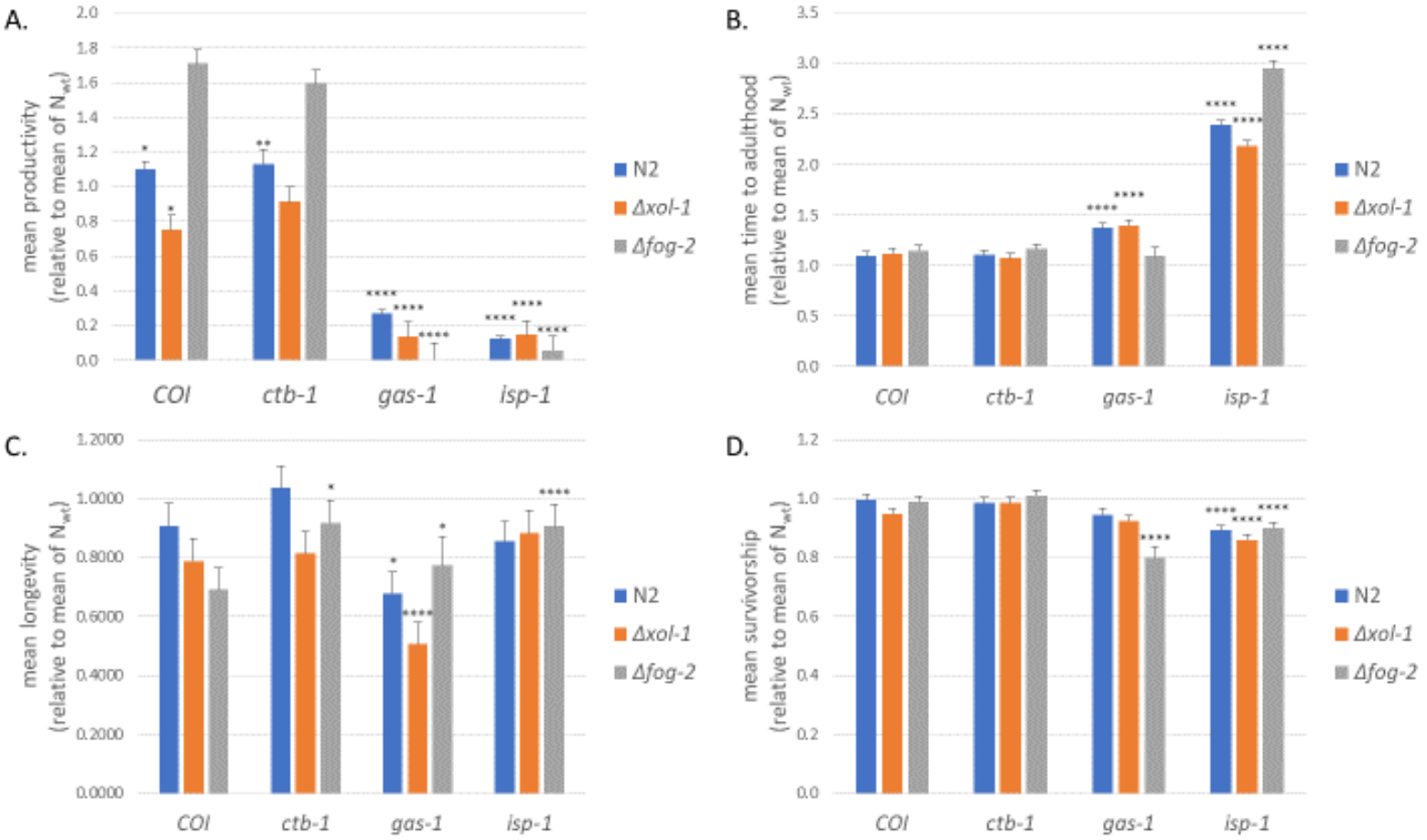

Figure V-2. Fitness trait means for N_{ctb}, N_{isp}, and N_{ctb}/N_{isp} double mutants.

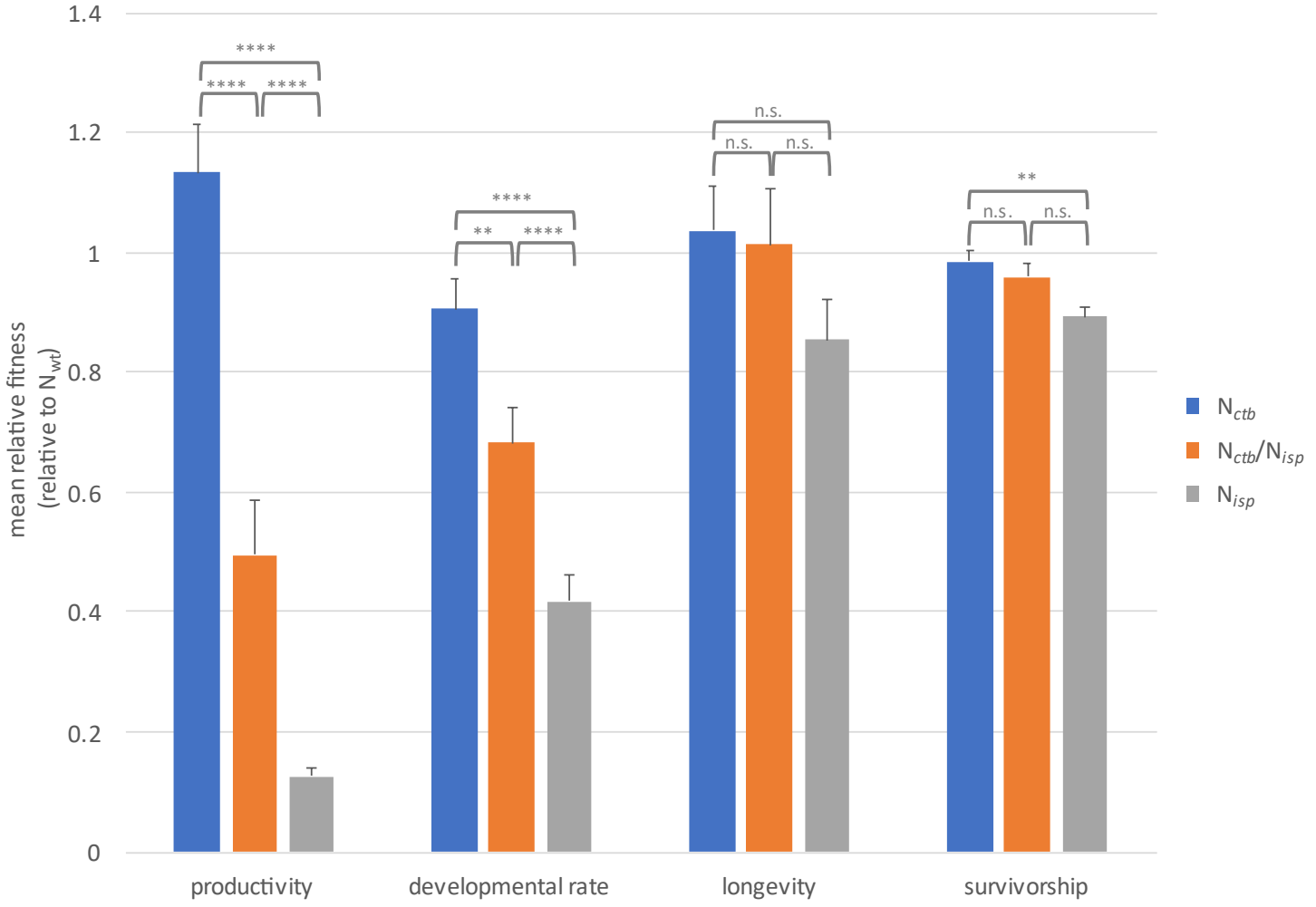

Figure V-3. Relative Oxygen Consumption Rate (OCR) in wild-type control lines.

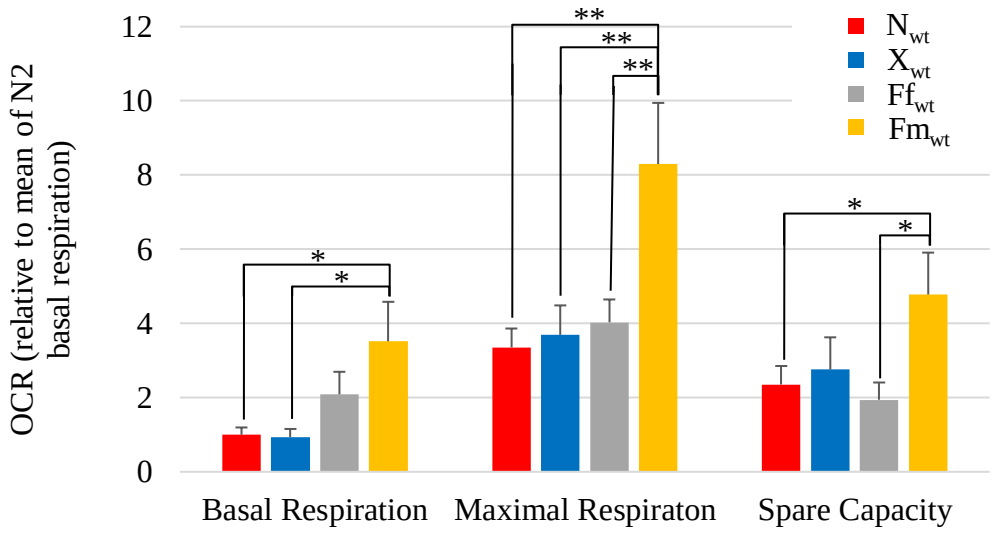

Figure V-4. Relative Oxygen Consumption Rate (OCR) in facultatively outcrossing (N2) electron transport chain mutant-bearing lines.

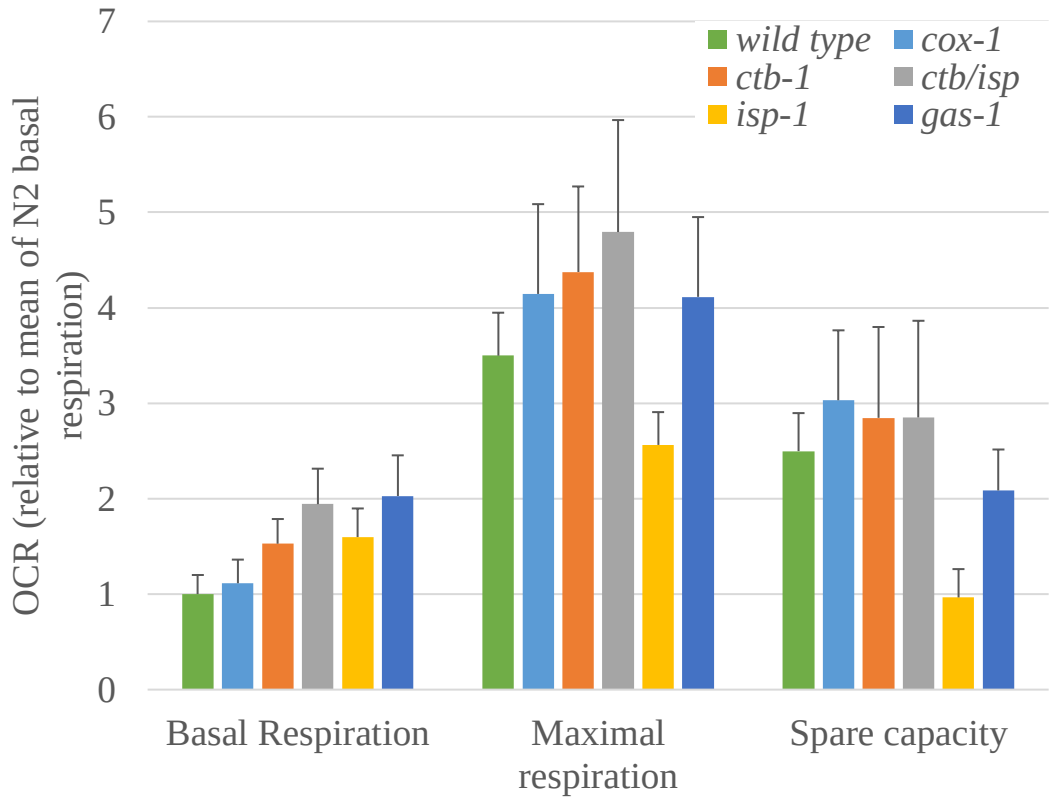

Figure V-5. Relative Oxygen Consumption Rate (OCR) in obligately selfing (Δ*xol-1*) electron transport chain mutant-bearing lines.

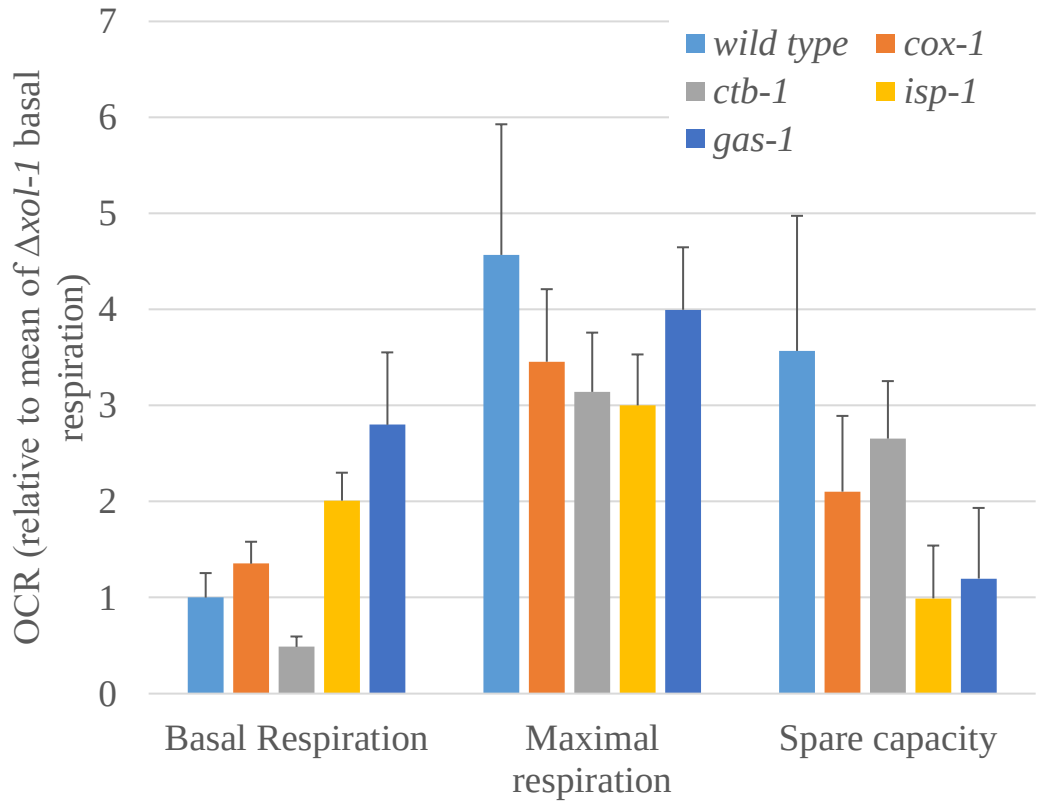

Figure V-6. Relative Oxygen Consumption Rate (OCR) in obligately outcrossing (Δ*fog-2*) electron transport chain mutant-bearing lines.

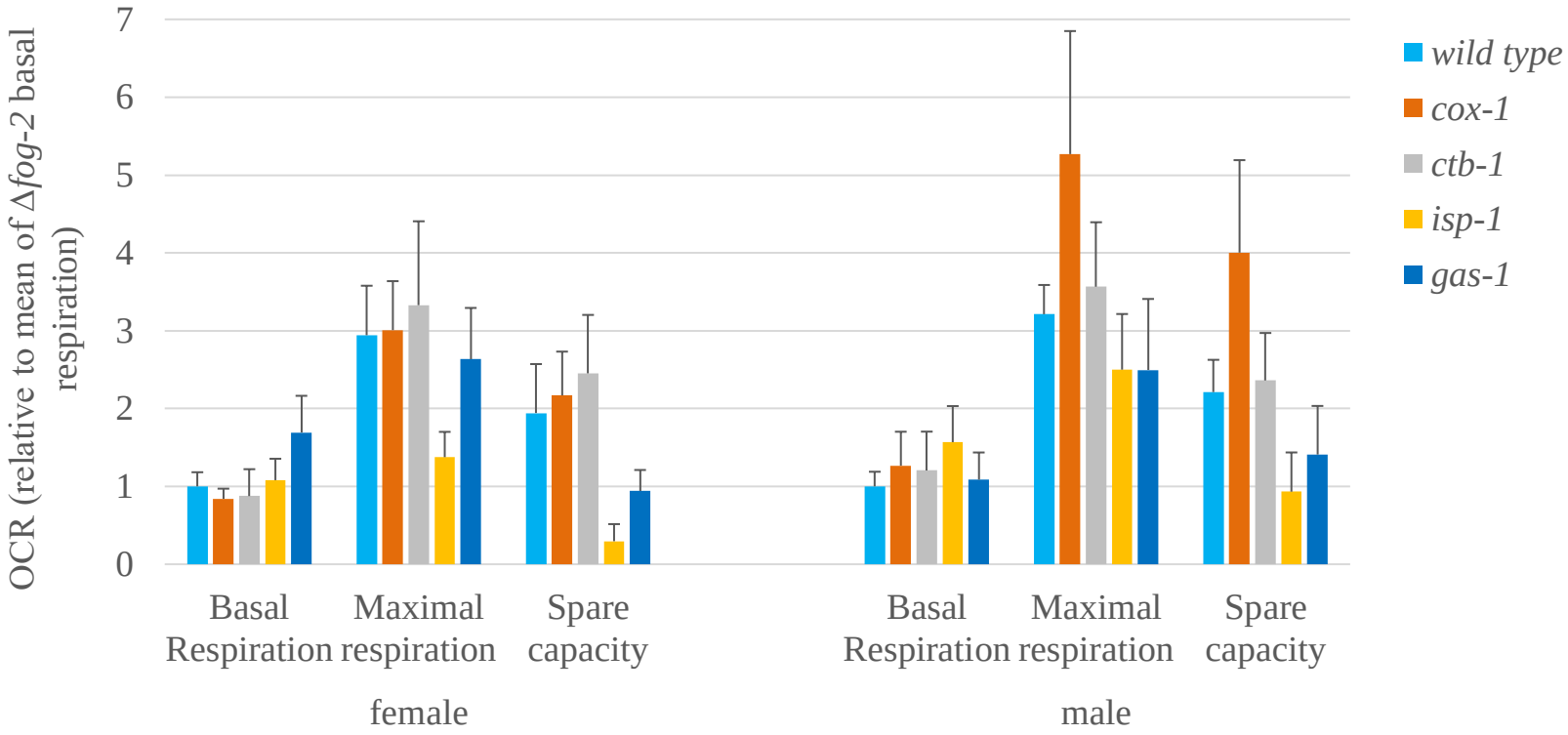

References

Andrews DGH. 2020. A new method for measuring the size of nematodes using image processing. *Biol Methods Protoc*. **5**(1):bpz020. (doi:10.1093/biomethods/bpz020)

Aw WC, Garvin MR, Melvin RG, Ballard JWO. 2017. Sex-specific influences of mtDNA mitotype and diet on mitochondrial functions and physiological traits in *Drosophila melanogaster*. *PLoS One*. **12**(11):e0187554. (doi:10.1371/journal.pone.0187554)

Azevedo L, Carneiro J, Van Asch B, Moleirinho A, Pereira F, Amorim A. 2009. Epistatic interactions modulate the evolution of mammalian mitochondrial respiratory complex components. *BMC Genomics*. **10**:266. (doi:10.1186/1471-2164-10-266)

Ballard JW, Whitlock MC. 2004. The incomplete natural history of mitochondria. *Mol Ecol* **13**:729-744. (doi:10.1046/j.1365-294x.2003.02063.x)

Benz R, McLaughlin S. 1983. The molecular mechanism of action of the proton ionophore FCCP (carbonylcyanide p-trifluoromethoxyphenylhydrazone). *Biophys J.* **41**(3):381-98. (doi:10.1016/S0006-3495(83)84449-X)

Burger JR, Hou C, Brown JH. 2019. Toward a metabolic theory of life history. *Proc Natl Acad Sci U S A*. **116**(52):26653-61. (doi:10.1073/pnas.1907702116)

Burton RS, Pereira RJ, Barreto FS. 2013. Cytonuclear genomic interactions and hybrid breakdown. *Annu.Rev. Ecol. Evol. Syst.* **44**:281-302. (doi:10.1534/genetics.107.080523)

Carroll J, Fearnley IM, Skehel JM, Shannon RJ, Hirst J, Walker JE. 2006. Bovine complex I is a complexof 45 different subunits. *J. Biol. Chem.* **281:**32724-7. (doi:10.1074/jbc.M607135200)

Chance B, Williams GR. 1955. Respiratory enzymes in oxidative phosphorylation. I. Kinetics of oxygen utilization. *J Biol Chem*. **217**(1):383-93.

Chinnery PF, Thorburn DR, Samuels DC, White SL, Dahl HM, Turnbull DM, Lightowlers RN, Howell N.2000. The inheritance of mitochondrial DNA heteroplasmy. *Trends in Genetics*. **16:**500-505. (doi:10.1016/s0168-9525(00)02120-x)

Christy SF, Wernick RI, Lue MJ, Velasco G, Howe DK, Denver DR, Estes S. 2017. Adaptive evolution under extreme genetic drift in oxidatively stressed *Caenorhabditis elegans*. *Genome Biol. Evol.* **9:**3008-22. (doi:10.1093/gbe/evx222)

Cutter AD, Payseur BA. 2003. Rates of deleterious mutation and the evolution of sex in *Caenorhabditis*. *J.Evol. Biol.* **16:**812-822. (doi:10.1046/j.1420-9101.2003.00596.x)

Cutter AD, Morran LT, Phillips PC. 2019. Males, outcrossing, and sexual selection in *Caenorhabditis* nematodes. *Genetics*. **213**(1):27-57. (doi:10.1534/genetics.119.300244)

Dingley SD, Polyak E, Ostrovsky J, Srinivasan S, Lee I, Rosenfeld AB, Tsukikawa M, Xiao R, Selak MA,Coon JJ, Hebert AS, Grimsrud PA, Kwon YJ, Pagliarini DJ, Gai X, Schurr TG, Hüttemann M, Nakamaru-Ogiso E, Falk MJ. 2014. Mitochondrial DNA variant in COX1 subunit significantly alters energy metabolism of geographically divergent wild isolates in *Caenorhabditis elegans*. *J. Mol. Biol.* **426**(11):2199-216. (doi:10.1016/j.jmb.2014.02.009)

Đorđević M, Stojković B, Savković U, Immonen E, Tucić N, Lazarević J, Arnqvist G. 2017. Sex-specific mitonuclear epistasis and the evolution of mitochondrial bioenergetics, ageing, and life history in seed beetles. *Evolution*. **71**(2):274-288. (doi:10.1111/evo.13109)

Drown DM, Preuss KM, Wade MJ. 2012. Evidence of a paucity of genes that interact with the mitochondrion on the X in mammals. *Genome Biol Evol*. **4**(8):763-8. (doi:10.1093/gbe/evs064)

Dubie JJ, Caraway AR, Stout MM, Katju V, Bergthorsson U. 2020 The conflict within: origin, proliferation and persistence of a spontaneously arising selfish mitochondrial genome. *Phil. Trans. R. Soc. B*. **375**:20190174. (doi:10.1098/rstb.2019.0174)

Feng J, Bussiere F, Hekimi S. 2001. Mitochondrial electron transport is a key determinant of life span in *Caenorhabditis elegans*. *Dev Cell* **1:**633-44. (doi:10.1016/s1534-5807(01)00071-5)

Garcia LR, LeBoeuf B, Koo P. 2007. Diversity in mating behavior of hermaphroditic and male-female Caenorhabditis nematodes. *Genetics*. **175**(4):1761-71. (doi:10.1534/genetics.106.068304)

Gemmell NJ, Metcalf VJ, Allendorf FW. 2004. Mother's curse: the effect of mtDNA on individual fitness and population viability. *Trends Ecol. Evol*. **19**:238-244. (doi:10.1016/j.tree.2004.02.002)

Glazier DS. 2005. Beyond the '3/4-power law': variation in the intra- and interspecific scaling of metabolic rate in animals. *Biol Rev Camb Philos Soc.* **80**(4):611-62. (doi:10.1017/S1464793105006834)

Gerencser AA, Neilson A, Choi SW, Edman U, Yadava N, Oh RJ, Ferrick DA, Nicholls DG, Brand MD. 2009. Quantitative microplate-based respirometry with correction for oxygen diffusion. *Anal Chem*. **81**(16):6868-78. (doi:10.1021/ac900881z)

Hargitai B, Kutnyánszky V, Blauwkamp TA, Steták A, Csankovszki G, Takács-Vellai K, Vellai T. 2009. *xol-1*, the master sex-switch gene in *C. elegans*, is a transcriptional target of the terminal sex-determining factor *TRA-1*. *Development*. **136**(23):3881-7. (doi:10.1242/dev.034637.)

Havird JC, Hall MD, Dowling DK. 2015. The evolution of sex: A new hypothesis based on mitochondrial mutational erosion: Mitochondrial mutational erosion in ancestral eukaryotes would favor the evolution of sex, harnessing nuclear recombination to optimize compensatory nuclear coadaptation. *Bioessays.* **37**:951-8. (doi:10.1002/bies.201500057)

Hill GE. 2014. Sex linkage of nuclear-encoded mitochondrial genes. *Heredity*. **112**(5):469-70. (doi:10.1038/hdy.2013.125)

Hill GE. 2015. Mitonuclear ecology. *Mol. Biol. Evol.* **32**:1917-1927. (doi:10.1093/molbev/msv104)

Hoekstra LA, Julick CR, Mika KM, Montooth KL. 2018. Energy demand and the context-dependent effects of genetic interactions underlying metabolism. *Evol Lett.* **2**(2):102-113. (doi:10.1002/evl3.47)

Immonen E, Collet M, Goenaga J, Arnqvist G. 2016. Direct and indirect genetic effects of sex-specific mitonuclear epistasis on reproductive ageing. *Heredity.* **116**(3):338-47. (doi:10.1038/hdy.2015.112)

Jafari G, Wasko BM, Tonge A, Schurman N, Dong C, Li Z, Peters R, Kayser EB, Pitt JN, Morgan PG, Sedensky MM, Crofts AR, Kaeberlein M. 2015. Tether mutations that restore function and suppress pleiotropic phenotypes of the *C. elegans isp-1(qm150)* Rieske iron-sulfur protein. *Proc. Natl. Acad. Sci. U. S. A.* **112**:e6148-57. (doi:10.1073/pnas.1509416112)

Katju V, LaBeau EM, Lipinski KJ, Bergthorsson U. 2008. Sex change by gene conversion in a *Caenorhabditis elegans fog-2* mutant. *Genetics*. **180**:669-72. (doi:10.1534/genetics.108.090035)

Katju V, Packard LB, Bu L, Keightley PD, Bergthorsson U. 2015 Fitness decline in spontaneous mutation accumulation lines of *Caenorhabditis elegans* with varying effective population sizes. *Evolution*. **69**:104-116. (doi:10.1111/evo.12554)

Katju V, Packard LB, Keightley PD. 2018 Fitness decline under osmotic stress in *Caenorhabditis elegans* populations subjected to spontaneous mutation accumulation at varying population sizes. *Evolution.* **72**:1000-1008. (doi:10.1111/evo.13463)

Kayser EB, Sedensky MM, Morgan PG. 2004. The effects of complex I function and oxidative damage on lifespan and anesthetic sensitivity in *Caenorhabditis elegans. Mech. Ageing Dev.* **125:**455-64. (doi:10.1016/j.mad.2004.04.002)

Keaney TA, Wong HWS, Dowling DK, Jones TM, Holman L. 2020. Sibling rivalry versus mother's curse: can kin competition facilitate a response to selection on male mitochondria? *Proc Biol Sci*. **287**(1930):20200575. (doi:10.1098/rspb.2020.0575)

Konrad A, Thompson O, Waterston RH, Moerman DG, Keightley PD, Bergthorsson U, Katju V. 2017. Mitochondrial mutation rate, spectrum and heteroplasmy in *Caenorhabditis elegans* spontaneous mutation accumulation lines of differing population size. *Mol. Biol. Evol*. **34**:1319-1334. (doi:10.1093/molbev/msx051)

Koopman M, Michels H, Dancy BM, Kamble R, Mouchiroud L, Auwerx J, Nollen EA, Houtkooper RH. 2016. A screening-based platform for the assessment of cellular respiration in *Caenorhabditis elegans*. *Nat Protoc*. **11**(10):1798-816. (doi:10.1038/nprot.2016.106)

Lang BF, Gray MW, Burger G. 1999. Mitochondrial genome evolution and the origin of eukaryotes. *Annu. Rev. Genet*. **33**:351-97. (doi:10.1146/annurev.genet.33.1.351)

Lee Y, Hwang W, Jung J, Park S, Cabatbat JJ, Kim PJ, Lee SJ. 2016. Inverse correlation between longevity and developmental rate among wild *C. elegans* strains. *Aging*. **8:**986-999. (doi:10.18632/aging.100960)

Lemire B. 2005. Mitochondrial genetics. *WormBook* 1-10. (doi:10.1895/wormbook.1.25.1)

Lewis JA, Fleming JT. 1995. Basic culture methods. *Methods Cell Biol*. **48**:3-29. (doi:10.1007/978-1-61779-452-0_12)

Lynch M. 1996. Mutation accumulation in transfer RNAs: molecular evidence for Muller's ratchet in mitochondrial genomes. *Mol. Biol. Evol.* **13**:209-220. (doi:10.1093/oxfordjournals.molbev.a025557)

Moore BT, Jordan JM, Baugh LR. 2013. WormSizer: high-throughput analysis of nematode size and shape. *PLoS One*. **8**(2):e57142. (doi:10.1371/journal.pone.0057142)

Morales HE, Pavlova A, Amos N, Major R, Kilian A, Greening C, Sunnucks P. 2018. Concordant divergence of mitogenomes and a mitonuclear gene cluster in bird lineages inhabiting different climates. *Nat Ecol Evol*. **2**:1258-1267. (doi:10.1038/s41559-018-0606-3)

Mossman JA, Tross JG, Li N, Wu Z, Rand DM. 2016. Mitochondrial-nuclear interactions mediate sex-specific transcriptional profiles in *Drosophila*. *Genetics*. **204**(2):613-630. (doi:10.1534/genetics.116.192328)

Mossman JA, Tross JG, Jourjine NA, Li N, Wu Z, Rand DM. 2017. Mitonuclear interactions mediate transcriptional responses to hypoxia in *Drosophila*. *Mol Biol Evol*. **34**(2):447-466. (doi:10.1093/molbev/msw246)

Nagarajan-Radha V, Aitkenhead I, Clancy DJ, Chown SL, Dowling DK. 2020. Sex-specific effects of mitochondrial haplotype on metabolic rate in *Drosophila melanogaster* support predictions of the Mother's Curse hypothesis. *Philos Trans R Soc Lond B Biol Sci.* **375**(1790):20190178. (doi:10.1098/rstb.2019.0178)

Neiman M, Hehman G, Miller JT, Logsdon JM, Taylor DR. 2010. Accelerated mutation accumulation in asexual lineages of a freshwater snail. *Mol. Biol. Evol*. **27**:954-963. (doi:10.1093/molbev/msp300)

Nickens KP, Wikstrom JD, Shirihai OS, Patierno SR, Ceryak S. 2013. A bioenergetic profile of non-transformed fibroblasts uncovers a link between death-resistance and enhanced spare respiratory capacity. *Mitochondrion*. **13**(6):662-7. (doi:10.1016/j.mito.2013.09.005)

Osada, N, Akashi H. 2012. Mitochondrial-nuclear interactions and accelerated compensatory evolution: Evidence from the primate cytochrome c oxidase complex. Mol. *Biol. Evol.* **29**:337-46. (doi:10.1093/molbev/msr211)

Paland S, Lynch M. 2006. Transitions to asexuality result in excess amino acid substitutions. *Science*. **311**:990-992. (doi:10.1126/science.1118152)

Pfleger J, He M, Abdellatif M. 2015. Mitochondrial complex II is a source of the reserve respiratory capacity that is regulated by metabolic sensors and promotes cell survival. *Cell Death Dis.* **6**(7):e1835. (doi:10.1038/cddis.2015.202)

Plesnar-Bielak A, Labocha MK, Kosztyła P, Woch KR, Banot WM, Sychta K, Skarboń M, Prus MA, Prokop ZM. 2017. Fitness effects of thermal stress differ between outcrossing and selfing populations in *Caenorhabditis elegans*. *Evol Biol.* **44**(3):356-364. (doi:10.1007/s11692-017-9413-z)

Radzvilavicius AL, Hadjivasiliou Z, Pomiankowski A, Lane N. 2016. Selection for mitochondrial quality drives evolution of the germline. *PLoS Biol*. **14**(12):e2000410. (doi:10.1371/journal.pbio.2000410)

Radzvilavicius AL, Kokko H, Christie JR. 2017. Mitigating mitochondrial genome erosion without recombination. *Genetics*. **3**:1079-1088. (doi:10.1534/genetics.117.300273)

Rand DM. 2008. Mitigating mutational meltdown in mammalian mitochondria. *PLoS Biol*. **6**:e35. (doi:10.1371/journal.pbio.0060035)

Rand DM, Mossman JA. 2020. Mitonuclear conflict and cooperation govern the integration of genotypes, phenotypes and environments. *Philos Trans R Soc Lond B Biol Sci.* **375**(1790):20190188. (doi:10.1098/rstb.2019.0188)

Rane HS, Smith JM, Bergthorsson U, Katju V. 2010. Gene conversion and DNA sequence polymorphism in the sex-determination gene *fog-2* and its paralog *ftr-1* in *Caenorhabditis elegans*. *Mol Biol Evol*. **27**(7):1561-9. (doi:10.1093/molbev/msq039)

Sackton TB, Haney RA, Rand DM. 2003. Cytonuclear coadaptation in Drosophila: disruption of cytrochrome c oxidase activity in backcross genotypes. *Evolution* **57**:2315-25. (doi:10.1111/j.0014-3820.2003.tb00243.x)

Schedl T, Kimble J. 1988. *fog-2*, a germ-line-specific sex determination gene required for hermaphrodite spermatogenesis in *Caenorhabditis elegans*. *Genetics*. **119**(1):43-61. (doi:10.1093/genetics/119.1.43)

Schindelin J, Arganda-Carreras I, Frise E, Kaynig V, Longair M, Pietzsch T, Preibisch S, Rueden C, Saalfeld S, Schmid B, Tinevez JY, White DJ, Hartenstein V, Eliceiri K, Tomancak P, Cardona A. 2012. Fiji: an open-source platform for biological-image analysis. *Nat Methods*. **9**(7):676-82. (doi:10.1038/nmeth.2019)

Stiernagle T. 2006. Maintenance of *C. elegans*. *WormBook*. **11**:1-11. (doi:10.1895/wormbook.1.101.1)

Suthammarak W, Yang YY, Morgan PG, Sedensky MM. 2009. Complex I function is defective in complex IV-deficient *Caenorhabditis elegans*. *J Biol Chem* **284**:6425-35. (doi:10.1074/jbc.M805733200)

Theologidis I, Chelo IM, Goy C, Teotónio H. 2014. Reproductive assurance drives transitions to self-fertilization in experimental *Caenorhabditis elegans*. *BMC Biol*. **12**:93. (doi:10.1186/s12915-014-0093-1)

Tsubaki M. 1993. Fourier-transform infrared study of azide binding to the Fea3-CuB binuclear site of bovine heart cytochrome C oxidase: new evidence for a redox-linked conformational change at the binuclear site. *Biochemistry*. **32**(1):174-82. (doi: 10.1021/bi00052a023)

Wade MJ. 2014. Paradox of mother's curse and the maternally provisioned offspring microbiome. *Cold Spring Harb Perspect Biol*. **6**(10):a017541. (doi:10.1101/cshperspect.a017541)

Wernick RI, Estes S, Howe DK, Denver DR. 2016. Paths of heritable mitochondrial DNA mutation and heteroplasmy in reference and *gas-1* strains of *Caenorhabditis elegans*. *Front. Genet.* **7**:1-12. (doi:10.3389/fgene.2016.00051)

Will Y, Hynes J, Ogurtsov VI, Papkovsky DB. 2006. Analysis of mitochondrial function using phosphorescent oxygen-sensitive probes. *Nat Protoc*. **1**(6):2563-72. (doi:10.1038/nprot.2006.351)

Wolff JN, Pichaud N, Camus MF, Côté G, Blier PU, Dowling DK. 2016. Evolutionary implications of mitochondrial genetic variation: mitochondrial genetic effects on OXPHOS respiration and mitochondrial quantity change with age and sex in fruit flies. *J Evol Biol*. **29**(4):736-47. (doi:10.1111/jeb.12822)

Wu M, Neilson A, Swift AL, Moran R, Tamagnine J, Parslow D, Armistead S, Lemire K, Orrell J, Teich J, Chomicz S, Ferrick DA. 2007. Multiparameter metabolic analysis reveals a close link between attenuated mitochondrial bioenergetic function and enhanced glycolysis dependency in human tumor cells. *Am J Physiol Cell Physiol*. **292**(1):C125-36. (doi:10.1152/ajpcell.00247.2006)

Xu S, Schaack S, Seyfert A, Choi E, Lynch M, Cristescu ME. 2012. High mutation rates in the mitochondrial genomes of *Daphnia pulex*. *Mol. Biol. Evol*. **29**:763-769. (doi:10.1093/molbev/msr243)

Yadava N, Nicholls DG. 2007. Spare respiratory capacity rather than oxidative stress regulates glutamate excitotoxicity after partial respiratory inhibition of mitochondrial complex I with rotenone. *J Neurosci*. **27**(27):7310-7. (doi:10.1523/JNEUROSCI.0212-07.2007)

Zaidi AA, Wilton PR, Su MS, Paul IM, Arbeithuber B, Anthony K, Nekrutenko A, Nielsen R, Makova KD. 2019. Bottleneck and selection in the germline and maternal age influence transmission of mitochondrial DNA in human pedigrees. *Proc Natl Acad Sci U S A*. **116**(50):25172-25178. (doi:10.1073/pnas.1906331116)

CONCLUSION

The evolution of eukaryotes and mitochondria is tightly tied to one another. Despite this, the evolution of mitochondria has not received the same level of attention as that of eukaryotes. This is partially due to the difficulty of generating heteroplasmic mitochondrial mutations and performing controlled experiments with them in their host organism. The studies reported here have taken advantage of lines created by Konrad et al. (2017). These lines spontaneously generated a variety of mitochondrial mutations at a high frequency within the model organism *Caenorhabditis elegans* during a long-term experimental evolution experiment. This provided a unique system to experimentally test what forces drive the evolution and inheritance of mitochondrial mutations.

Most of this dissertation focused on how deleterious mutations evade selection and rise to high frequencies within individuals, taking advantage of selfish genetic drive. In the first study (chapter II), we analyzed the fitness effects and population dynamics of a mitochondrial genome containing a novel 499 bp deletion in *ctb-1* (Δ*ctb-1*). Δ*ctb-1* reached a high heteroplasmic frequency of 96% during experimental evolution and was linked to additional spontaneous mutations in *nd5* and *tRNA-Asn*. The Δ*ctb-1* mutant mitotype imposed a significant fitness cost, including a 65% and 52% reduction in productivity and competitive fitness, respectively, relative to individuals bearing wild-type (WT) mitochondria. When competed against WT mitochondrial DNA (mtDNA) bearing worms, deletion-bearing worms were rapidly purged within a few

generations in experimental populations. In contrast, the Δ*ctb-1* mitotype was able to persist in large populations comprising heteroplasmic individuals only, although the average intracellular frequency of Δ*ctb-1* exhibited a slow decline owing to competition among individuals bearing different frequencies of the heteroplasmy. Within experimental lines subjected to severe population bottlenecks (n = 1), the relative intracellular frequency of Δ*ctb-1* increased, which is a hallmark of selfish drive. Δ*ctb-1* also resulted in an elevated mtDNA copy number. However, a positive correlation between Δ*ctb-1* and WT mtDNA copy number suggests a mechanism that increases total mtDNA without discerning the Δ*ctb-1* mitotype from the WT mtDNA.

In chapter III, we continued to explore the selfish behavior of the Δ*ctb-1* mitotype. The regular cryopreservation of the original experimental line at several time intervals during its evolution provided an opportunity to dissect the sequential origin and fitness effects of the various mutations comprising this selfish mitochondrial genome.

First, we investigated whether subsequent mtDNA mutations present in the Δ*ctb-1* mitotype compensate for the deleterious effects of preceding ones, as had been seen with mutations associated with dosage compensation and the nuclear electron transport chain (ETC) mutations. Second, we investigated whether a particular class of mutations confers selfish behavior in mitochondria. We assayed fitness across four life-history traits in backcrossed ancestral lines with WT nuclear genomes and heteroplasmic mutation-bearing mtDNA. We found that the addition of each subsequent mitochondrial mutation reduced overall fitness in the backcrossed lines. We then propagated ancestral lines containing each combination of mutations by bottlenecking to reduce

interindividual competition. This allowed us to track the intraindividual frequency of heteroplasmy over evolutionary time and to determine if selfish drive could be detected. Without interindividual competition acting upon these lines, a mean increase in heteroplasmic frequency across replicates could be attributed to an intraindividual selfish drive.

We found evidence of selfish drive for three of the four mutations. Interestingly, the only line that did not show clear evidence of selfish drive was a frameshift insertion in *nd5*. However, a subsequent insertion in *nd5* at the same location did confer selfish drive. We found that selfish drive can be seen in a variety of different classes of mitochondrial mutations, but we found no evidence for compensatory effects of each subsequent mutation. We were unable to disentangle the contribution of the original deletion from the selfish behavior of each subsequent mutation. It is therefore possible that the subsequent mutations lack a selfish drive of their own but serve to enhance that of the original deletion.

In chapter IV, we examined the evolutionary dynamics of another mtDNA deletion and compared it to Δ*ctb-1*. We analyzed the fitness effects and population dynamics of a mitochondrial genome containing a 1185 bp deletion in *COI* (Δ*COI*). Like Δ*ctb*-1, Δ*COI* reached a high heteroplasmic frequency of 82% during experimental evolution. Δ*COI* also imposed a significant fitness cost on its host. Bearing Δ*COI* imposed a 28.5% reduction in productivity relative to wild type, far less than the 65% reduction imposed by Δ*ctb-1*. Also, like Δ*ctb-1*, the Δ*COI* mitotype persists in large populations comprising heteroplasmic individuals only, with the heteroplasmic

frequency of Δ*COI* slowly declining over time. Where Δ*COI* and Δ*ctb-1* differ is in their within-individual selfish drive. In experimental lines subjected to severe population bottlenecks ($N = 1$), the relative intracellular frequency of Δ*COI* increased in the original mutation accumulation background but not in backcrossed lines with WT nDNA and Δ*COI* mtDNA. One possible explanation for this difference is that the frequency of Δ*COI* could be near a threshold in heteroplasmic frequency, above which worms are no longer viable and Δ*COI* cannot increase. Alternatively, there could be some mitonuclear interacting factors present that permit selfish drive of Δ*COI* in the mutation accumulation background or inhibit selfish drive it in the wild-type background. Either explanation highlights the context dependance of selfish genetic drive. The similarity in both origin and evolutionary dynamics to the previously identified Δ*ctb-1* mitotype provides a new tool to test what aspects of mitochondrial biology affect the fate of new mtDNA mutations and their selfish behavior.

The final study (chapter V) diverted from the question of selfish mitotypes and instead examined the effect of ETC mutations in male and female *C. elegans* in a variety of sexual systems. Using two nuclear ETC mutations (*isp-1(150)* and *gas-1(fc21)*), two mitochondrial ETC mutations (*ctb-1(189)* and *cox-1(chpIR)*), in three sex systems, we measured fitness traits of lines for each ETC/sexual system combination. We also measured mitochondrial respiration in hermaphrodites from the obligately selfing and facultatively outcrossing lines, and in males and females from the obligately outcrossing lines. We found that both nuclear ETC mutations caused some mitochondrial dysfunction. Conversely, we found little evidence for mitochondrial dysfunction in

either of the mitochondrial ETC mutations. We also found little evidence for sex-specific effects of any of our ETC mutations. We did, however, find some evidence for sex system-specific differences in the deleterious effects of ETC mutation. Obligately outcrossing *C. elegans* had especially low developmental rate and productivity when bearing either of the nuclear ETC mutants.

All these studies have established new tools for studying mitochondrial biology and evolutionary dynamics. Future research is needed to capitalize on the experimental models established here. While the first three studies characterize and isolate several new selfishly acting mitotypes, none of these studies directly test hypotheses related to why the selfishly acting mitotypes have this selfish drive.

Because many of the known selfish mitotypes bear deletions, it is possible that the selfish drive of these mitotypes is due to the faster replication of smaller mtDNA (Clark et al. 2012). This theory has gained additional support with the observation that *C. elegans* mtDNA are replicated as a single long multimer (Lewis et al. 2015), which could potentially contain more copies of mtDNA per round of replication if the mtDNA molecules were shortened by a deletion. With a panel of *C. elegans* mtDNA deletions of varying sizes, which we have contributed to here, it is now possible to measure how mtDNA replication rate varies with the size of the deletion.

Another aspect of mtDNA selfishness that needs to be explored is the role of fission and fusion. Modeling has predicted that fusion and fission should modulate the efficiency of a host cell in purging deleterious mtDNA (Tam et al. 2015). Increasing fusion is predicted to maintain energetic homeostasis but mask the effect of deleterious

mtDNA, while increasing fission is predicted to increase selection against deleterious mtDNA but also lessen the energy available to the host cell. With the growing panel of heteroplasmic deletion-bearing mtDNA available and the ability to inhibit fusion/fission control genes like *dyn-1* (Nakayama et al. 2009) with RNAi, these models can easily be tested with *C. elegans*.

These are just a few examples of the numerous ways that the lines generated in these studies could be used to further understand the fundamental principles of mitochondrial evolution. We still do not have the nuanced understanding of mitochondrial biology called for in the beginning of this piece, but we do have a better understanding of evolutionary dynamics of selfish mitochondrial deletions in *C. elegans*. We also have several new models that can be used to test our assumptions about the little powerhouses within us all.

References

Clark KA, Howe DK, Gafner K, Kusuma D, Ping S, Estes S, Denver DR. 2012. Selfish little circles: transmission bias and evolution of large deletion-bearing mitochondrial DNA in *Caenorhabditis briggsae* nematodes. *PLoS One*. **7**(7):e41433. (doi:10.1371/journal.pone.0041433)

Konrad A, Thompson O, Waterston RH, Moerman DG, Keightley PD, Bergthorsson U, Katju V. 2017. Mitochondrial mutation rate, spectrum and heteroplasmy in *Caenorhabditis elegans* spontaneous mutation accumulation lines of differing population size. *Mol Biol Evol*. **34**(6):1319-1334. (doi:10.1093/molbev/msx051)

Lewis SC, Joers P, Willcox S, Griffith JD, Jacobs HT, Hyman BC. 2015. A rolling circle replication mechanism produces multimeric lariats of mitochondrial DNA in *Caenorhabditis elegans*. *PLoS Genet*. **11**(2):e1004985. (doi:10.1371/journal.pgen.1004985)

Nakayama Y, Shivas JM, Poole DS, Squirrell JM, Kulkoski JM, Schleede JB, Skop AR. 2009. Dynamin participates in the maintenance of anterior polarity in the *Caenorhabditis elegans* embryo. Dev Cell. **16**(6):889-900. (doi:10.1016/j.devcel.2009.04.009)

Tam ZY, Gruber J, Halliwell B, Gunawan R. 2015. Context-dependent role of mitochondrial fusion-fission in clonal expansion of mtDNA mutations. *PLoS Comput Biol*. **11**(5):e1004183. (doi:10.1371/journal.pcbi.1004183)